

AD-A142 537

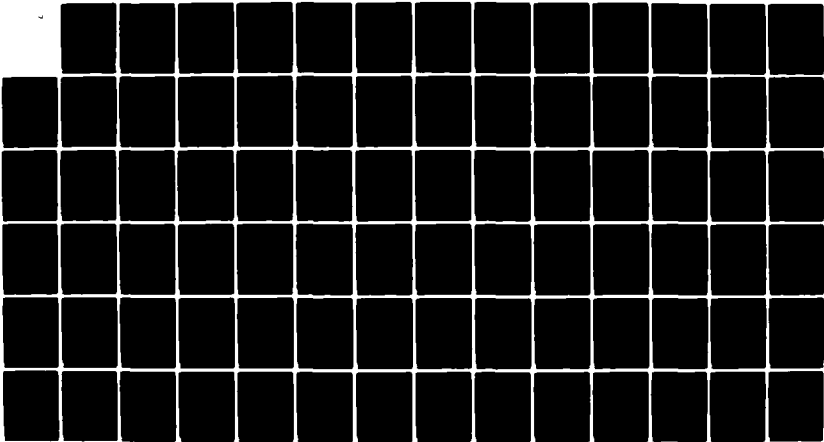
THE TEMPERATURE SENSITIVITY OF DOUBLY ROTATED QUARTZ
RESONATORS(U) RIO GRANDE ASSOCIATES HOUSTON TX
R R BELAND NOV 83 SCIENTIFIC-2 AFGL-TR-84-0078
F19628-81-C-0128

1/1

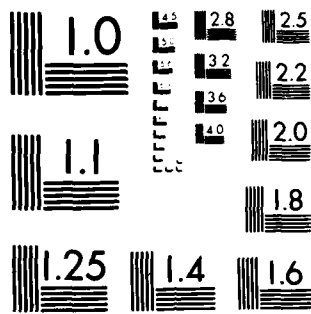
UNCLASSIFIED

F/G 9/1

NL



END
DATE
FILMED
8-84
DTIC



MICROCOPY RESOLUTION TEST CHART
NATIONAL BUREAU OF STANDARDS-1963 A

12

AFGL-TR-84-0078

THE TEMPERATURE SENSITIVITY OF
DOUBLY ROTATED QUARTZ RESONATORS

Robert R. Beland

AD-A142 537

Rio Grande Associates
1 Allen Center, Suite 100
Houston, Texas 77002

Scientific Report No. 2

November 1983

Approved for public release; distribution unlimited

DTIC FILE COPY

AIR FORCE GEOPHYSICS LABORATORY
AIR FORCE SYSTEMS COMMAND
UNITED STATES AIR FORCE
HANSCOM AFB, MASSACHUSETTS 01731

84 06 22 005

This report has been reviewed by the ESD Public Affairs Office (PA) and is releasable to the National Technical Information Service (NTIS).

This technical report has been reviewed and is approved for publication.

P Tsipouras

PAUL TSIPOURAS
Contract Manager

P Tsipouras

PAUL TSIPOURAS, Chief
Analysis & Techniques Branch
Information Resources Management Division

FOR THE COMMANDER

Eunice C. Cronin

EUNICE C. CRONIN, Director
Information Resources Management Division

Qualified requestors may obtain additional copies from the Defense Technical Information Center. All others should apply to the National Technical Information Service.

If your address has changed, or if you wish to be removed from the mailing list, or if the addressee is no longer employed by your organization, please notify AFGL/DAA, Hanscom AFB, MA 01731. This will assist us in maintaining a current mailing list.

Do not return copies of this report unless contractual obligations or notices on a specific document requires that it be returned.

Unclassified

SECURITY CLASSIFICATION OF THIS PAGE (When Data Entered)

REPORT DOCUMENTATION PAGE		READ INSTRUCTIONS BEFORE COMPLETING FORM
1. REPORT NUMBER AFGL-TR-84-0078	2. GOVT ACCESSION NO. AD-A242 537	3. RECIPIENT'S CATALOG NUMBER
4. TITLE (and Subtitle) THE TEMPERATURE SENSITIVITY OF DOUBLY ROTATED QUARTZ RESONATORS		5. TYPE OF REPORT & PERIOD COVERED Scientific Report No. 4
		6. PERFORMING ORG. REPORT NUMBER
7. AUTHOR(s) Robert R. Beland		8. CONTRACT OR GRANT NUMBER(s) F19628-81-C-0128
9. PERFORMING ORGANIZATION NAME AND ADDRESS Rio Grande Associates 1 Allen Center Suite 100 Houston, TX 77002		10. PROGRAM ELEMENT, PROJECT, TASK AREA & WORK UNIT NUMBERS 62101F 9993XXXX
11. CONTROLLING OFFICE NAME AND ADDRESS Air Force Geophysics Laboratory Hanscom AFB, MA 01731 Monitor: Paul Tsipouras/RMA		12. REPORT DATE November 1983
		13. NUMBER OF PAGES 81
14. MONITORING AGENCY NAME & ADDRESS (if different from Controlling Office)		15. SECURITY CLASS. (of this report) Unclassified
		15a. DECLASSIFICATION/DOWNGRADING SCHEDULE
16. DISTRIBUTION STATEMENT (of this Report) Approved for public release: distribution unlimited		
17. DISTRIBUTION STATEMENT (of the abstract entered in Block 20, if different from Report)		
18. SUPPLEMENTARY NOTES		
19. KEY WORDS (Continue on reverse side if necessary and identify by block number) Quartz plates; piezoelectric plate vibrations; temperature behavior; temperature sensitivity; quartz resonators; doubly rotated quartz; temperature stability		
20. ABSTRACT (Continue on reverse side if necessary and identify by block number) Thickness-mode quartz resonators have long been used for timing and frequency control. It is well known that a change in temperature results in a change in the resonance frequencies of such quartz plates. Thus, a major requirement for precision frequency applications is that these temperature deviations are minimized. This report summarizes a detailed numerical investigation of the temperature sensitivity of doubly rotated quartz resonators. Various measures of sensitivity are used for the temperature range -40 to 80°C. Several cuts of quartz with stable temperature behavior are described and compared.		

TABLE OF CONTENTS

	<u>Page</u>
ABSTRACT	4
ACKNOWLEDGEMENTS	5
LIST OF FIGURES	6
LIST OF TABLES	7
1. INTRODUCTION	8
2. THEORY	9
3. TEMPERATURE BEHAVIOR	17
4. NUMERICAL RESULTS	23
5. CONCLUSION	80
REFERENCES	81

ABSTRACT

Thickness-mode quartz resonators have long been used for timing and frequency control. It is well known that a change in temperature results in a change in the resonance frequencies of such quartz plates. Thus, a major requirement for precision frequency applications is that these temperature deviations are minimized. This report summarizes a detailed numerical investigation of the temperature sensitivity of doubly rotated quartz resonators. Various measures of sensitivity are used for the temperature range -40 to 80°C . Several cuts of quartz with stable temperature behavior are described and compared.

ACKNOWLEDGEMENTS

This work was performed in support of A. Kahan of RADC. Indeed, it was Mr. Kahan who suggested the general framework for this investigation and provided the subroutine for calculating the temperature coefficients of quartz. For these reasons, as well as for informative discussions, the author wishes to acknowledge his invaluable contribution.

Accession For		
NTIS GRA&I	<input checked="" type="checkbox"/>	
DTIC TAB	<input type="checkbox"/>	
Unannounced	<input type="checkbox"/>	
Justification	<input type="checkbox"/>	
By _____		
Distribution/ _____		
Availability Codes		
Avail and/or		
Dist	Special	
A-1		



LIST OF FIGURES

	<u>Page</u>
Figure 1: PLATE GEOMETRY	9
Figure 2: SINGLY AND DOUBLY ROTATED CRYSTAL PLATES: COORDINATE SYSTEMS	15
Figure 3: COUPLING CONSTANTS	24-27
Figure 4: RFD CURVE FOR AT CUT	28
Figure 5: RFD CURVE FOR BT CUT	30
Figure 6: LOCI OF FIRST ORDER ZERO TEMPERATURE COEFFICIENTS	31
Figure 7: INTEGRAL MEASURE OF TEMPERATURE SENSITIVITY . . .	33-43
Figure 8: INTEGRAL MINIMA FOR B MODE	44
Figure 9: INTEGRAL MINIMA FOR C MODE	45
Figure 10: RFD CURVES FOR C MODE INTEGRAL MINIMUM WITH $\phi = 0$, $\theta = 35.1304$ AND $\theta \pm 10'$	47
Figure 11: RFD CURVES FOR B MODE INTEGRAL MINIMUM WITH $\phi = 60^\circ$, $\theta = 49.3833$ AND $\theta \pm 10'$	48
Figure 12: RFD CURVES FOR C MODE INTEGRAL MINIMUM WITH $\phi = 27$, $\theta_m = 34.0644$ AND $\theta \pm 10'$	49
FIGURE 13: RFD CURVES FOR C MODE INTEGRAL MINIMUM WITH $\phi = 42$, $\theta = 33.2906$ AND $\theta \pm 10'$	50
Figure 14: COUPLING CONSTANT VERSUS ϕ FOR C MODE INTEGRAL MINIMIZED WITH RESPECT TO θ	52
Figure 15: EIGENVALUES VERSUS ϕ FOR C MODE INTEGRAL MINIMIZED WITH RESPECT TO θ	53
Figure 16: RANGE MEASURE OF TEMPERATURE SENSITIVITY	55-65
Figure 17: DIFFERENCE MEASURE OF TEMPERATURE SENSITIVITY . .	69-79

LIST OF TABLES

	Page
Table 1: MINIMA USING MEASURES M_1 , M_2 AND M_3	66

THE TEMPERATURE SENSITIVITY OF DOUBLY ROTATED QUARTZ RESONATORS

1.

INTRODUCTION

Thickness-mode quartz resonators have long been used for timing and frequency control. It is well known that a change in temperature results in a change in the resonance frequencies of such quartz plates. Thus, a major requirement for precision frequency applications is that these temperature deviations are minimized. This report summarizes a detailed numerical investigation of the temperature sensitivity of doubly rotated quartz resonators. Various measures of sensitivity are used for the temperature range -40 to 80°C . Several cuts of quartz with stable temperature behavior are described and compared.

2.

THEORY

We begin by summarizing the theory of piezoelectric plate vibrations. We assume the geometry of the plate depicted in Figure 1. The plate is of thickness $2h$ and has the y -axis as a normal. Furthermore, it is assumed to be infinite in extent in the x - z plane. These geometrical considerations imply that $\frac{\partial}{\partial z}$ and $\frac{\partial}{\partial x}$ vanish for the field quantities and we thus have one-dimensional motion in the y -direction, i.e., the so-called simple thickness modes of vibration.

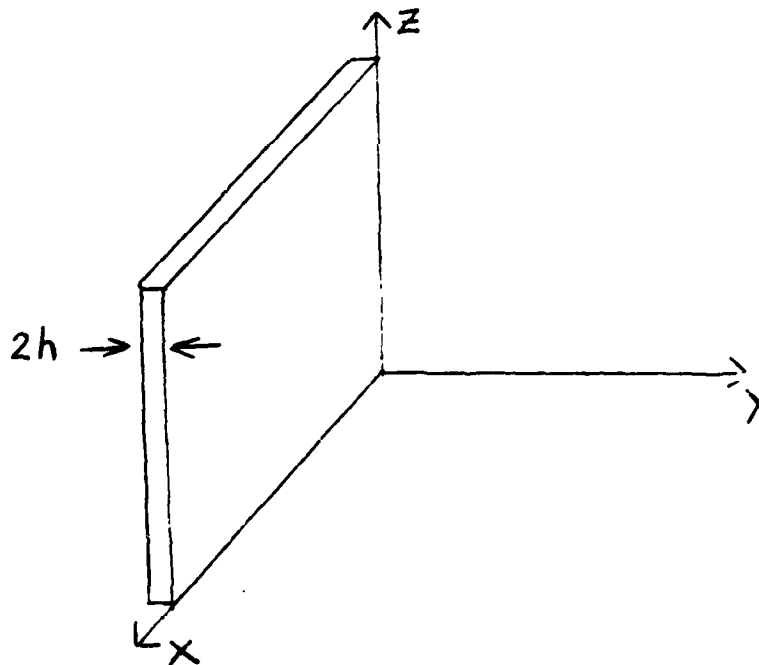


Figure 1: PLATE GEOMETRY

In the following, a subscripted index following a comma denotes differentiation with respect to that spatial index. To further simplify the notation, we will adopt the summation convention that repeated indices are to be summed over. The stress equations of motion are:

$$T_{ij,i} = \rho \ddot{\mu}_j \quad (1)$$

where T_{ij} is the stress tensor, ρ the material density (assumed constant) and μ_j is the j th component of the displacement vector. Under the assumption of an infinitesimal deformation, we have the Cauchy strain tensor:

$$S_{ij} = \frac{1}{2} (\mu_{i,j} + \mu_{j,i}). \quad (2)$$

The electromagnetic characterization of the problem is achieved using a quasi-static approximation which produces the equations for the electric displacement D_i , the electric field E_i , and potential

$$D_{i,i} = 0 \quad (3)$$

$$E_j = -\varphi_{,j} \quad (4)$$

The remaining equations are obtained from thermodynamic considerations. Let the material under consideration be characterized by the elastic stiffness tensor at constant electric field, C_{ijkl} , the piezoelectric stress tensor, e_{ijk} , and the dielectric tensor at constant strain ϵ_{ij} . These material constants are related to the field quantities by the linear piezoelectric constitutive relations:

$$T_{ij} = C_{ijkl}S_{kl} - e_{nij}E_n \quad (5)$$

$$D_i = e_{ikl}S_{kl} + \epsilon_{in}E_n \quad (6)$$

Equations 1-6 can be combined, yielding the simplified 4 equations:

$$C_{ijkl}u_{k,li} + e_{kij}\varphi_{,ki} = \rho \ddot{\mu}_j \quad (7)$$

$$e_{ikl}u_{k,li} - \epsilon_{ik}\varphi_{,ki} = 0 \quad (8)$$

Our geometrical considerations imply that $\varphi_{,li} u_{k,li}$ vanish unless $l=i=2$, so 7 and 8 become for the infinite plate:

$$C_{2jk2}u_{k,22} + e_{22j}\varphi_{,22} = \rho \ddot{\mu}_j \quad (9)$$

$$e_{2k2}u_{k,22} - \epsilon_{22}\varphi_{,22} = 0 \quad (10)$$

We now use (10) in (9), yielding

$$\left(c_{2jk2} + \frac{e_{22j} e_{2k2}}{\epsilon_{22}} \right) u_{k,22} = -\rho \omega^2 u_j \quad (11)$$

where u is assumed to have a harmonic time dependence. We define the piezoelectrically stiffened elastic constants by:

$$\bar{c}_{2jk2} = c_{2jk2} + \frac{e_{22j} e_{2k2}}{\epsilon_{22}} \quad (12)$$

Then (11) becomes a wave equation:

$$\bar{c}_{2jk2} u_{k,22} + \rho \omega^2 u_j = 0 \quad (13)$$

Note that this is really 3 coupled equations. The solutions we seek are acoustic plane waves of the form:

$$u_j(x,y,z,t) = \beta_j e^{i\left(\frac{\omega x}{v} - \omega t\right)} \quad (14)$$

where β_j is a constant. Substitution of (14) into (13) yields the equation

$$\bar{c}_{2jk2} \beta_k - \rho v^2 \beta_j = 0 \quad (15)$$

If we define the "matrix" \bar{c} such that $\bar{c}_{jk} = \bar{c}_{2jk2}$, then (15) may be written as:

$$\bar{c} \vec{\beta} - \lambda \vec{\beta} = 0 \quad (16)$$

where $\lambda = \rho v^2$ and $\vec{\beta}$ is the vector with components β_1 , β_2 , and β_3 . In this form, we clearly have an eigenvalue problem (although, strictly speaking, \bar{c} is not a matrix, i.e., a second rank tensor). The eigenvalues, $\lambda_{(n)}$, determine the propagation velocities of the three modes by:

$$v_{(i)} = \left(\frac{\lambda_{(i)}}{\rho} \right)^{1/2} \quad (17)$$

The solution of the eigenvalue problem yields 3 roots, or modes, which are ordered by the relation:

$$\lambda_a \geq \lambda_b \geq \lambda_c \quad (18)$$

and the convention is to refer to the modes by the letters a, b and c. The eigenvector corresponding to a mode gives the direction cosines of the displacement.

In addition to the eigenvalues and eigenvectors, there is another parameter which is important in characterizing the modes. This is the piezoelectric coupling constant, which is a measure of the ratio of electrical energy to mechanical energy of the vibrations. Following Ballato (1977) and Tiersten (1969), we define the coupling constant of mode m by:

$$k_{(m)}^2 = \left(\beta_j^{(m)} e_{22j} \right)^2 / \lambda_{(m)} \epsilon_{22} \quad (19)$$

where $\beta_j^{(m)}$ is the eigenvector corresponding to $\lambda_{(m)}$. It is worth emphasizing that the eigenvalues, eigenvectors and coupling constants are completely determined by the material constants for the thickness modes of infinite plates; these parameters are independent of the boundary conditions. The resonance frequencies, in contrast, depend critically on the boundary conditions. The conditions that we impose are that the surfaces are traction-free and driven by a sinusoidal voltage:

$$T_{j2} = T_{2j} = 0 \quad \text{at } y = \pm h \quad (20)$$

$$\varphi = \pm \varphi_0 e^{i\omega t} \quad \text{at } y = \pm h \quad (21)$$

where we have assumed that the plate is of thickness 2h. We apply these boundary conditions to our general solution which is a linear combination of the modal eigenvectors. The result is a transcendental equation whose solutions give the allowable frequencies of vibration for the plate. This equation can be expressed in the form (Tiersten [1969]):

$$\sum_{n=1}^3 k_{(n)}^2 \frac{\tan (wh/v_{(n)})}{wh/v_{(n)}} = 1 \quad (22)$$

The solutions to this equation yield the resonance frequencies. This equation cannot be solved in general and demonstrates the coupling of the resonance frequencies by the boundary conditions. In the general case, the frequency solutions to (22) cannot be identified with a certain mode. Fortunately, we can approximate (22) by a simpler equation when the coupling constants are small. This approximation is very reasonable for quartz, where $k_{(n)}$ is usually less than 0.10 (10%). If the eigenvalues are well separated in addition to the coupling constants being small, then the resonance frequencies can be approximated by the solutions to the uncoupled equation

$$k_n^2 \frac{\tan (wk/v_n)}{(wk/v_n)} = 1 \quad (23)$$

(Ballato & Iafrate [1976]). Note that in this approximation the modal resonances are independent. The solution to (23) can in turn be approximated for small k_n by using the Laurent series expansion of $\tan x$ about $x = \Pi/2$:

$$w_{rm} = (2m + 1) \frac{\Pi}{2} \frac{v_n}{n} \left[1 - \frac{4k_n^2}{\Pi^2 (2m + 1)^2} \right] \quad (24)$$

where $m = 0, 1, \dots$. Note that the first term is just the solution to

$$\tan \frac{wh}{v_n} = \infty \quad (25)$$

The correction term is clearly negligible for high overtones, i.e., for large m (Bechmann et al [1962]). We shall neglect this correction in the following and approximate the resonance frequencies by the solution to (25):

$$w_{rm} = (2m + 1) \frac{\Pi}{2} \frac{v_n}{h} \quad (26)$$

Converting these angular frequencies to cycles per unit time, the resonance frequencies are given by

$$f_{rm} = (2m + 1) \frac{v_n}{4h} \quad (27)$$

The theory we have summarized so far applies to a general, anisotropic piezoelectric substance; there are no constraints placed on the material constants. The most general piezoelectric substance is an arbitrarily anisotropic (triclinic) crystal without center of symmetry. In this case, there are 45 independent material constants required to specify the elastic, piezoelectric and dielectric tensors. However, we are interested in the properties of doubly rotated quartz, so we need not consider such an arbitrary substance. Quartz is a member of the trigonal, trapezohedral crystal class (32, D_3) (see, e.g., Mason [1950]). In the crystalline coordinate system, there are only 10 independent material constants (Mason [1950], Tiersten [1969], Bechmann [1956]): 6 elastic constants, 2 piezoelectric constants and 2 dielectric constants. These constants have been measured by Bechmann (1956). The elastic, piezoelectric and dielectric tensors for an arbitrary cut of quartz may be determined by applying the tensor transformation rules to the tensors in the crystalline coordinate system. The most general transformation between two coordinate systems is given by the Euler angle formulation. (Goldstein [1950]). Such a transformation is specified by the Euler angles (λ, μ, θ) (using the convention of Goldstein). We are, however, interested in doubly rotated quartz crystals; the plate orientations are specified by the two angles ϕ and θ relative to the crystal axes (see Figure 2). The case of both ϕ and θ being zero results in the so-called Y-plate (i.e., y-axis normal to plate) with material constants given by those in the crystal system. For non-zero ϕ and θ , the material constants are determined by applying the transformation x to the unrotated tensors, where

$$x = \begin{bmatrix} -\sin\phi \cos\theta & \cos\phi \cos\theta & \sin\theta \\ \sin\phi \sin\theta & -\cos\phi \sin\theta & \cos\theta \\ \cos\phi & \sin\phi & 0 \end{bmatrix} \quad (28)$$

If we denote the tensors relative to the crystal axes by primes, the elastic, piezoelectric and dielectric tensors for the doubly rotated cuts are given by:

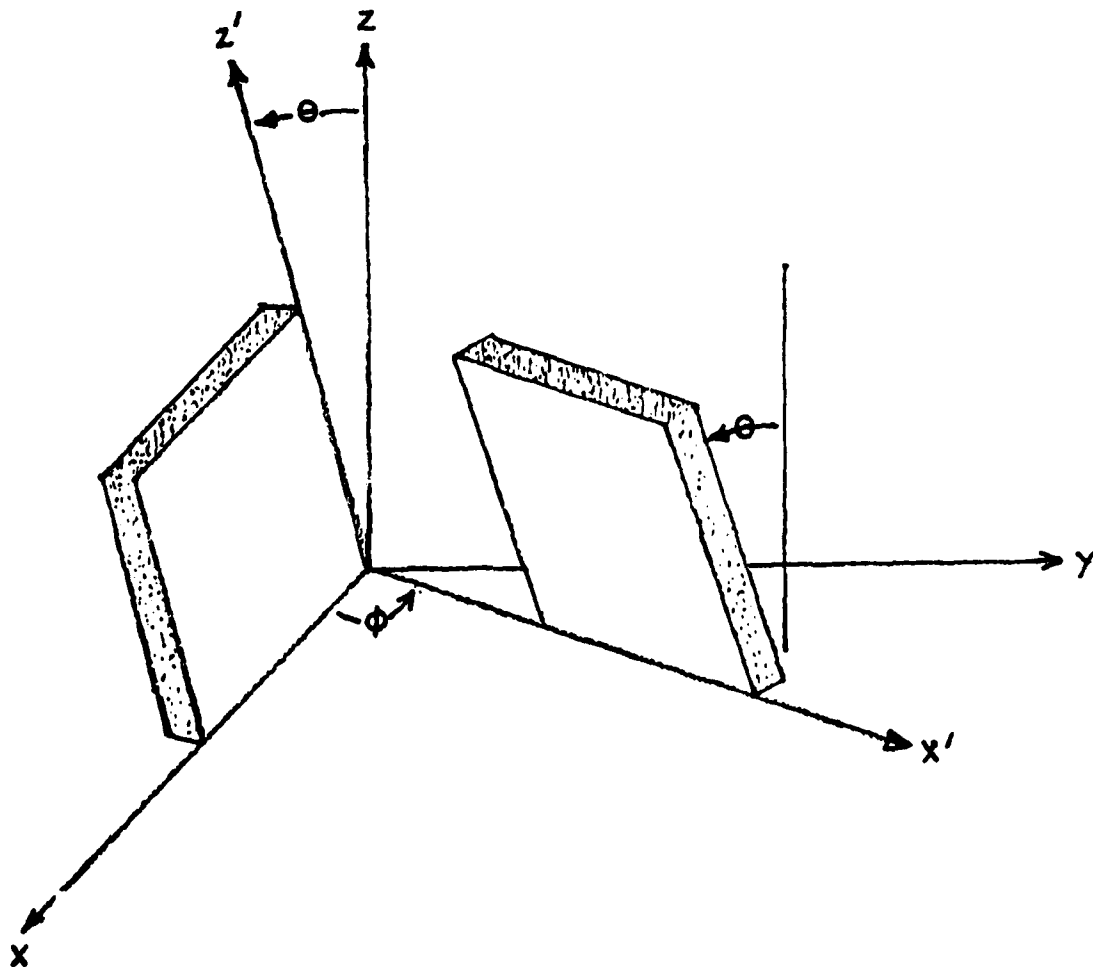


Figure 2: SINGLY AND DOUBLY ROTATED CRYSTAL PLATES:

COORDINATE SYSTEMS

$$C_{ijkl} = x_{im}x_{jn}x_{ko}x_{lp}C'_{mnop}$$

$$e_{ijk} = x_{il}x_{jm}x_{kn}e'_{lmn} \quad (29)$$

$$\hat{\epsilon}_{ij} = x_{ik}x_{jl}\hat{\epsilon}'_{kl}$$

Thus, given ϕ and θ , we calculate the material constants from (29). The eigenvalues, eigenvectors, coupling constants and approximate resonance frequencies are then calculated using these rotated tensors.

3.

TEMPERATURE BEHAVIOR

The resonance frequencies of piezoelectric plates are functions of temperature. The standard approach to this temperature behavior is phenomenological and assumes that the plate is in thermal equilibrium. We then assume that the equilibrium resonance frequency is an analytic function of temperature and expand it in a Taylor series about a reference state with frequency f_0 and temperature T_0 :

$$f = f_0 + \sum_{n=1}^{\infty} \left(\frac{1}{n!} \left. \frac{\partial^{(n)} f}{\partial T^{(n)}} \right|_{T=T_0} \right) (T-T_0)^n \quad (30)$$

We may rewrite this in terms of a fractional change in frequency:

$$\frac{f-f_0}{f_0} = \frac{\Delta f_0}{f_0} = \sum_{n=1}^{\infty} \left[\frac{1}{n!} \frac{1}{f_0} \left. \frac{\partial^{(n)} f}{\partial T^{(n)}} \right|_{T=T_0} \right] (T-T_0)^n \quad (31)$$

The standard notation for the temperature expansion coefficients is $T_f^{(n)}$, or explicitly:

$$T_f^{(n)} = \frac{1}{n! f_0} \left. \frac{\partial^{(n)} f}{\partial T^{(n)}} \right|_{T=T_0} \quad (32)$$

Indeed, we may write the temperature expansion of any quantity g about a reference state (g_0, T_0) as:

$$\frac{g-g_0}{g_0} = \sum_{n=1}^{\infty} T_g^{(n)} (T-T_0)^n. \quad (33)$$

It has been empirically established that a cubic expansion suffices to adequately describe the temperature effects on the quartz resonances (Bechmann [1956], Ballato [1977]). We shall refer to the cubic frequency expansion as the relative frequency difference function, $\Delta f/f$:

$$\frac{\Delta f}{f} = \sum_{n=1}^3 T_f^{(n)} (T-T_0)^n \quad (34)$$

Furthermore, we will assume that a cubic expansion suffices to describe the temperature behavior of other material parameters, such as the elastic constants. This is a reasonable approximation provided the temperature range is small.

We shall now proceed to relate the temperature coefficients of the relative frequency difference function to the temperature coefficients of the material parameters for quartz. We shall do so only for the fundamental frequencies. We have, from (27), the modal frequencies for an infinite plate of thickness $2k$:

$$f_n = \frac{1}{4h} \sqrt{\frac{\lambda_n}{\rho}} \quad (35)$$

We shall approximate the infinite plate by a finite one of dimensions d and l . This is reasonable provided $d \gg 2h$ and $l \gg 2h$. The density is then given by

$$\rho = \frac{M}{2hld} \quad (36)$$

The modal frequencies are thus:

$$f_n = \frac{1}{2} \sqrt{\frac{\lambda_n^2 ld}{2hM}} \quad (37)$$

where M is the plate mass. Straightforward differentiation gives:

$$T_f^{(1)} = \frac{1}{2} T_n^{(1)} - \frac{1}{2} T_h^{(1)} + \frac{1}{2} T_l^{(1)} + \frac{1}{2} T_d^{(1)} \quad (38)$$

Note that the temperature coefficients $T_l^{(1)}$, $T_d^{(1)}$ and $T_h^{(1)}$ are just the coefficients of thermal expansion in the x , y and z directions. These are

measurable quantities. The temperature coefficient of the eigenvalue, $T_{\lambda_n}^{(1)}$, can be expressed in terms of the material constants. The characteristic equation (16) yields a cubic for λ_n , which we write as:

$$\lambda^3 - A \lambda^2 + B \lambda + D = 0 \quad (39)$$

After differentiation and algebraic manipulations, we obtain:

$$T_{\lambda_n}^{(1)} = \left(\frac{1}{\lambda_n} \right) \left[\frac{\lambda_n^2 A T_A^{(1)} - \lambda_n B T_B^{(1)} - D T_D^{(1)}}{3 \lambda_n^2 - 2 A \lambda_n + B} \right] \quad (40)$$

The temperature coefficients of A, B and D are determined by the eigenvalue equation. We have:

$$A = \square_{11} + \square_{22} + \square_{33} \quad (41)$$

$$B = \square_{11} \square_{22} + \square_{22} \square_{33} + \square_{11} \square_{33} \\ - \square_{23}^2 - \square_{13}^2 - \square_{12}^2 \quad (42)$$

$$D = \square_{11} \square_{23}^2 + \square_{22} \square_{13}^2 + \square_{33} \square_{12}^2 \\ - \square_{11} \square_{22} \square_{33} - 2 \square_{12} \square_{23} \square_{33} \\ - 2 \square_{12} \square_{23} \square_{13} \quad (43)$$

where

$$\square_{2jk2} = C_{2jk2} + \frac{e_{22j} e_{2k2}}{\epsilon_{22}} \quad (44)$$

and for ease of notation, we have written \square_{jk} instead of \square_{2jk2} .

In a straightforward but tedious fashion, the temperature coefficients of A, B and C may be found to be:

$$T_A^{(1)} = \frac{1}{A} \left\{ \begin{matrix} \square_{11} T_{\square_{11}}^{(1)} + \square_{22} T_{\square_{22}}^{(1)} + \square_{33} T_{\square_{33}}^{(1)} \end{matrix} \right\} \quad (45)$$

$$T_B^{(1)} = \frac{1}{B} \left\{ \begin{matrix} \square_{11} \square_{22} T_{\square_{11}}^{(1)} + T_{\square_{22}}^{(1)} + \square_{22} \square_{33} T_{\square_{22}}^{(1)} + T_{\square_{33}}^{(1)} \\ + \square_{33} \square_{11} T_{\square_{33}}^{(1)} + T_{\square_{11}}^{(1)} - 2 \square_{23}^2 T_{\square_{23}}^{(1)} \\ - 2 \square_{13}^2 T_{\square_{13}}^{(1)} - 2 \square_{12}^2 T_{\square_{12}}^{(1)} \end{matrix} \right\} \quad (46)$$

$$T_D^{(1)} = \frac{1}{D} \left\{ \begin{matrix} \square_{11} T_{\square_{11}}^{(1)} \square_{23}^2 - \square_{22} \square_{33} + 2 \square_{23} T_{\square_{23}}^{(1)} \square_{11} \square_{23} - \square_{12} \square_{13} \\ + \square_{22} T_{\square_{22}}^{(1)} \square_{31}^2 - \square_{33} \square_{11} + 2 \square_{31} T_{\square_{31}}^{(1)} \square_{22} \square_{31} - \square_{23} \square_{21} \\ + \square_{33} T_{\square_{33}}^{(1)} \square_{12} - \square_{11} \square_{22} + 2 \square_{12} T_{\square_{12}}^{(1)} \square_{33} \square_{12} - \square_{31} \square_{32} \end{matrix} \right\} \quad (47)$$

The last step in this derivation of the first order temperature coefficient of frequency is to relate the temperature coefficients of \square_{ij} to those of the elastic, piezoelectric and dielectric constants. This is done using equation (44). We shall assume that the temperature variation of the piezoelectric and dielectric constants can be neglected compared to that of the elastic constants. Thus, from (44), we have in this approximation:

$$T_{\square_{jk}}^{(1)} = \frac{\square_{jk}}{C_{2jk2}} T_C^{(1)} \quad (48)$$

Let us summarize these results. We have seen how the first order temperature coefficient of the relative frequency difference function may be calculated from the material constants and from the first order temperature coefficients of the elastic constants and the coefficients of thermal expansion. The steps in this calculation are straightforward but algebraically tedious. The calculation of the second and third order temperature coefficients of frequency in terms of the coefficients of thermal expansion and the elastic constants follows the same procedure and will not be done here. (Kahan [1982], Ballato [1977]).

The temperature coefficients of the elastic constants and the coefficients of thermal expansion depend on the orientation angles of the quartz plate with respect to the crystalline axes. This clearly implies that the frequency temperature coefficients depend on these orientation angles. Thus, we need to know how to calculate the temperature coefficients of a particular plate given those in the crystalline axes. Therefore, we need to determine the transformation properties of the temperature coefficients. We will consider a general tensor of order n , denoted by $g_{i_1, \dots, i_n}(T)$ where we have explicitly included the temperature dependence. Now, for any temperature T , the transformation between any 2 coordinate systems is specified by:

$$g_{j_1, \dots, j_n}(T) = x_{j_1, k_1} \dots x_{j_n, k_n} g'_{k_1, \dots, k_n}(T) \quad (49)$$

where x_{ij} is the coordinate transformation from the primed to the unprimed axes. We therefore have:

$$\begin{aligned} \Delta g_{j_1, \dots, j_n}(T) &= g_{j_1, \dots, j_n}(T) - g_{j_1, \dots, j_n}(T_0) \\ &= x_{j_1, k_1} \dots x_{j_n, k_n} \Delta g'_{k_1, \dots, k_n}(T) \end{aligned} \quad (50)$$

Now, the temperature expansions in the 2 coordinate systems may be written:

$$\Delta g_{i_1, \dots, i_n}^{(T)} = g_{i_1, \dots, i_n}^{(T_0)} \left[\sum_{j=1} T_{g_{i_1, \dots, i_n}}^{(j)} (T-T_0)^j \right] \quad (51)$$

and for the primed axes:

$$\Delta g'_{k_1, \dots, k_n}^{(T)} = g'_{k_1, \dots, k_n}^{(T_0)} \left[\sum_{j=1} T_{g'_{k_1, \dots, k_n}} (T-T_0)^j \right] \quad (52)$$

(In (51) and (52), there is no implied summation.)

Combining (50), (51) and (52), and equating like powers of $(T-T_0)$, we obtain the following relation between the temperature coefficients in the two coordinate systems:

$$T_{g_{i_1, \dots, i_n}}^{(j)} = \frac{1}{g_{i_1, \dots, i_n}} x_{i_1, k_1} \dots x_{i_n, k_n} T_{g'_{k_1, \dots, k_n}}^{(j)} \quad (53)$$

Note that in this formula there is no implied summation over the indices i_1, \dots, i_n on the right-hand side. Using the transformation rule (53), the temperature coefficients of the elastic constants (a fourth rank tensor) for a doubly rotated plate can be calculated from those in the crystalline coordinate system using the coordinate transformation (28). Similarly, the coefficient of thermal expansion, a vector (i.e., first rank tensor) can also be calculated from (53). The temperature coefficients of frequency can thus be calculated for any doubly rotated quartz plate from those of thermal expansion and the elastic coefficients in the crystalline system. Indeed, the coefficients for the elastic constants in the crystalline system were determined by Bechmann (1956) by transforming the measured coefficients of various standard cuts of quartz.

NUMERICAL RESULTS

We shall now use the theory of the previous two sections to perform calculations for doubly rotated quartz plates. All calculations were performed on the Air Force Geophysics Lab's (AFGL) CDC 6600 computer. The material constants and their temperature coefficients are those given by Bechmann et al (1962).

We begin by depicting in Figure 3 the values of the coupling constants for the three modes of quartz. The coupling constants were calculated from (19) for the doubly rotated cuts. Ballato (1977) presented similar graphs using a different definition of the angles defining the doubly rotated cuts. The curves of Figure 3 are a representative sampling of the coupling constant for doubly rotated cuts. (Due to the symmetry of the quartz crystal lattice, we need only consider ϕ in the range $(0^\circ, 60^\circ)$ and θ in the range $(0^\circ, 90^\circ)$). We shall have frequent recourse to these curves in the following search for cuts with desirable temperature characteristics; for a cut to be useful, it must have a reasonable amount of piezoelectric coupling.

The widespread applications of quartz plates owe much to the early discovery of the AT cut ($\phi = 0^\circ$, $\theta = 35.0931^\circ$). From Figure 3, we see that the AT cut has a relatively high ($\sim 9\%$) coupling constant for the C mode and zero coupling for modes a and b. In Figure 4, we plot the relative frequency difference function (mode C) about the reference temperature $T_0 = 25^\circ\text{C}$ for the temperature range $(-40, 80)$. The graph exhibits the temperature stability that makes the AT cut the preferred choice in many applications. This stability derives from the flatness of the curve in the vicinity of 25°C . This flatness is, of course, a consequence of the derivative vanishing at 25° , or equivalently, the first order temperature coefficient of frequency (for mode C) having a zero at $\phi = 0^\circ$ and $\theta = 35.0931$.

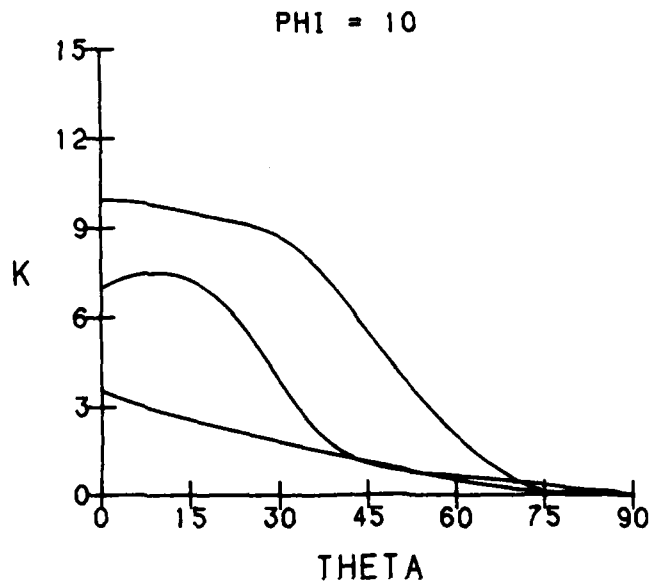
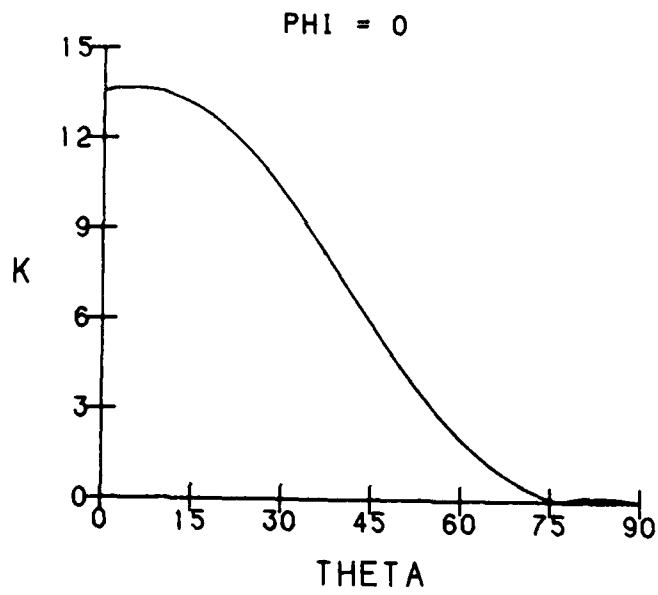


Figure 3: COUPLING CONSTANTS

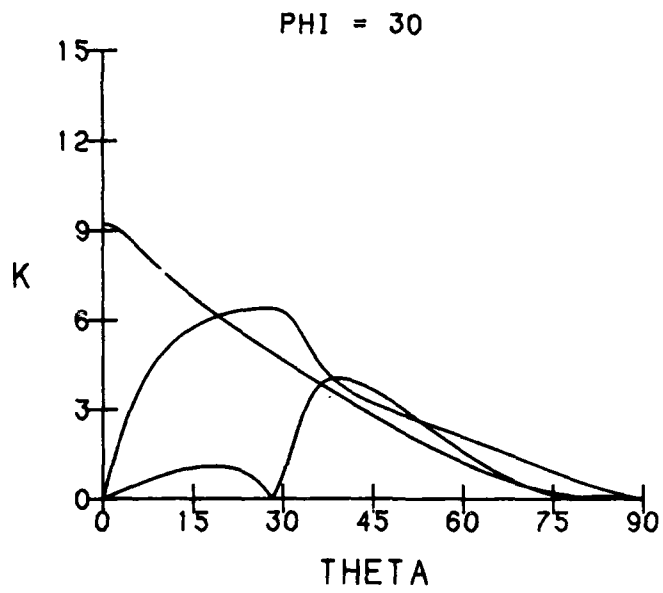
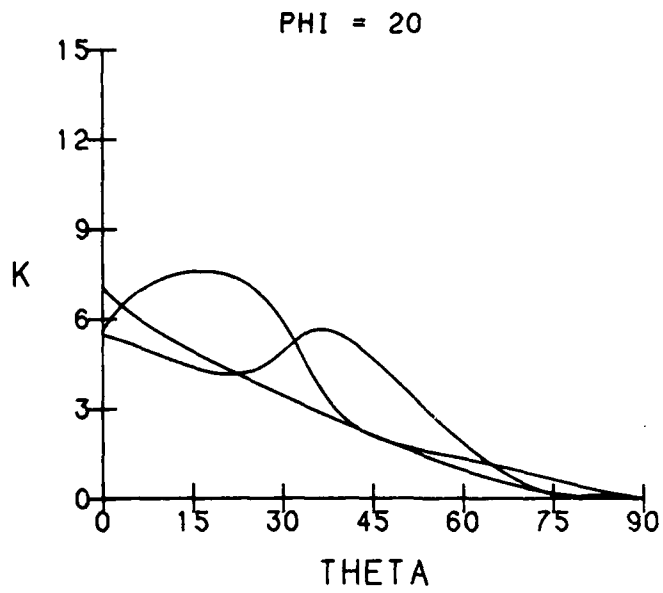


Figure 3: COUPLING CONSTANTS (continued)

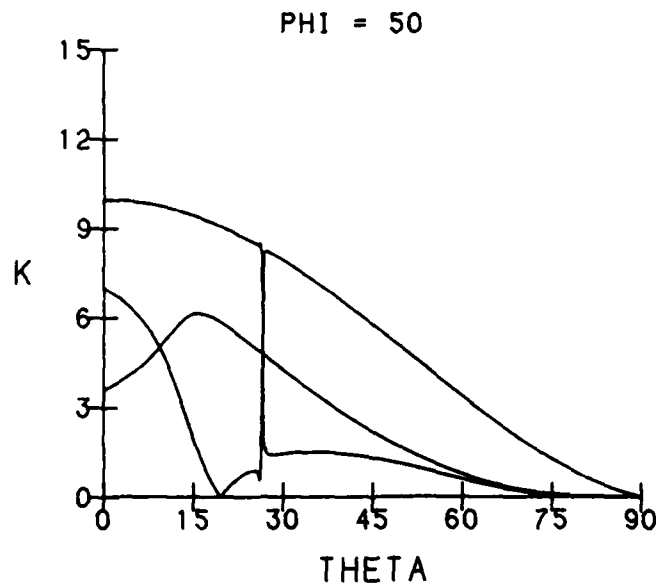
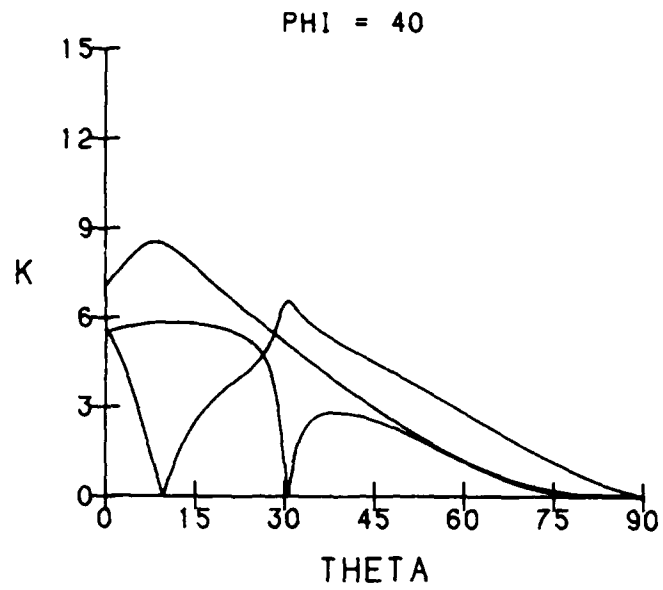


Figure 3: COUPLING CONSTANTS (continued)

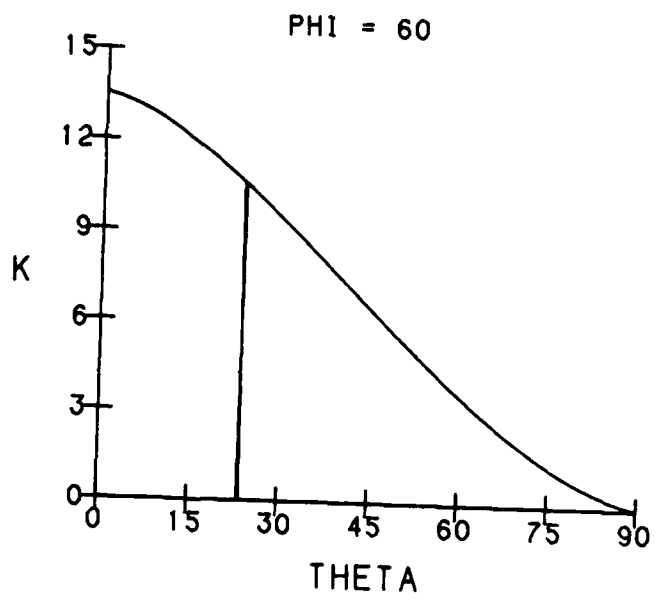


Figure 3: COUPLING CONSTANTS (continued)

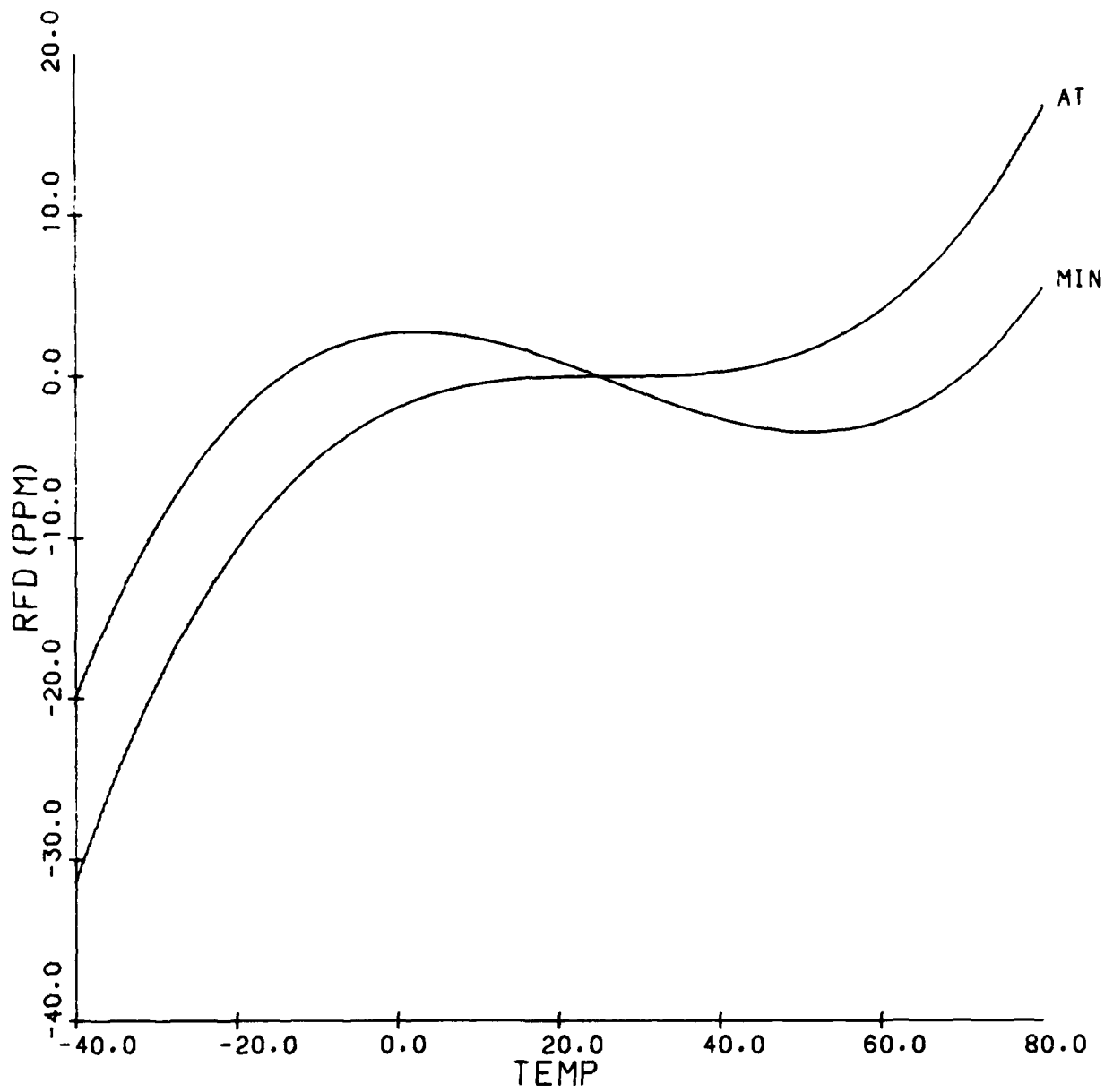


Figure 4: RFD CURVE FOR AT CUT

Another of the commonly used cuts is the BT cut, defined by $\phi = 60^\circ$ and $\theta = 48.9942^\circ$. The relative frequency difference for mode b is displayed in Figure 5. Like the AT cut, the BT cut owes its temperature stability to the vanishing of the first order temperature coefficient of frequency. The general shapes of the AT and BT frequency curves are, however, very different. The BT curve is parabolic; it is the second order temperature coefficient which dominates the cubic frequency expansion. In contrast, the AT curve is clearly of cubic form. These 2 general forms, i.e., parabolic and cubic, are representative of the shapes of the relative frequency difference curves for arbitrary ϕ and θ .

The common feature of the AT and BT cuts that makes these cuts useful is the vanishing of the first order temperature coefficients. Bechmann et al (1962) mapped out the locations of the zeroes in the first order temperature coefficient. In Figure 6, the loci of zeroes is displayed for modes b and c (mode a has no zeroes). This previous work represents a search for quartz cuts with stable temperature behavior using a very "local" measure of sensitivity. If the first order temperature coefficient vanishes, the changes in frequency due to a small deviation in temperature from 25°C will also be small (order of $(T-T)^2$). However, large temperature deviations may produce large changes in frequency, as is evident for the AT and BT cuts from Figures 4 and 5.

In many applications, the range of temperature variation is too large to rely on a local measure of sensitivity. For these cases, a more "global" measure is required, that is, a measure which takes into account the variations over the entire temperature interval of interest. Furthermore, modern electronic devices are capable of compensating for or correcting small frequency changes; this is accomplished by following a known relative frequency difference curve.

The first "global" measure that we will consider uses an integral measure of temperature sensitivity. Specifically, the measure is the integral of the absolute value of the relative frequency difference from

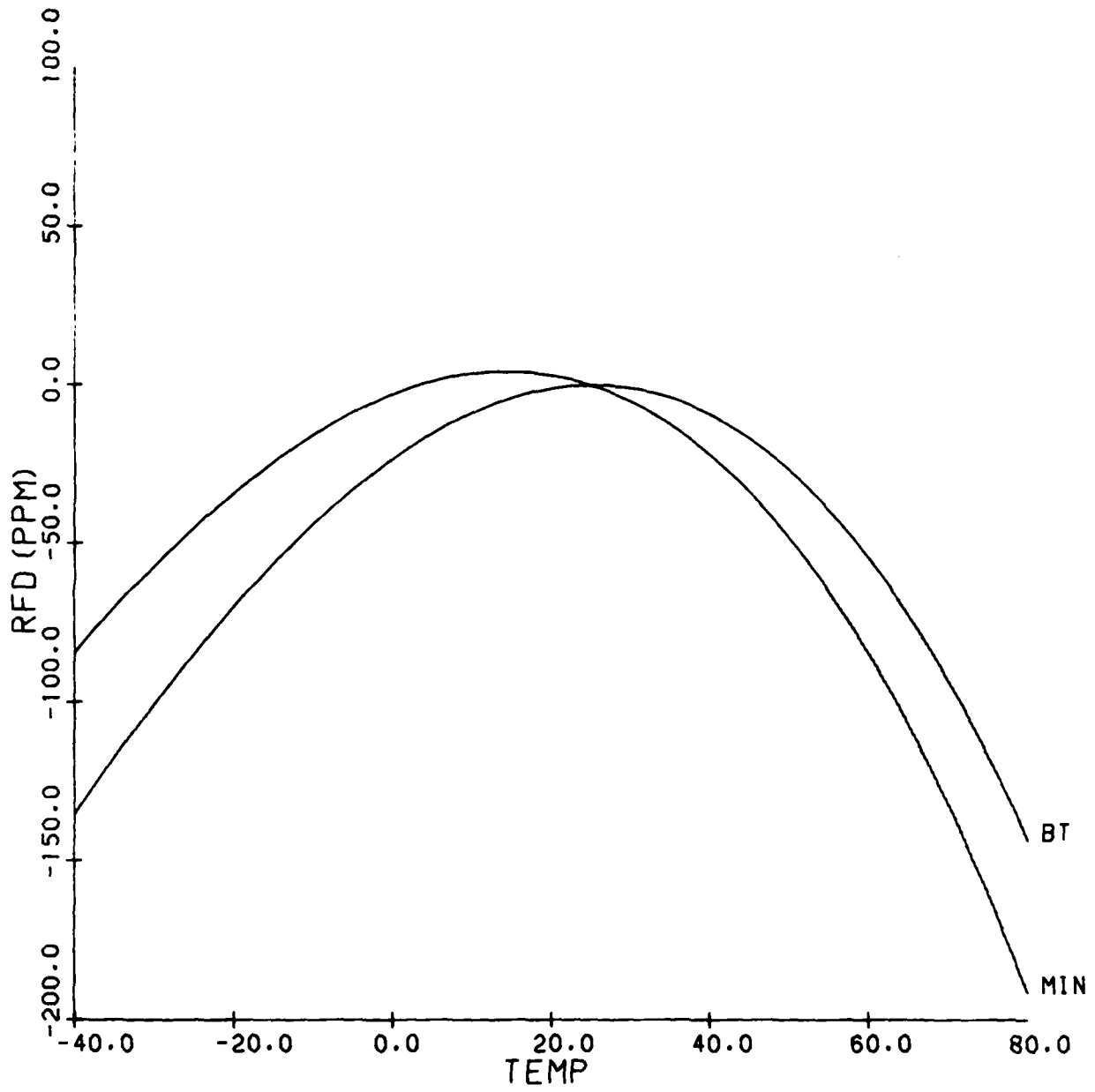


Figure 5: RFD CURVE FOR BT CUT

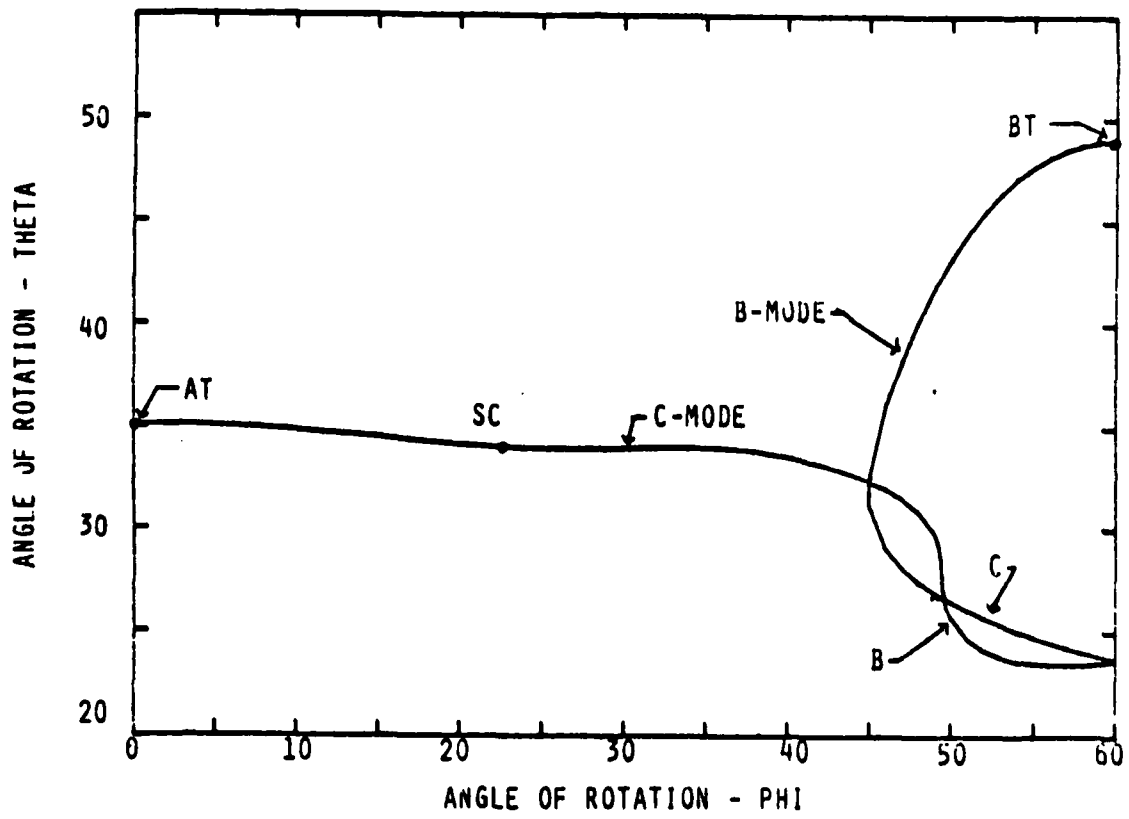


Figure 6: LOCI OF FIRST ORDER ZERO TEMPERATURE COEFFICIENTS

(courtesy of A. Kahan)

-40° to 80° , i.e.,

$$M_1(\phi, \theta) = \int_{-40}^{80} \left| \frac{\Delta f}{f} \right| dT \quad (54)$$

where the notation explicitly displays the dependence of the measure on the cut angles ϕ and θ . In Figure 7, we present the results of the calculations of $M_1(\phi, \theta)$ for the three modes of quartz plates. These curves give us a rough indication of the location and magnitudes of the minima in temperature sensitivity. The minima for mode a are seen to be very weak and will not be considered further. The minima for modes b and c are of reasonable order (i.e., relative magnitude of approximately 100) and warrant further investigation. The actual locations and magnitudes of the b and c mode minima were calculated by minimizing $M_1(\phi, \theta)$ with respect to θ for fixed ϕ . The results, for ϕ in increments of 1° , are given in Figure 8 for mode c and Figure 9 for mode b. The absolute minima for mode c occurs for $\phi = 0^\circ$, while for mode b, it occurs for $\phi = 60^\circ$. It is no coincidence that these are the ϕ -values of the AT and BT cuts, respectively. However, the θ values of the minima do not agree exactly with those of the AT and BT cuts; the minima do not have vanishing first order temperature coefficients. For mode c, the minima occurs at $\phi = 0^\circ$, $\theta = 35.1304^\circ$; for mode b, it occurs at $\phi = 60^\circ$, $\theta = 49.3833^\circ$. The relative frequency difference curves of these minima are given in Figures 4 and 5 along with the corresponding standard cut. The minima for modes b and c thus occur in very close proximity to the zeroes of the first order temperature coefficients. This is, in fact, true of all the minima displayed in Figures 8 and 9. Indeed, if we were to plot the ϕ and θ angles of the minima in Figures 8 and 9, we would produce a curve very similar to Figure 6, the loci of the zeroes of the first order temperature coefficient.

We have seen that the least sensitive cut, with respect to an integral measure is given by mode c. $\phi = 0^\circ$, $\theta = 35.1304^\circ$. The c mode minima is superior by more than a factor of 10 to the b mode minima. In fact, from Figure 8, we see that any c mode minima with $\phi < 50^\circ$ is superior to the b mode minima. However, we must use more than the magnitude of the minimum to compare different cuts effectively. The goal here is to find cuts that

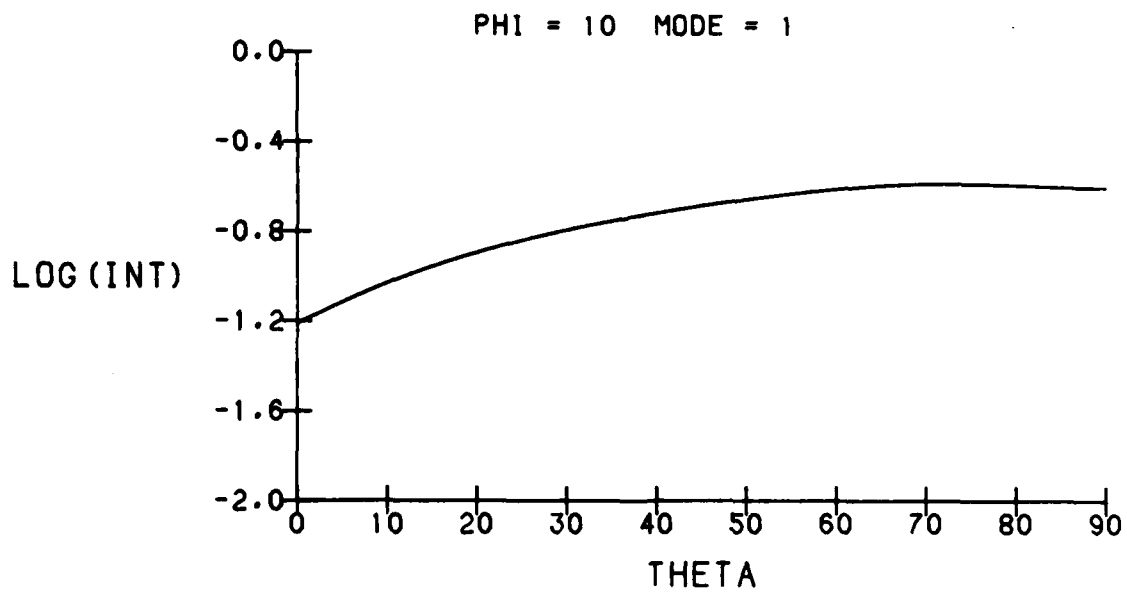
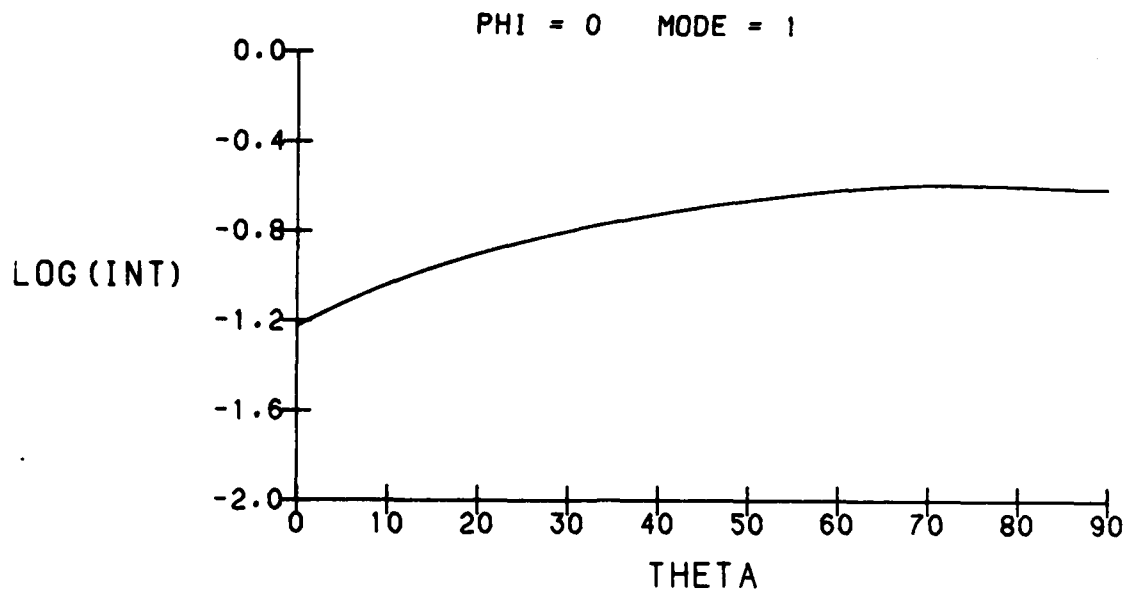


Figure 7: INTEGRAL MEASURE OF TEMPERATURE SENSITIVITY

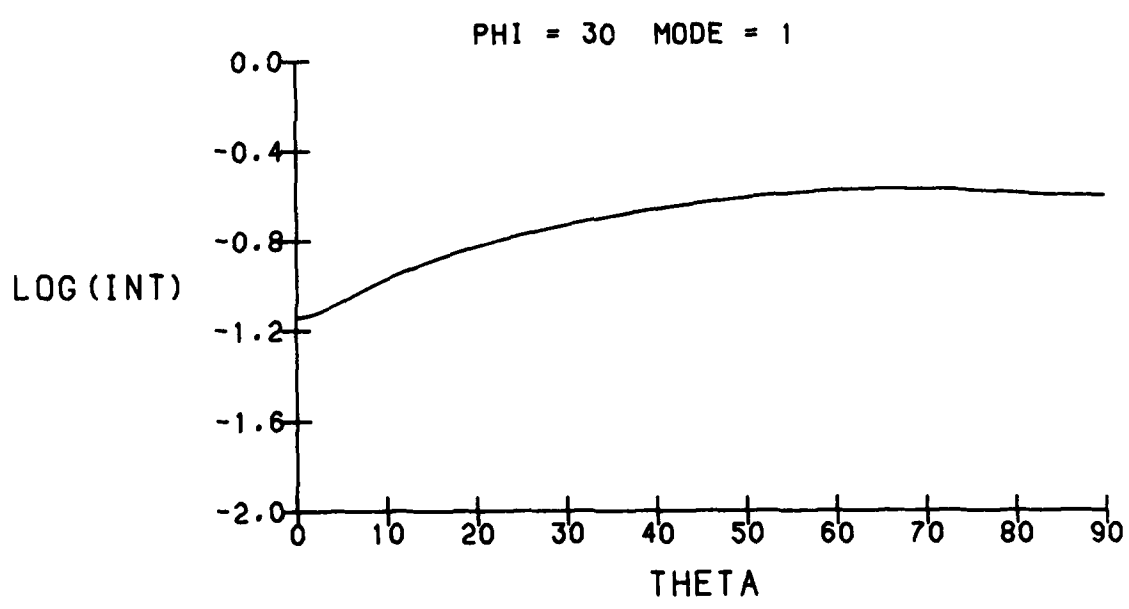
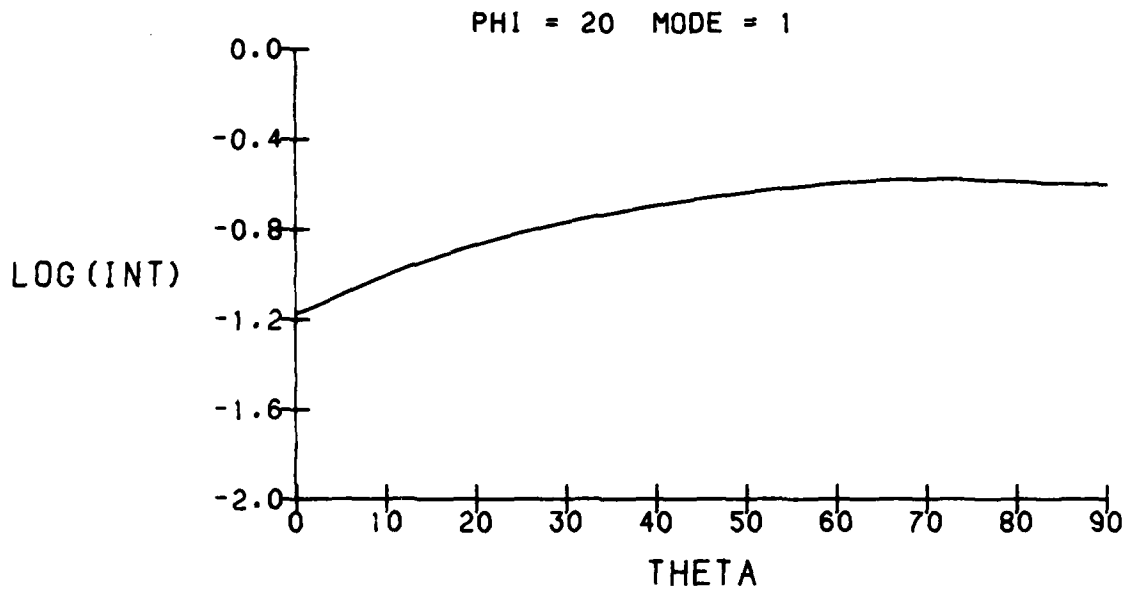


Figure 7: INTEGRAL MEASURE OF TEMPERATURE SENSITIVITY (continued)

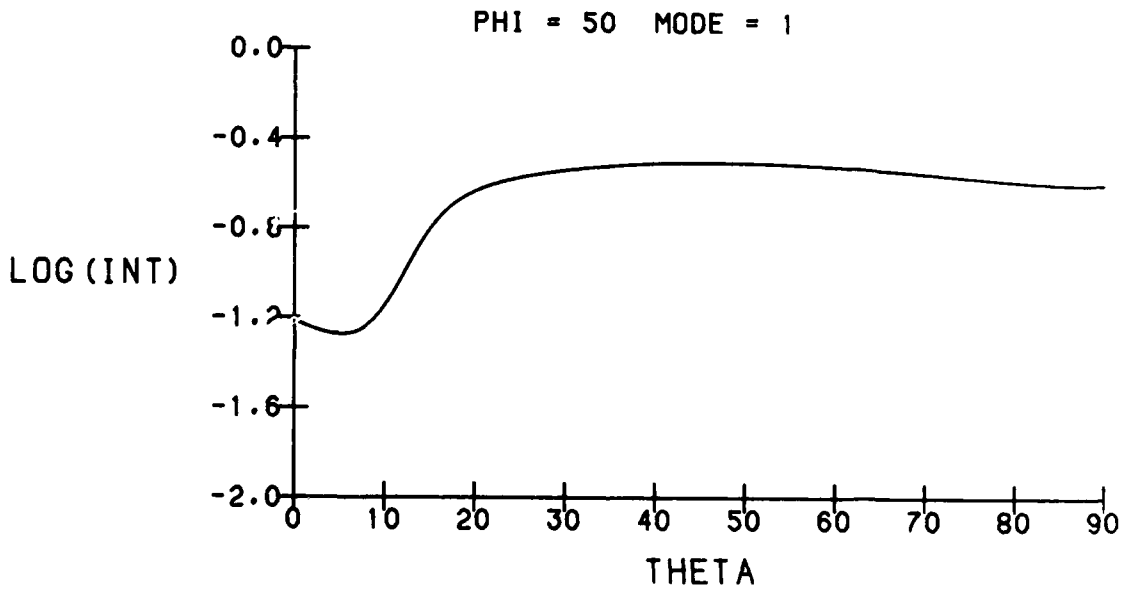
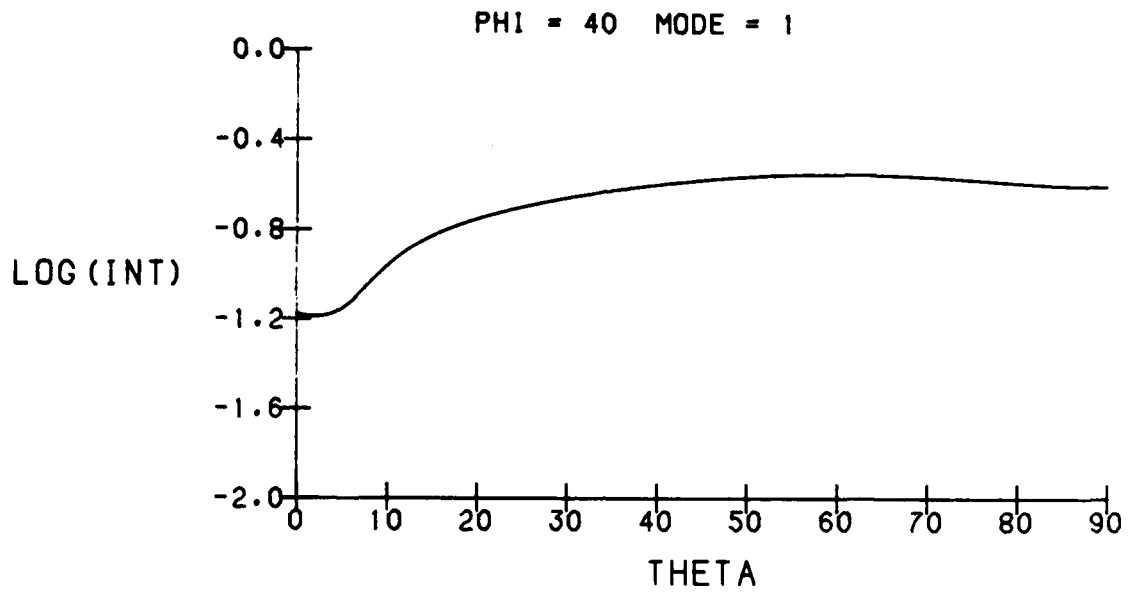


Figure 7: INTEGRAL MEASURE OF TEMPERATURE SENSITIVITY (continued)

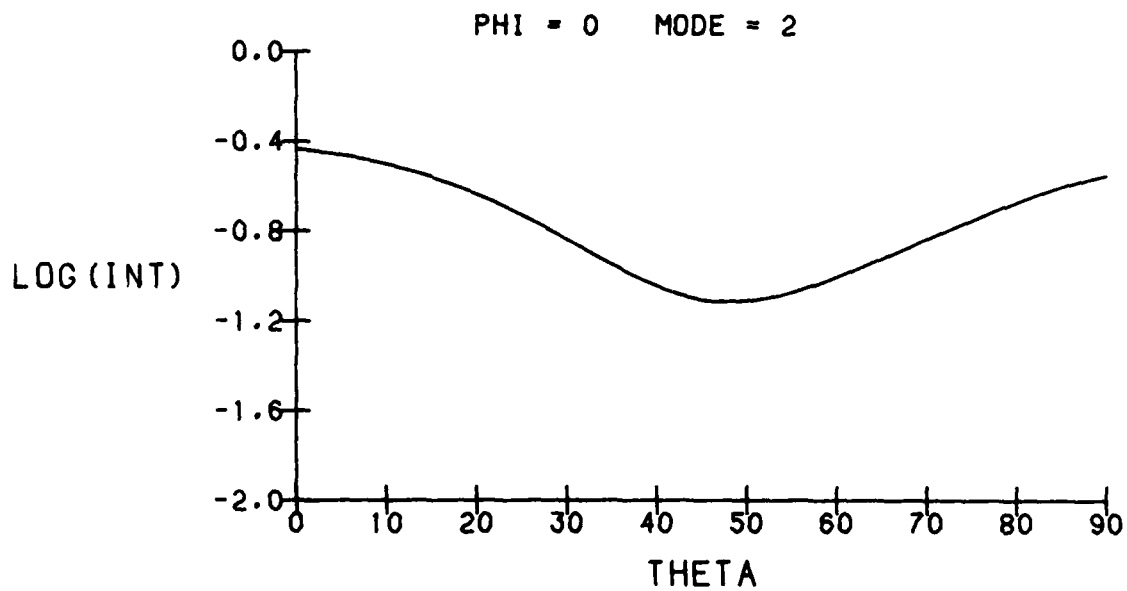
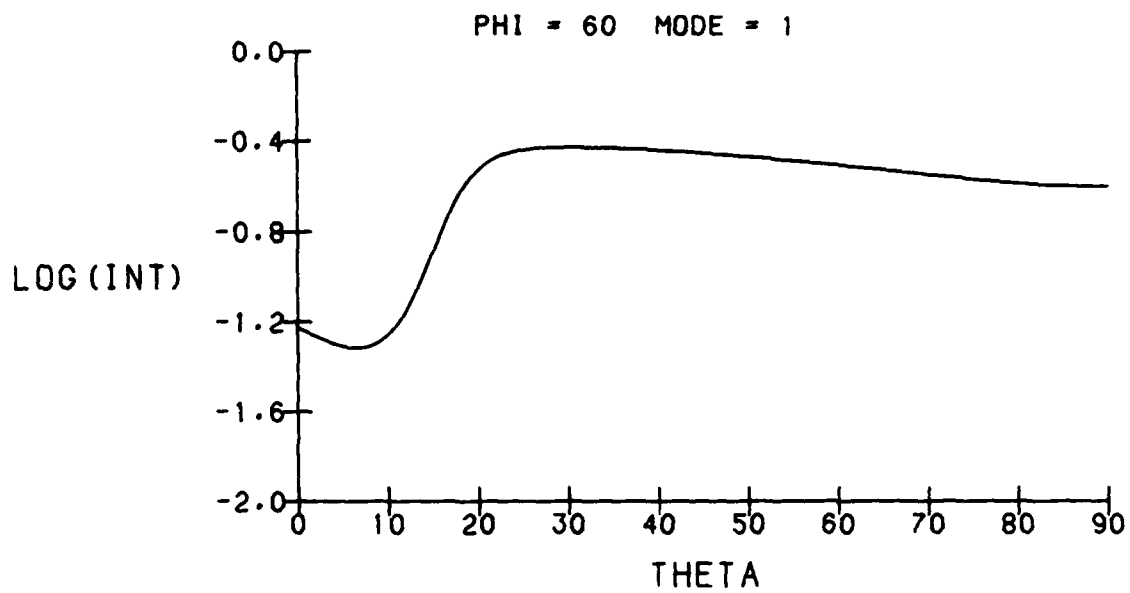


Figure 7: INTEGRAL MEASURE OF TEMPERATURE SENSITIVITY (continued)

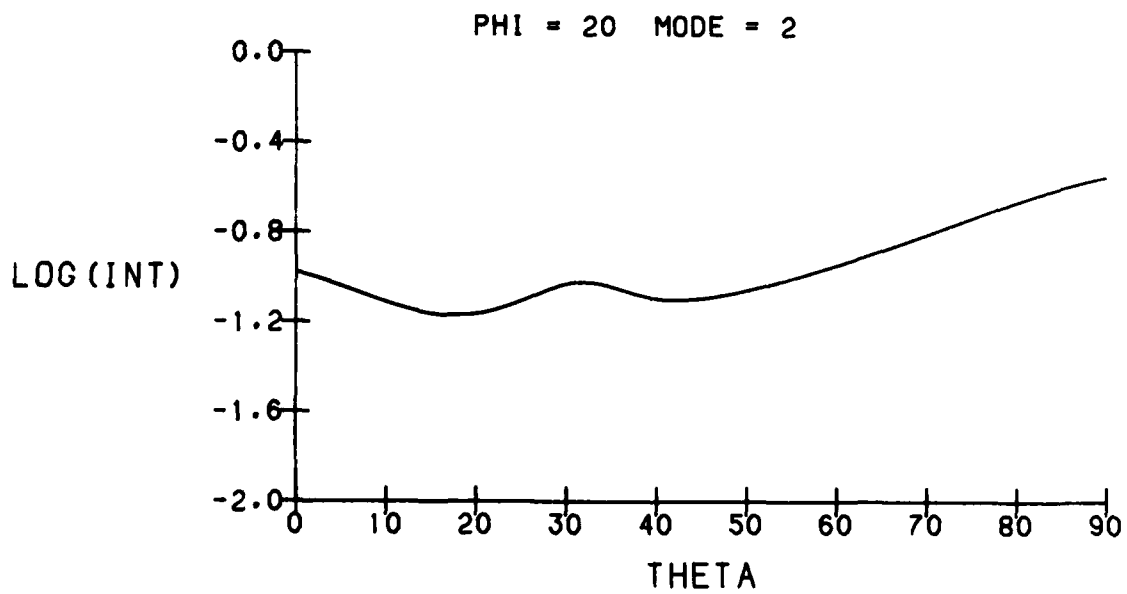
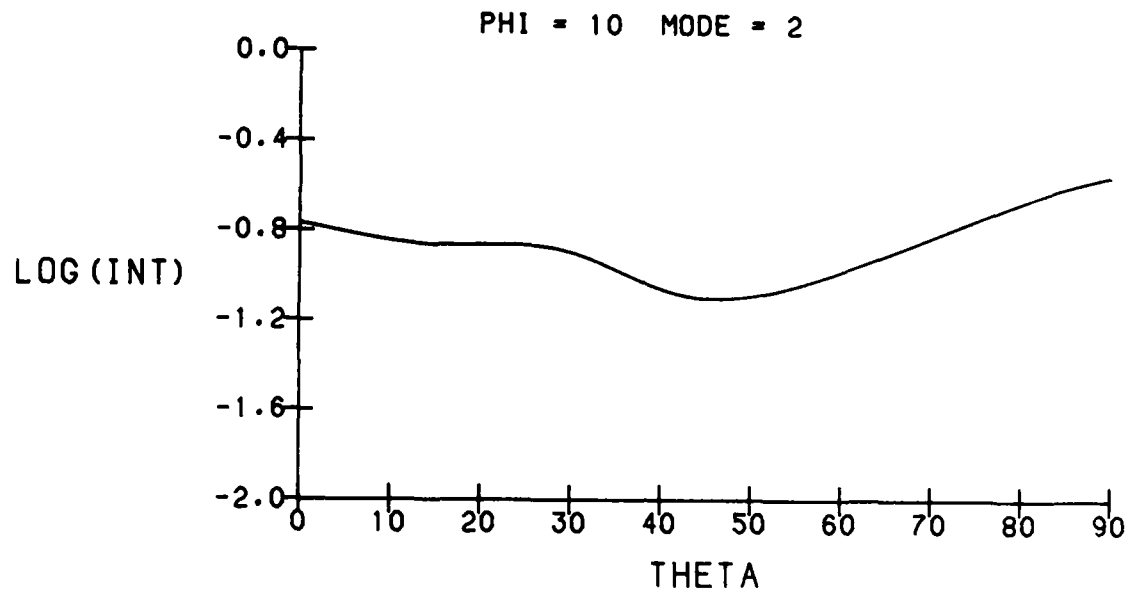


Figure 7: INTEGRAL MEASURE OF TEMPERATURE SENSITIVITY (continued)

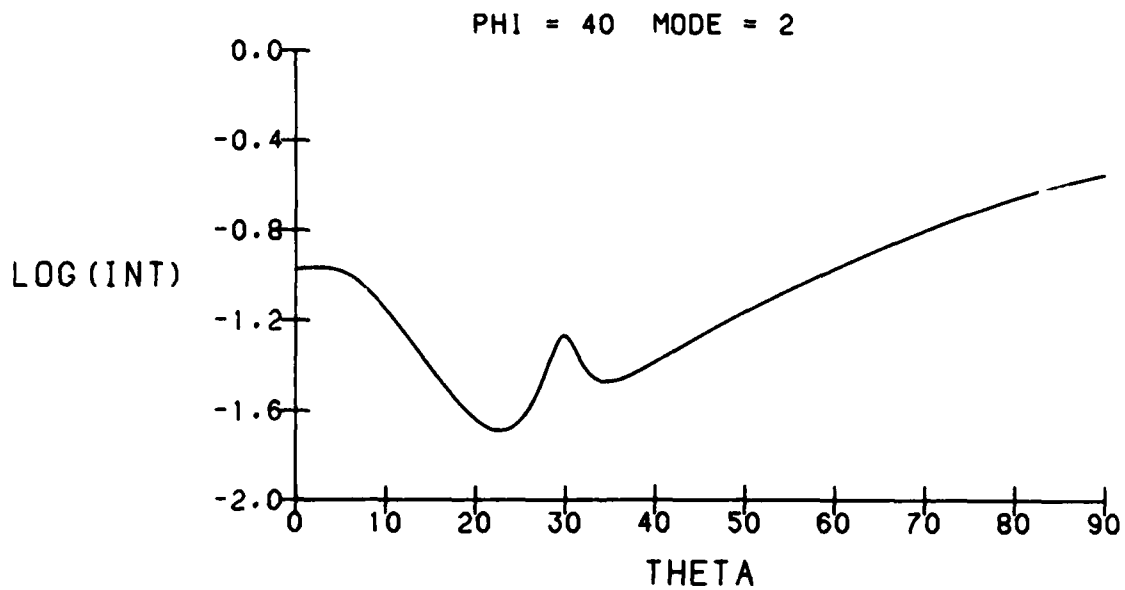
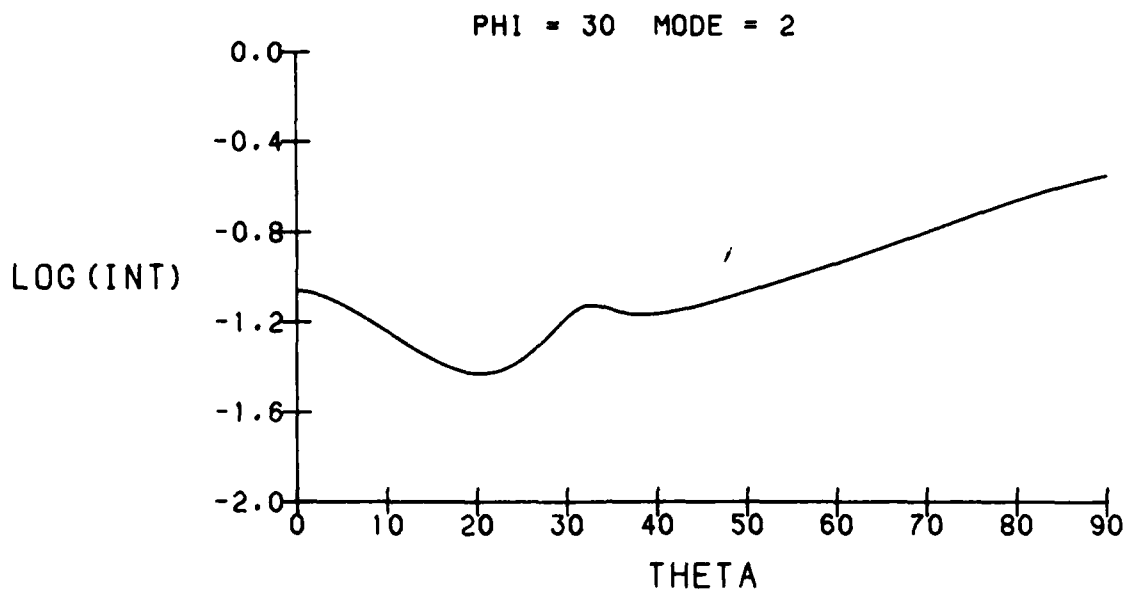


Figure 7: INTEGRAL MEASURE OF TEMPERATURE SENSITIVITY (continued)

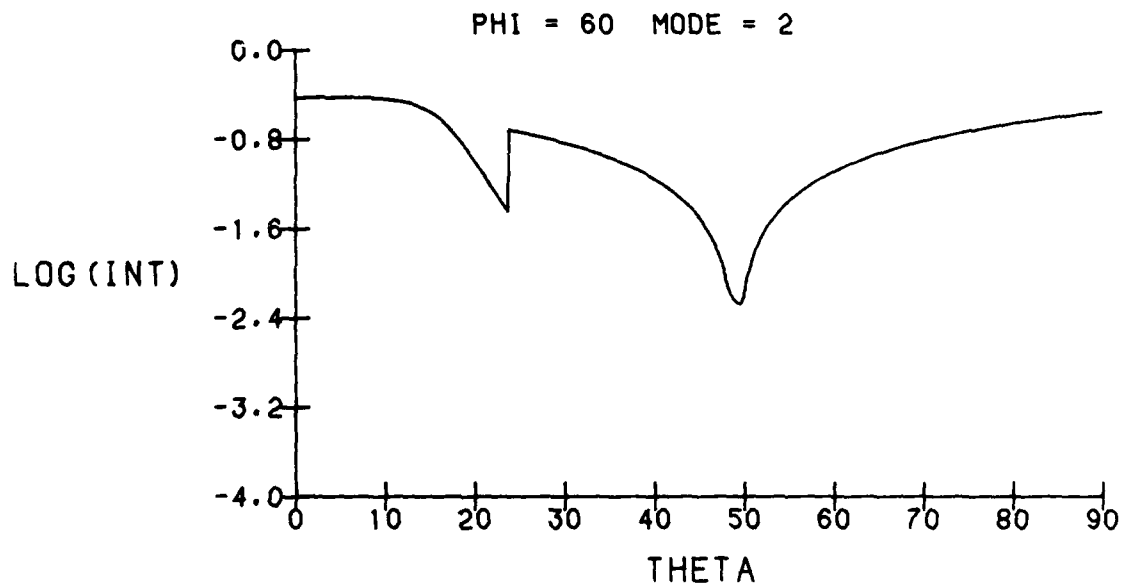
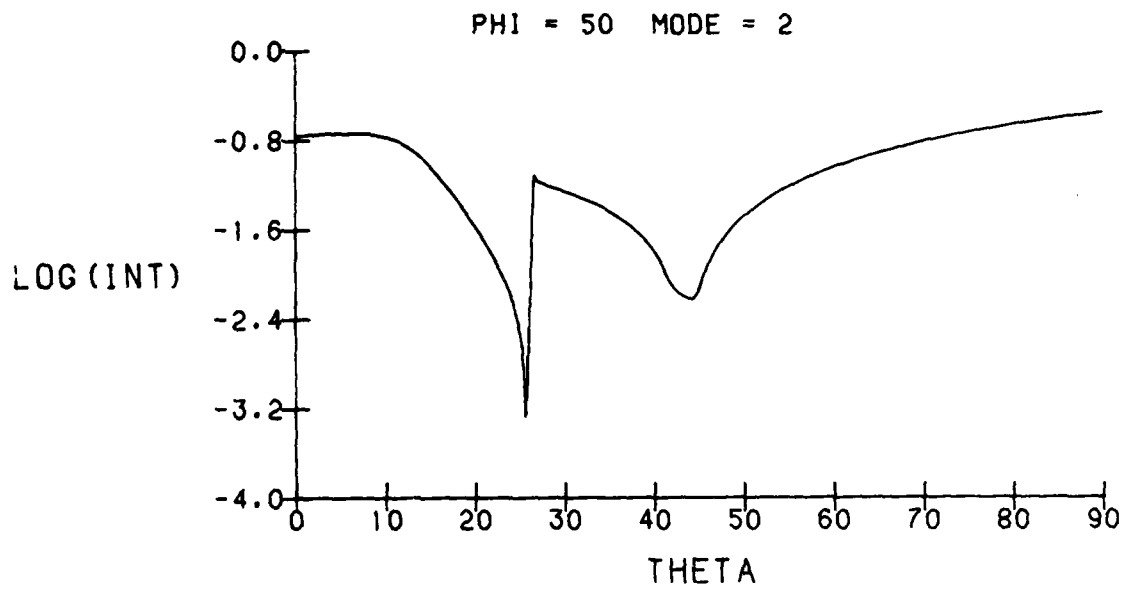


Figure 7: INTEGRAL MEASURE OF TEMPERATURE SENSITIVITY (continued)

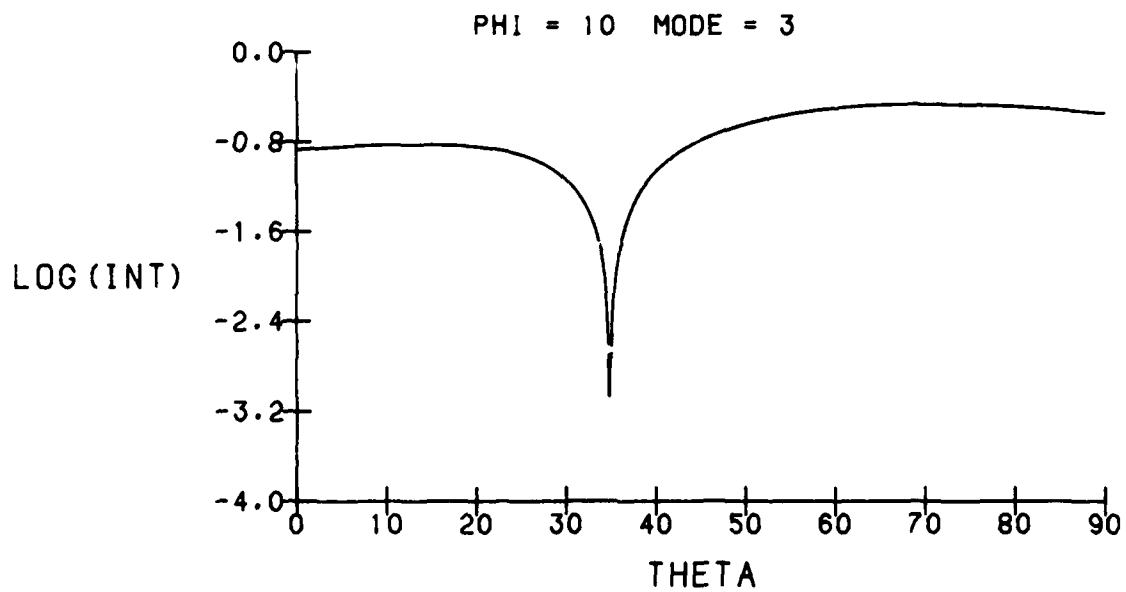
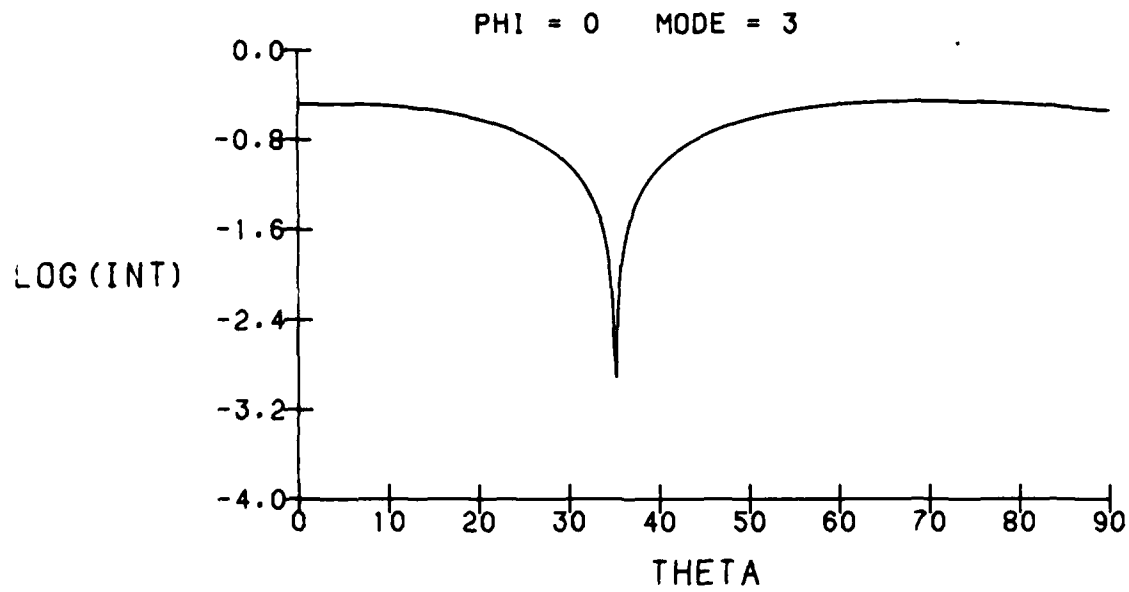


Figure 7: INTEGRAL MEASURE OF TEMPERATURE SENSITIVITY (continued)

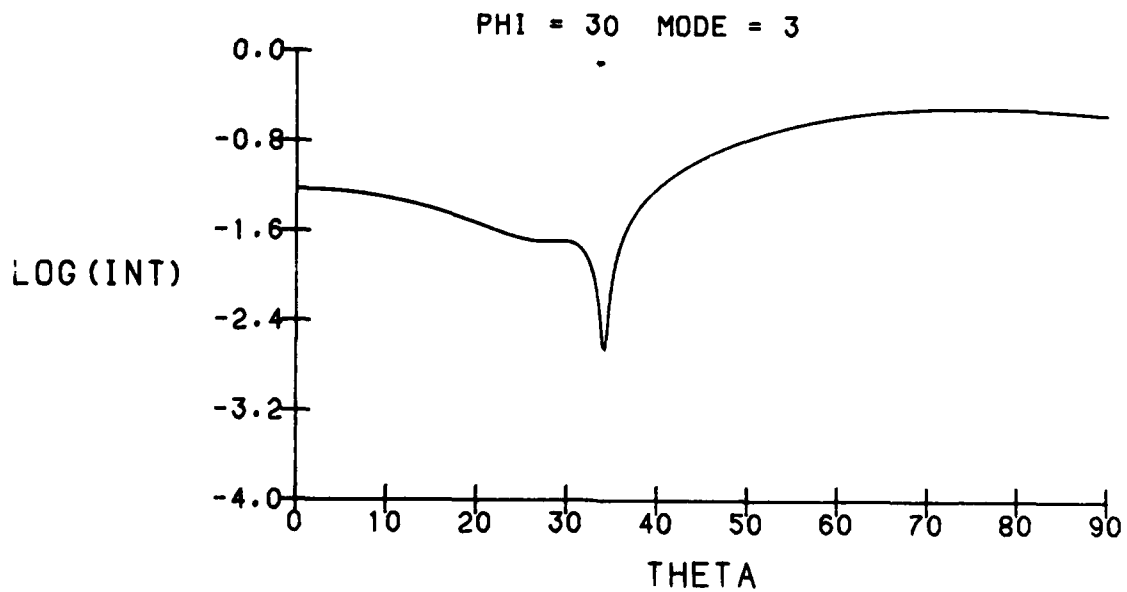
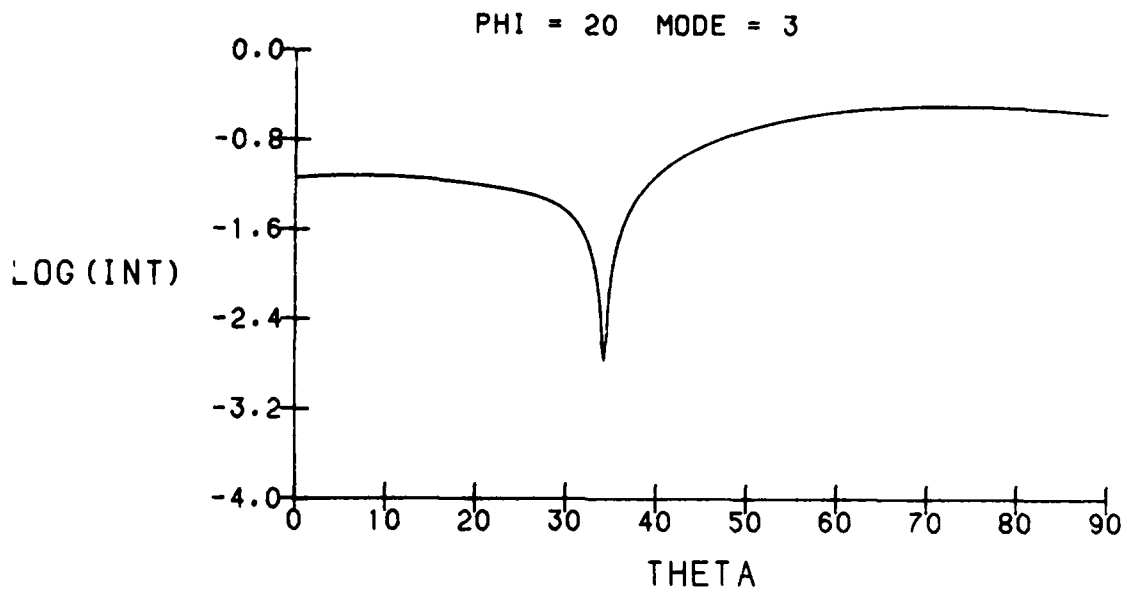


Figure 7: INTEGRAL MEASURE OF TEMPERATURE SENSITIVITY (continued)

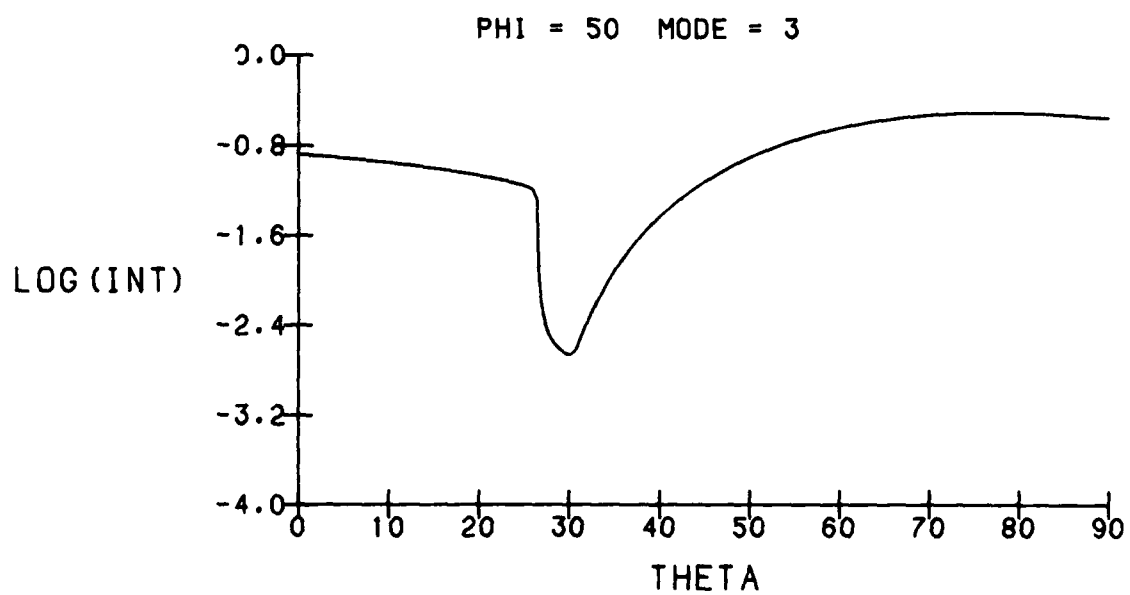
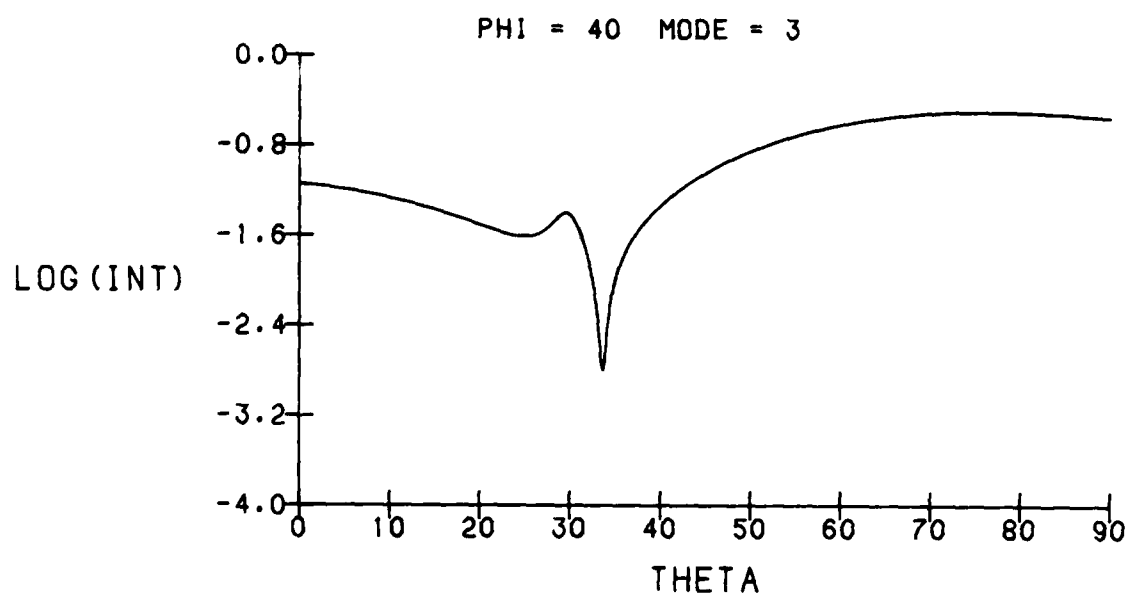


Figure 7: INTEGRAL MEASURE OF TEMPERATURE SENSITIVITY (continued)

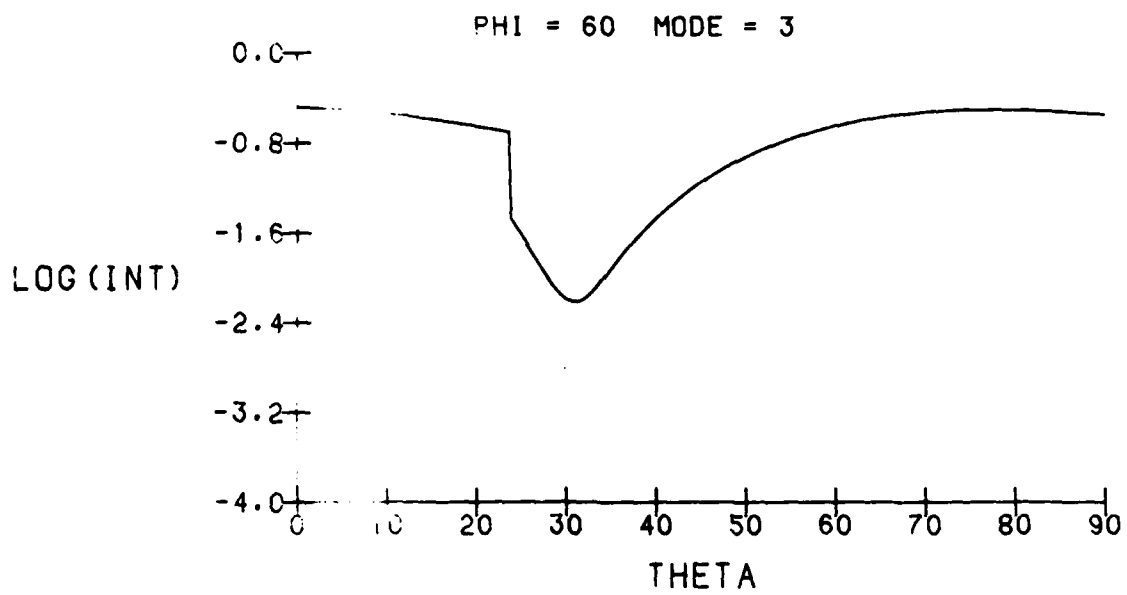


Figure 7: INTEGRAL MEASURE OF TEMPERATURE SENSITIVITY (continued)

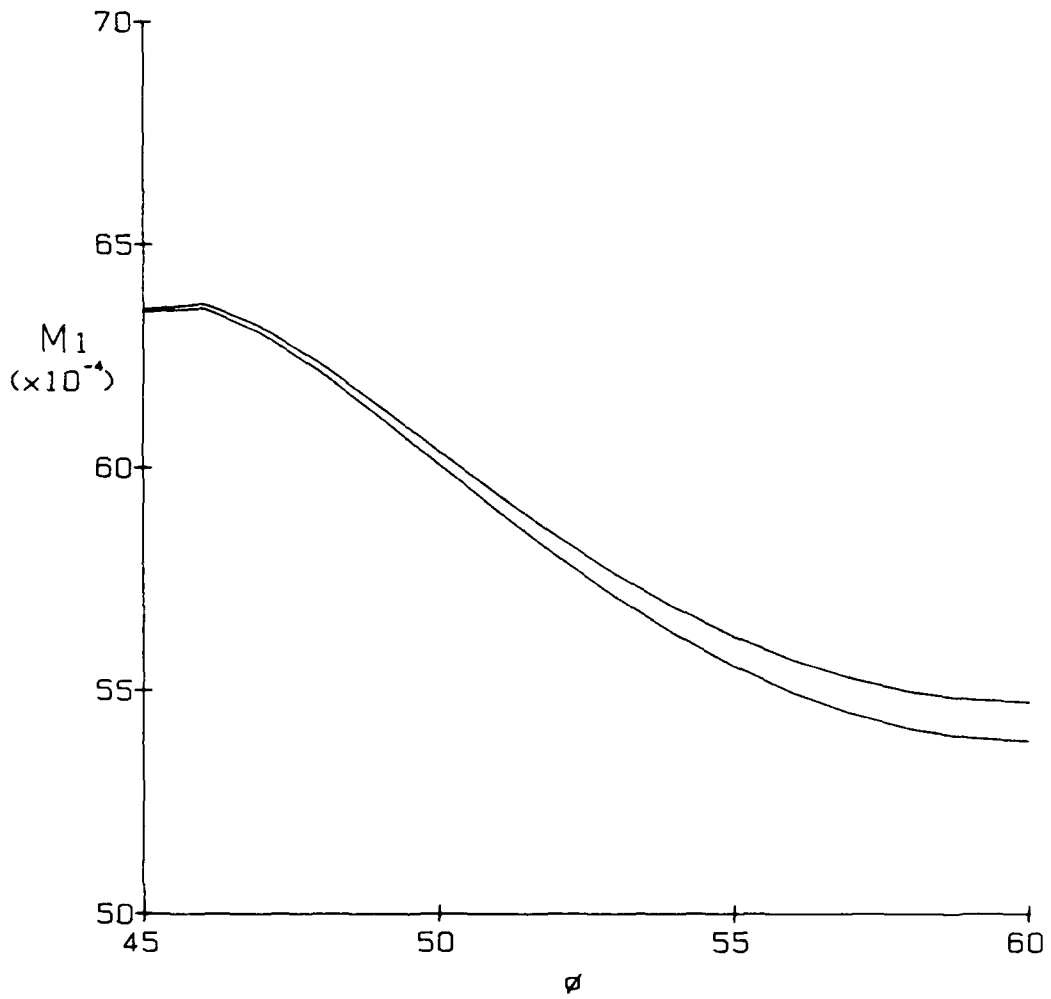


Figure 8: INTEGRAL MINIMA FOR b MODE
(MINIMA WITH RESPECT TO θ).

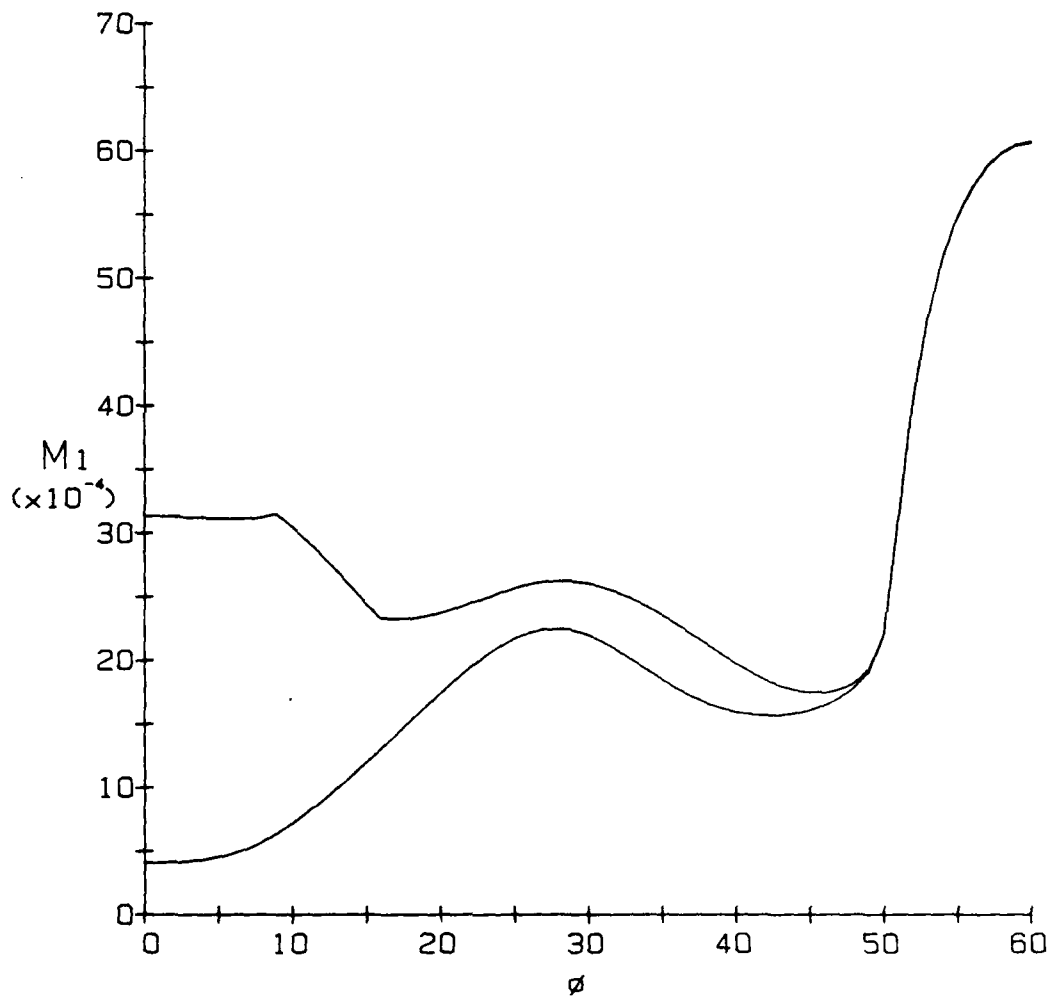


Figure 9: INTEGRAL MINIMA FOR C MODE
(MINIMA WITH RESPECT TO θ).

are useful and so various practical criteria must also be considered. The first such criterion we will treat is angle stability: for a minimum to be useful, the temperature sensitivity must not change greatly if the angle is changed slightly. Such angular deviations or errors are likely to occur in the manufacturing process. To evaluate this angular stability numerically, we will consider the effect of errors in the θ value of $10'$ (0.167°). For the minima in Figures 8 and 9, the integral measure was also calculated for the same ϕ value, but with θ changed by $+10'$ and $-10'$. The upper curves in Figures 8 and 9 represent the larger of the integrals for the $+10'$ and $-10'$ cases. It is thus a reasonable measure of angular stability. The deficiencies of the $\phi = 0^\circ$, mode c minimum are apparent: it is highly sensitive to small changes in angle. Indeed, a $10'$ change in θ produces a relative change in the integral measure of several hundred percent. This effect of small θ errors on the relative frequency difference is demonstrated in Figure 10. This angular instability is also demonstrated by the very sharp minima for mode c at $\phi = 0^\circ$ given in Figure 7. In contrast, the minima for $\phi = 60^\circ$ and mode b is seen in Figure 7 to be somewhat rounded and not as abrupt. This is borne out by Figure 9, where a $10'$ deviation in θ produces a relative change of about 2% in the temperature measure. Thus, the b mode minimum is very stable. This stability is exhibited by the relative frequency difference curves in Figure 11. Because of this extreme angular instability, the $\phi = 0^\circ$, c mode minimum cannot be practically considered. However, as mentioned previously, there are other c mode minima which have smaller minima than the b mode. Taking into account angular stability, inspection of Figure 8 reveals two candidates for useful c mode cuts: $\phi = 27^\circ$ ($\theta = 34.0644^\circ$) and $\phi = 42^\circ$ ($\theta = 33.2906^\circ$). The effect of theta errors on the relative frequency difference for these cuts is depicted in Figures 12 and 13.

A second practical criterion is, as mentioned earlier, the piezoelectric coupling constant. The mode b minimum ($\phi = 60^\circ$, $\theta = 49.3833^\circ$) is very close to the standard BT cut ($\phi = 60^\circ$, $\theta = 48.9942^\circ$). Thus, we would expect this minimum to satisfy most practical criteria with regard to the coupling constant. For this reason, we will restrict the calculations of coupling to the mode c minima, especially the two mentioned

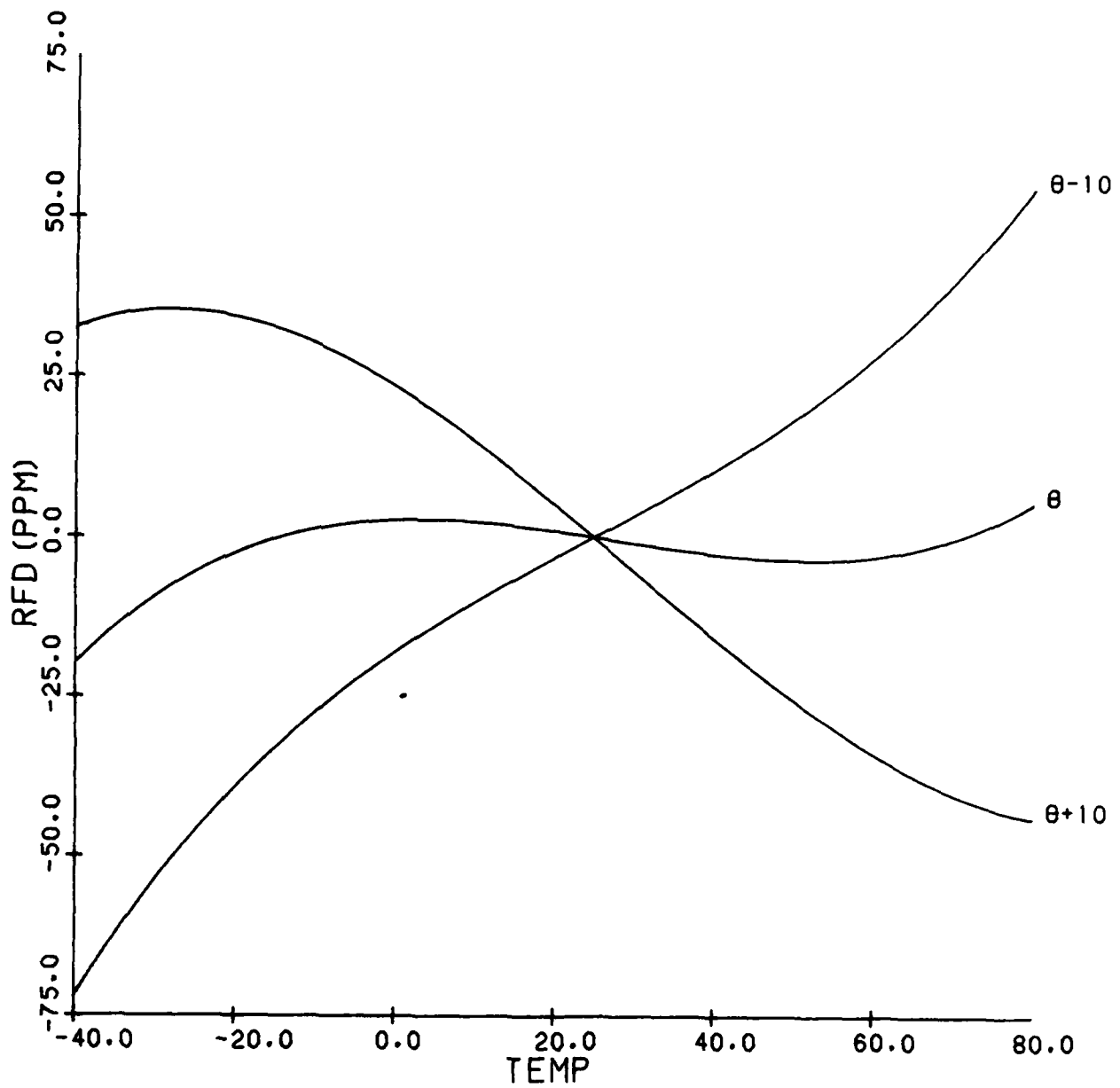


Figure 10: RFD CURVES FOR C MODE INTEGRAL MINIMUM WITH

$$\phi = 0, \theta = 35.1304 \text{ AND } \theta \pm 10'$$

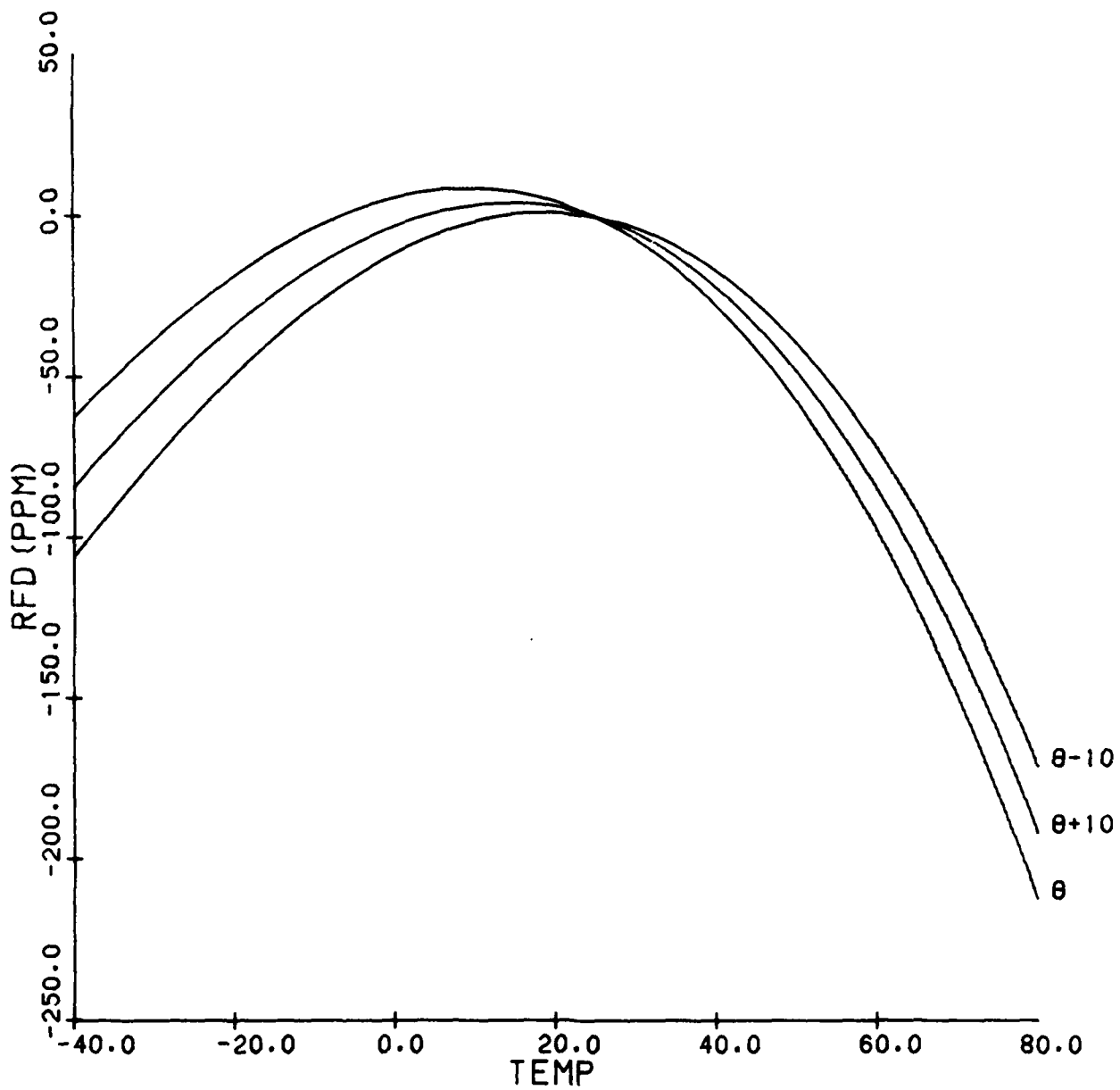


Figure 11: RFD CURVES FOR B MODE INTEGRAL MINIMUM WITH

$$\phi = 60, \theta = 49.3833 \text{ AND } \theta \pm 10'$$

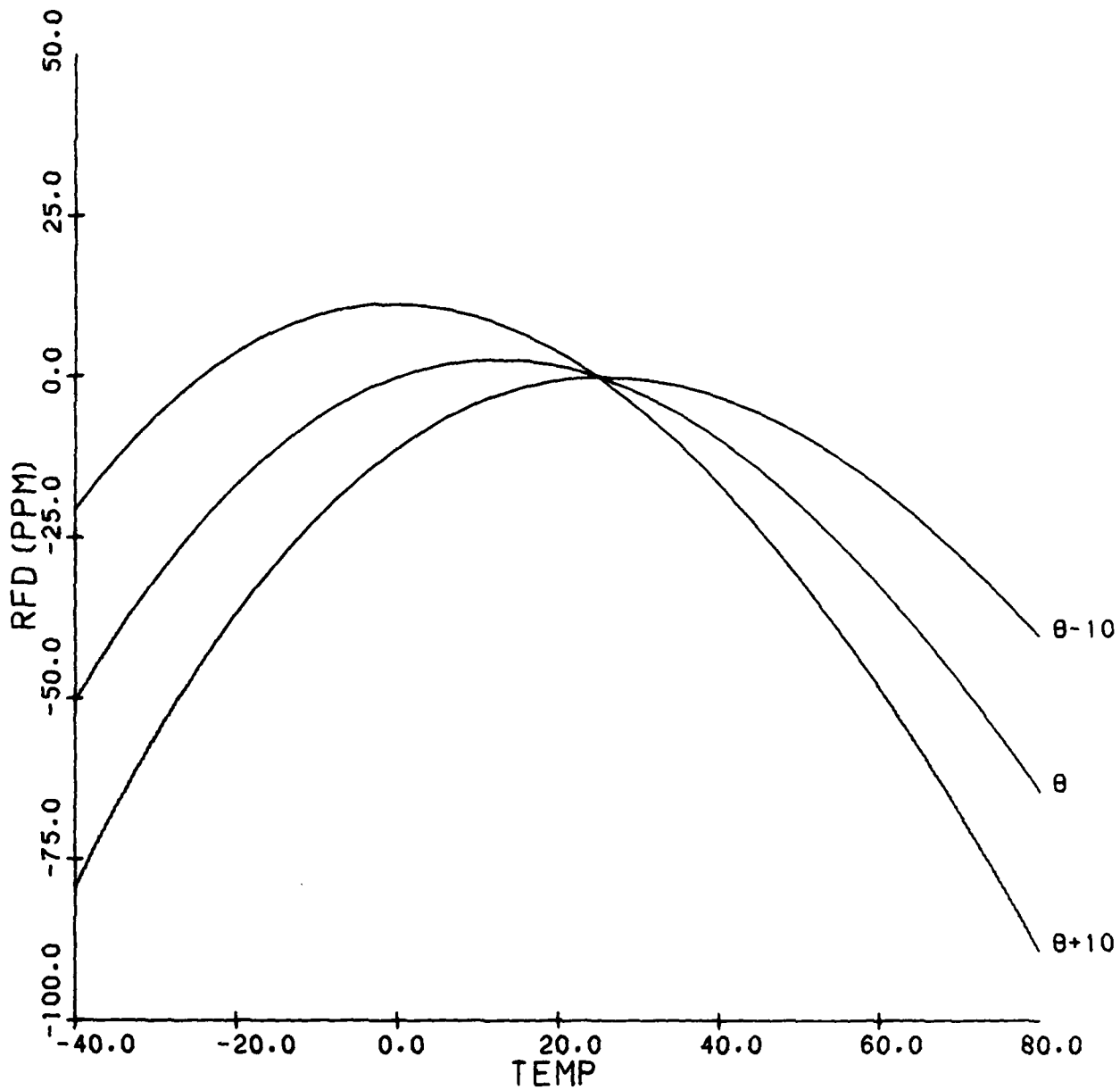


Figure 12: RFD CURVES FOR C MODE INTEGRAL MINIMUM WITH

$$\phi = 27, \theta = 34.0644 \text{ AND } \theta \pm 10'$$

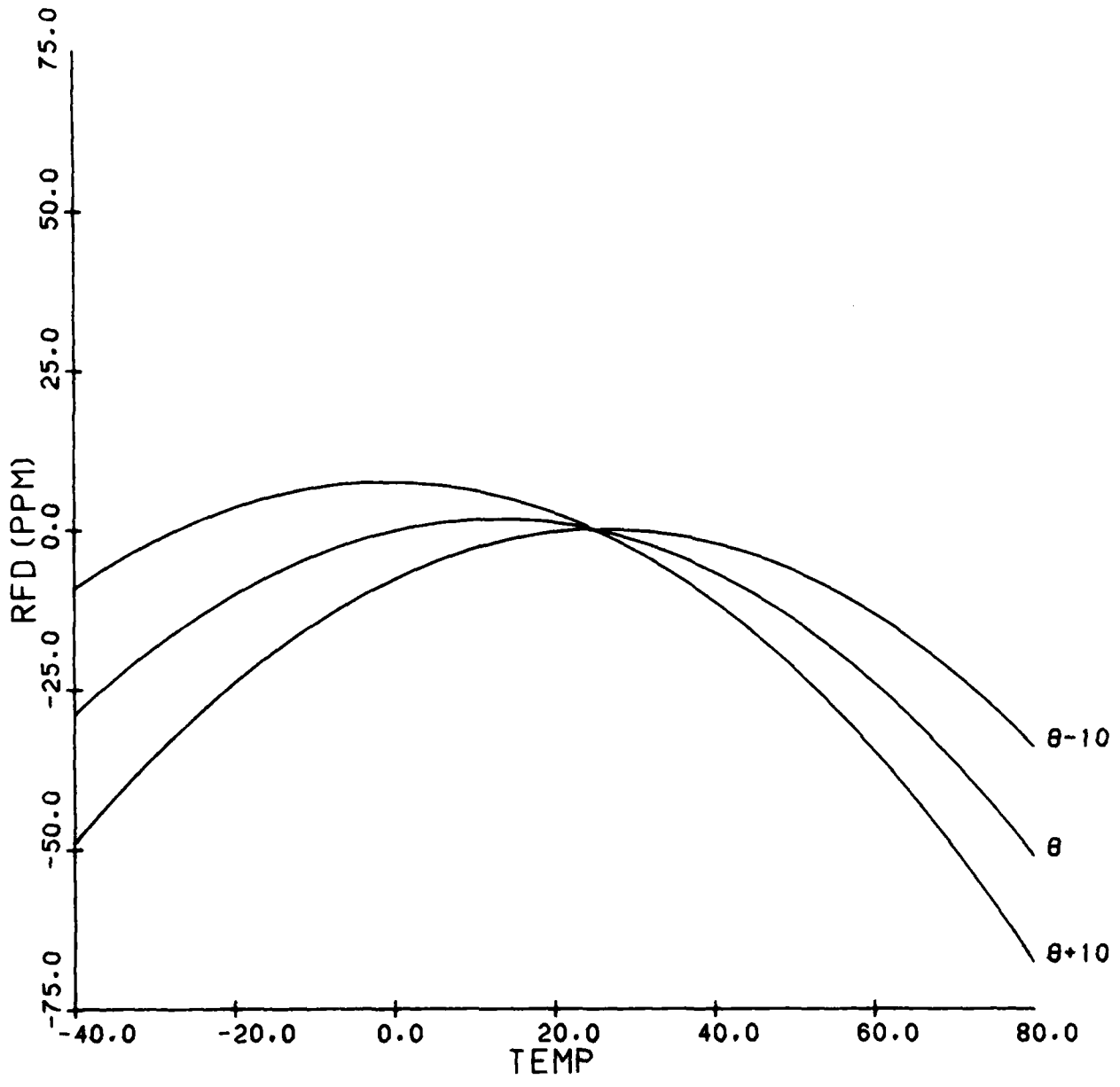


Figure 13: RFD CURVES FOR C MODE INTEGRAL MINIMUM WITH

$$\phi = 42, \theta = 33.2906 \text{ AND } \vartheta \pm 10'$$

above. In Figure 14, we display the results of the calculation of the coupling constant for mode c along the mode c minimum curve of Figure 8. This graph shows that for $\phi = 27^\circ$, the minimum has a coupling constant of about 3.7%, while it is approximately 2.2% for the $\phi = 42^\circ$ minimum. By comparison, the mode b minimum ($\phi = 60^\circ$) has larger piezoelectric coupling, approximately 5.5% (see Figure 3).

The last practical criterion we will consider pertains to the separation in frequency of the three modes. From equation (27) we have that the fundamental frequencies of the three modes may be written as:

$$f_n = \frac{1}{4h\sqrt{\rho}} \sqrt{\lambda_n} \quad . \quad (55)$$

In this form, it is clear that we may treat the separation of eigenvalues instead of frequency. In Figure 15, the eigenvalues of all 3 modes are plotted along the mode c minimum curve of Figure 8. For both of our prospective c-mode minima, the c-mode eigenvalue is well separated from those of the other two modes. This criterion is not really applicable to our b-mode minimum because, for $\phi = 60^\circ$ and $\theta = 49.3833^\circ$, the piezoelectric coupling vanishes for modes a and c (see Figure 3). There is thus no difficulty in this case due to the interference of the plate vibrations of the other modes. This is an advantage of the mode b minima over our 2 mode c minima, which have piezoelectric vibrations for all three modes present.

Let us summarize our results for the integral measure of temperature sensitivity. We have located four cuts which minimize this sensitivity and have outlined some of the advantages and disadvantages of these cuts. The absolute minimum ($\phi = 0^\circ$, mode c) is extremely sensitive to errors in the cut angles and this instability renders precision applications very difficult. Of the remaining three cuts, the weakest minimum ($\phi = 60^\circ$, mode b) possesses the greatest angular stability, the largest coupling constant, and has only one mode present. However, the range of variation of the relative frequency difference curve may be too large (i.e., the minimum too weak) to be practical.

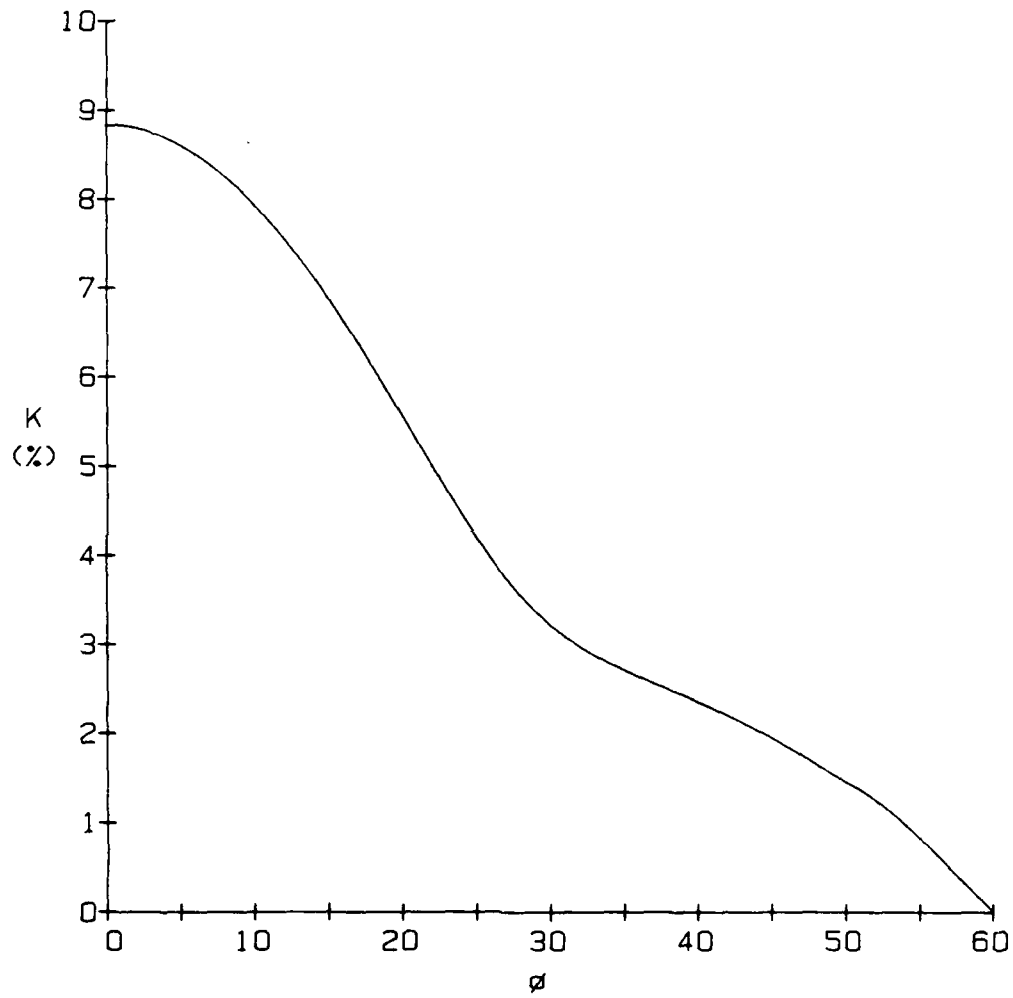


Figure 14: COUPLING CONSTANT VERSUS ϕ FOR C MODE
INTEGRAL MINIMIZED WITH RESPECT TO θ .

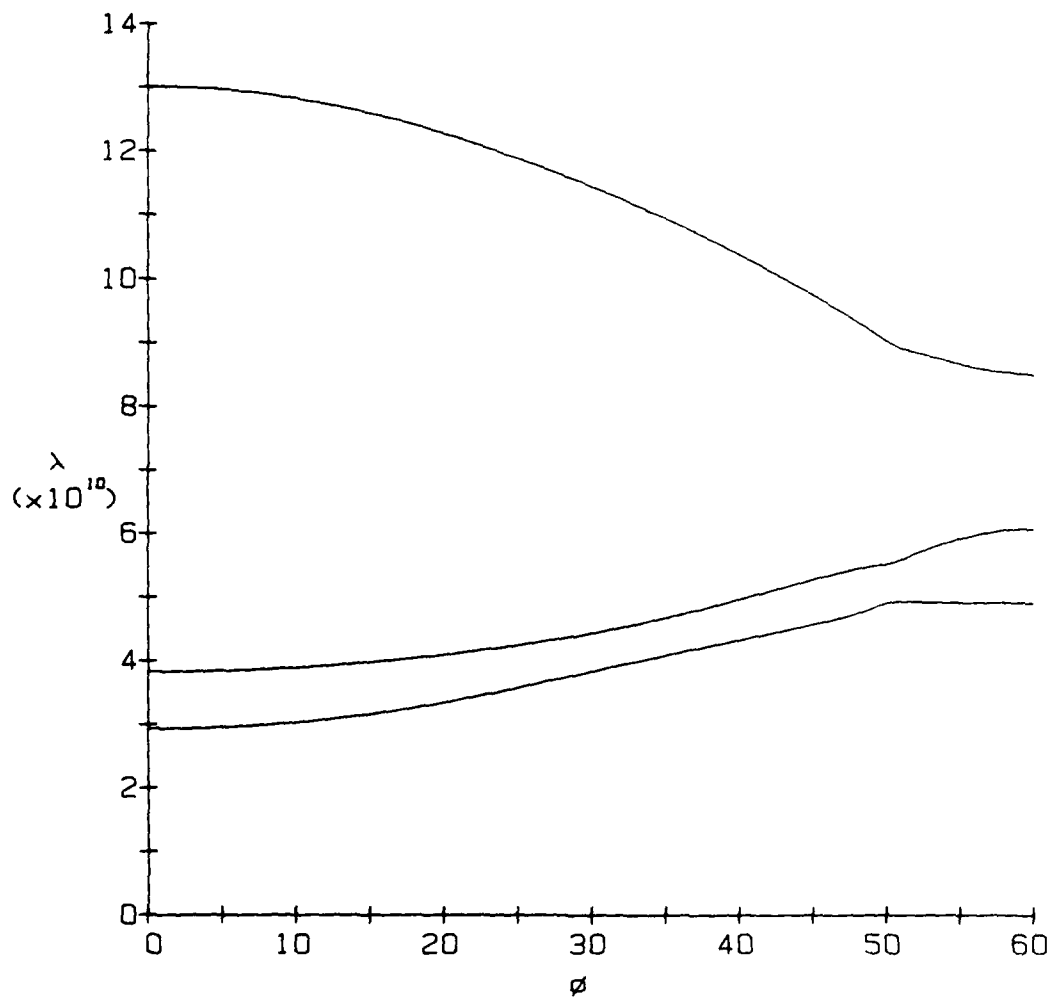


Figure 15: EIGENVALUES VERSUS ϕ FOR C MODE
 INTEGRAL MINIMIZED WITH RESPECT TO θ .

Next, we shall consider another measure of sensitivity. Define the range measure by:

$$M_2(\phi, \theta) = \left| \max \frac{\Delta f}{f} - \min \frac{\Delta f}{f} \right| \quad (56)$$

where the maximum and minimum are over the temperature range $(-40^\circ, 80^\circ)$. As for the integral measure, we calculate $M_2(\phi, \theta)$ for each mode for ϕ in increments of 10° and θ in the range 0° to 90° . The results are displayed in Figure 16. It is instructive to compare Figures 16 and 7. It is seen that the shapes of the curves are virtually identical. Similar calculations were performed for a third measure of temperature sensitivity using a slope

$$M_3(\phi, \theta) = \max \left| \frac{d}{dT} \frac{\Delta f}{f} \right| \quad (57)$$

The curves for this measure will be omitted since they are indistinguishable from those of the other two measures. For all three measures, the minima for mode a are weak and are not treated further. Using the measures M_2 and M_3 , curves of the minima for fixed ϕ were calculated for modes b and c for ϕ in increments of 1° . The resulting curves are not shown since they are identical in shape to Figures 8 and 9. It follows that the overall features of the temperature sensitivity using M_2 and M_3 are the same as for M_1 . In all three measures, we can identify three cuts ($\phi = 0^\circ, 27^\circ$ and 42°) which minimize the mode c sensitivity and one ($\phi = 60^\circ$) which minimizes that of mode b. We summarize the magnitudes and locations of these minima in Table 1. It can be seen that the locations of the minima for different measures differ only very slightly. Indeed, the angular locations of these minima deviate only slightly from the locations of zero first order temperature coefficients. It can also be shown that the features of these minima with regard to angular stability, coupling and frequency separation are the same for all three measures. The relative advantages and disadvantages of these 4 minima are the same for all three measures and are as stated earlier.

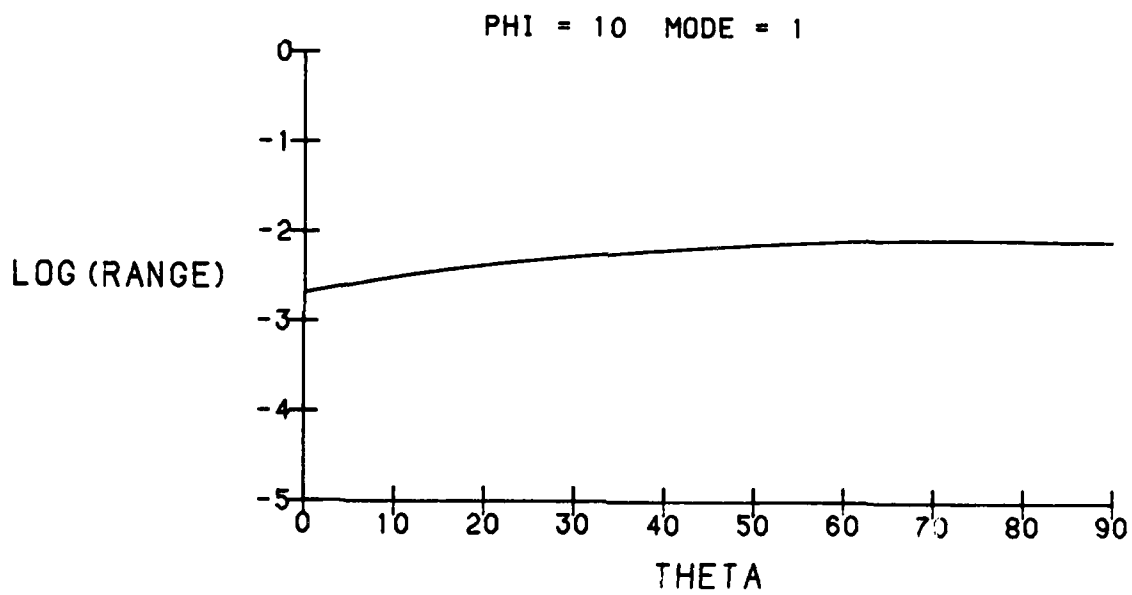
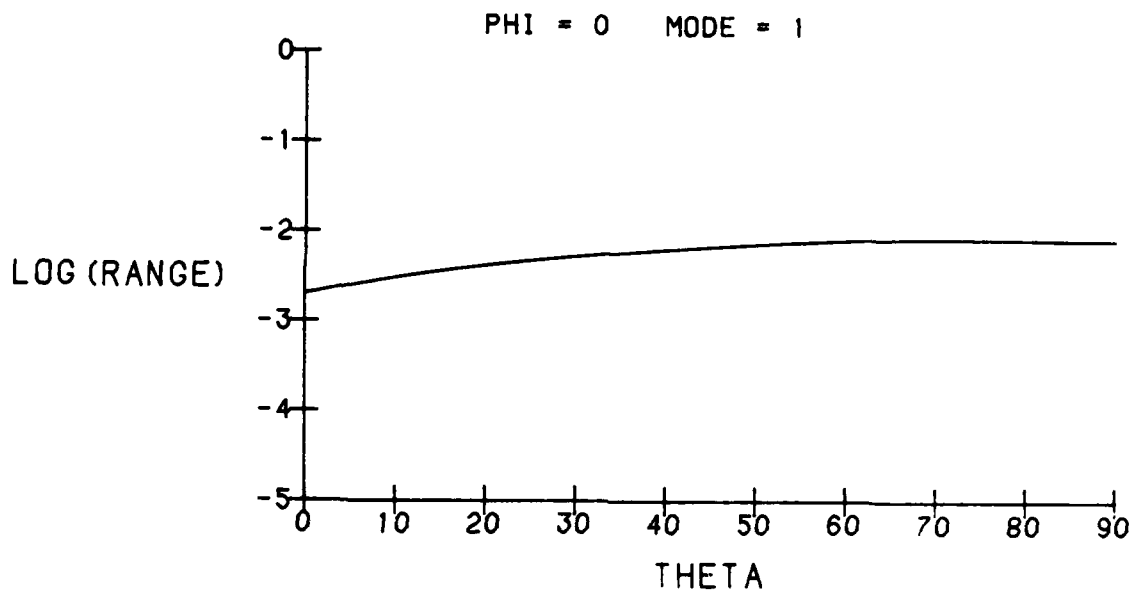


Figure 16: RANGE MEASURE OF TEMPERATURE SENSITIVITY

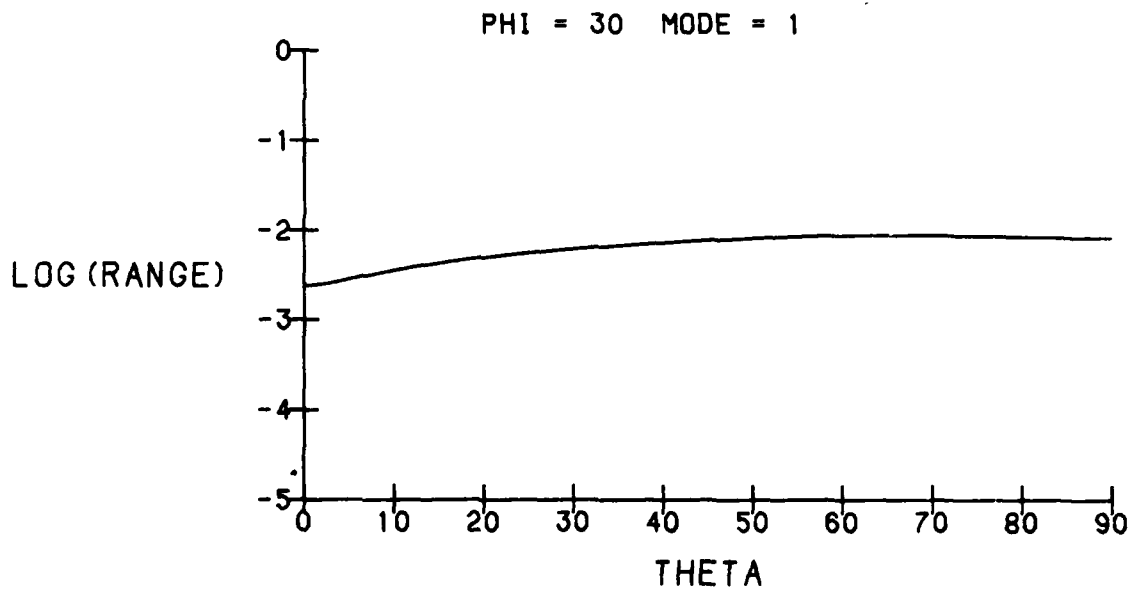
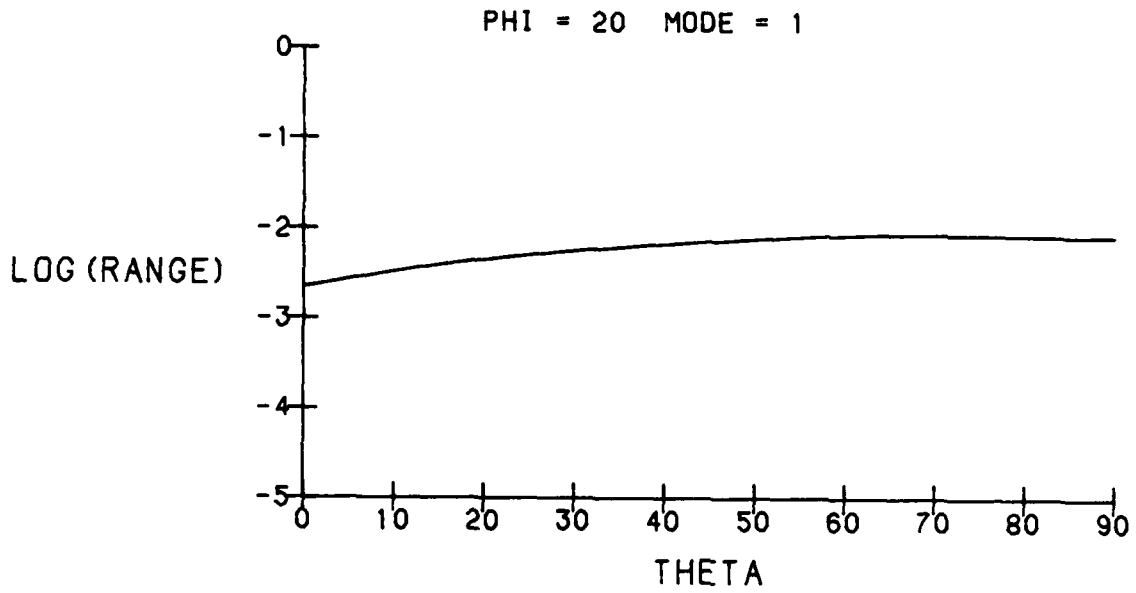


Figure 16: RANGE MEASURE OF TEMPERATURE SENSITIVITY (continued)

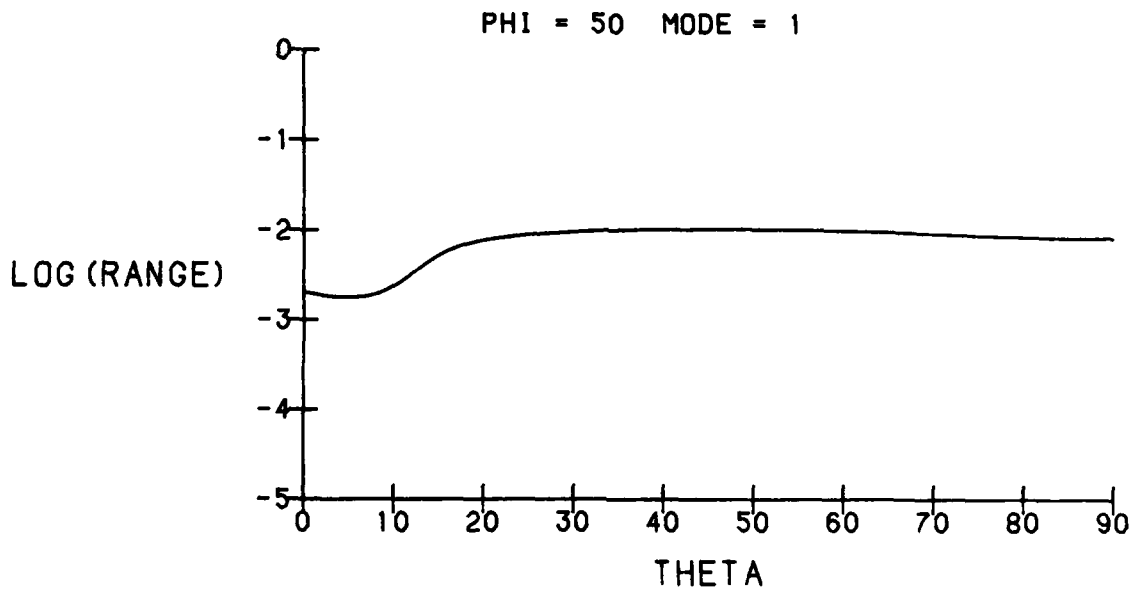
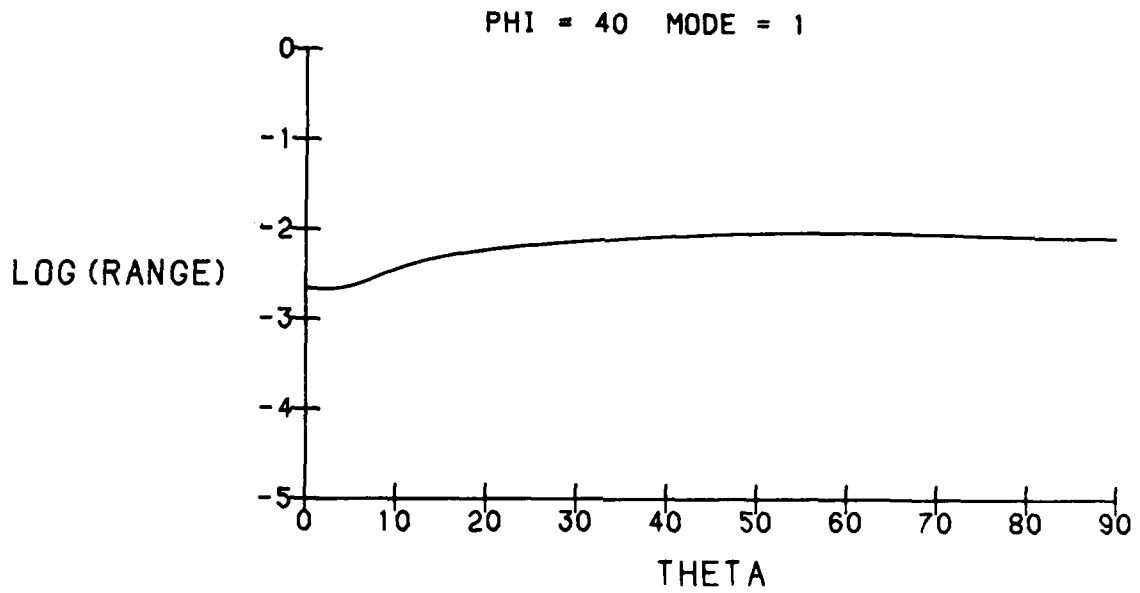


Figure 16: RANGE MEASURE OF TEMPERATURE SENSITIVITY (continued)

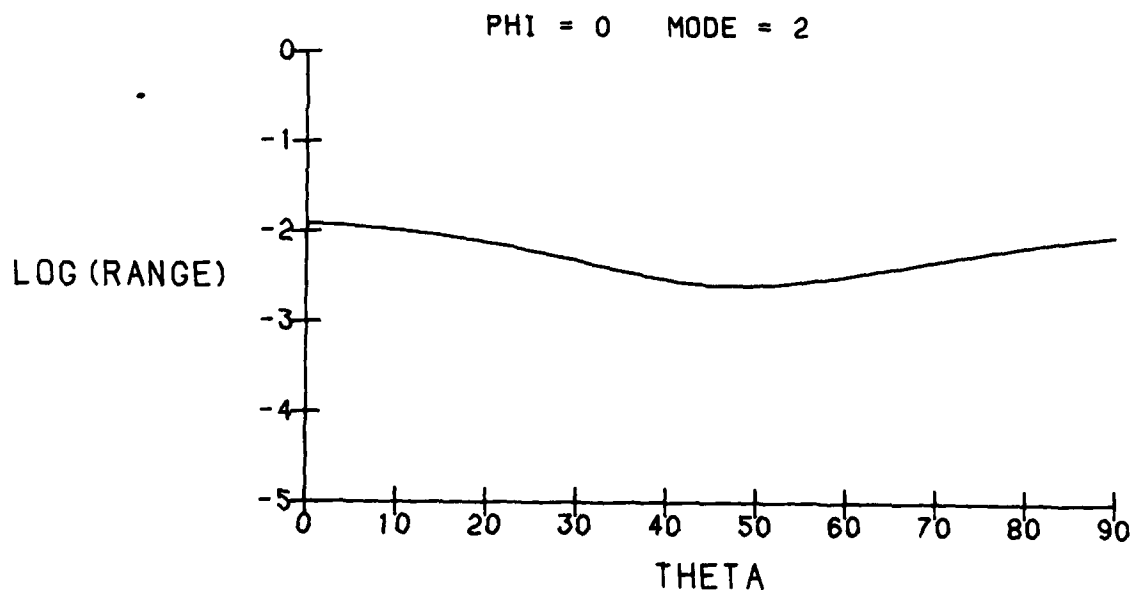
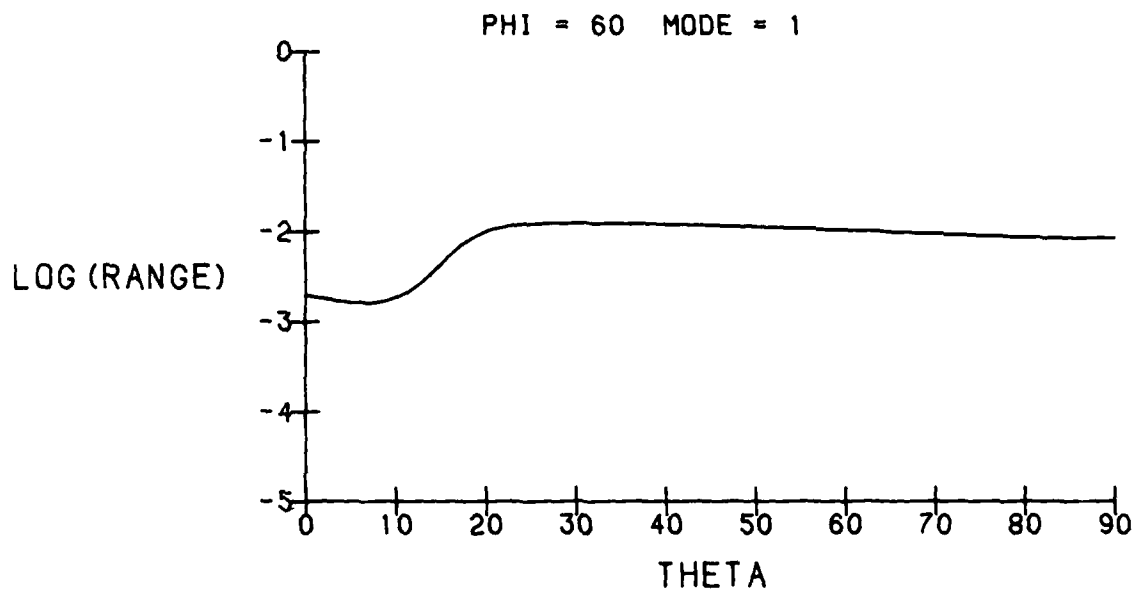


Figure 16: RANGE MEASURE OF TEMPERATURE SENSITIVITY (continued)

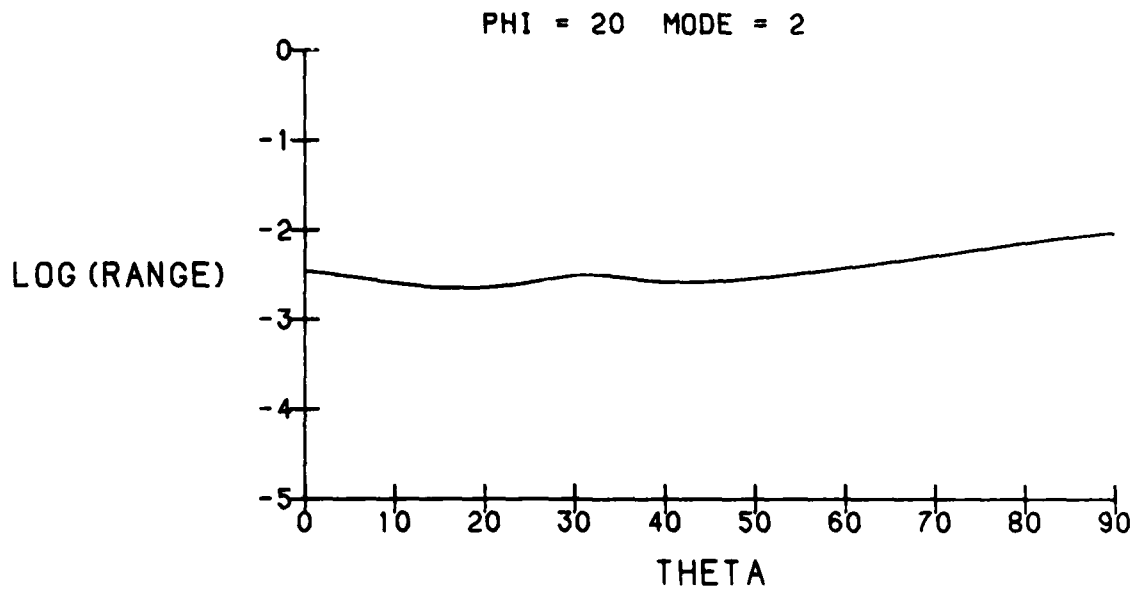
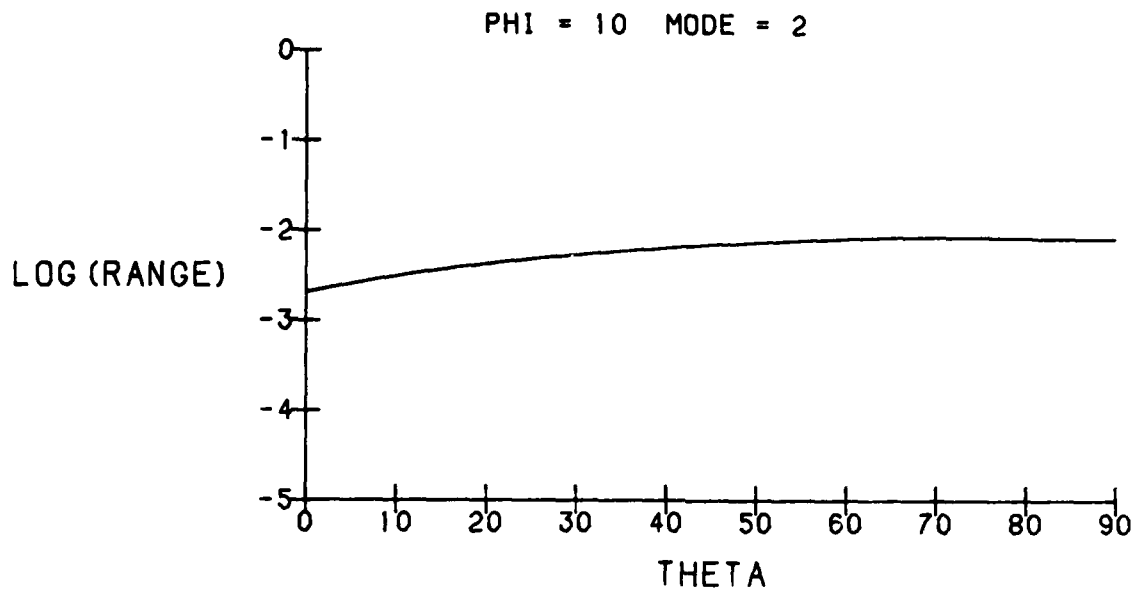


Figure 16: RANGE MEASURE OF TEMPERATURE SENSITIVITY (continued)

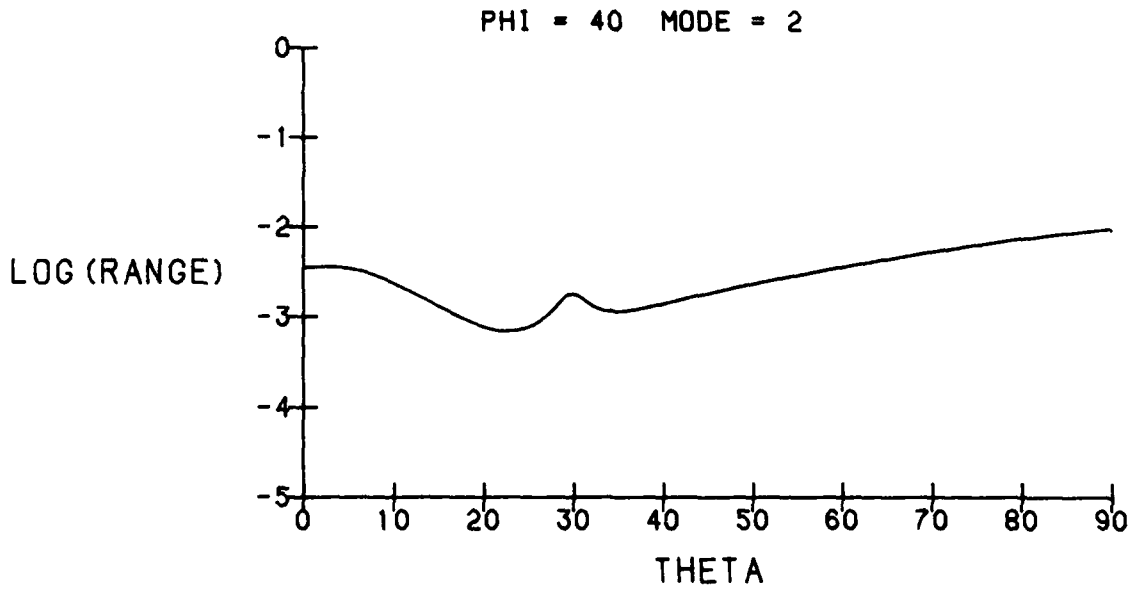
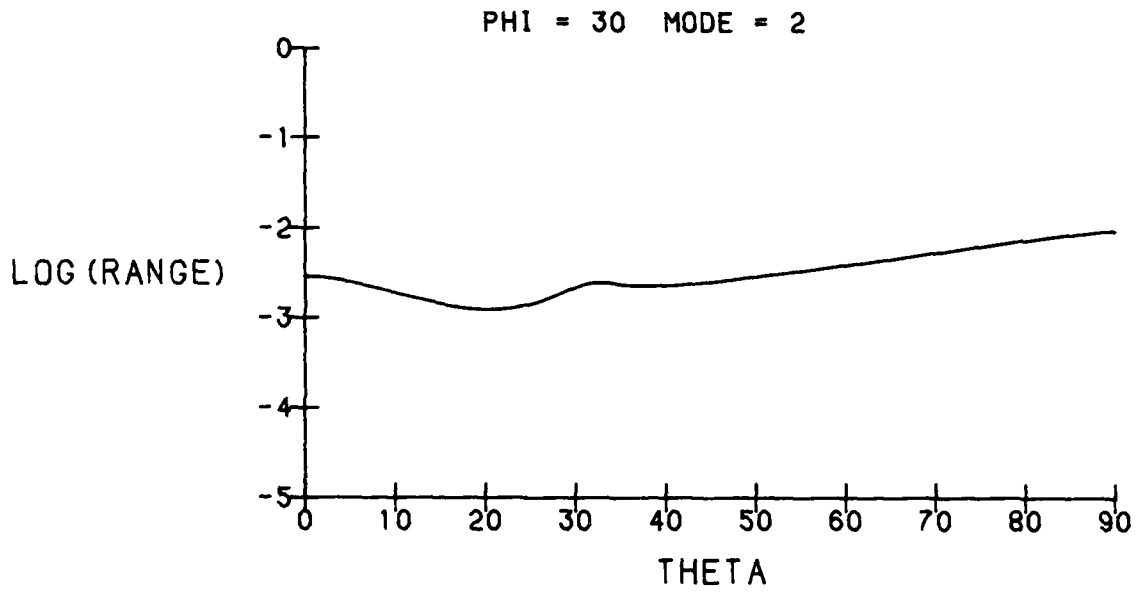


Figure 16: RANGE MEASURE OF TEMPERATURE SENSITIVITY (continued)

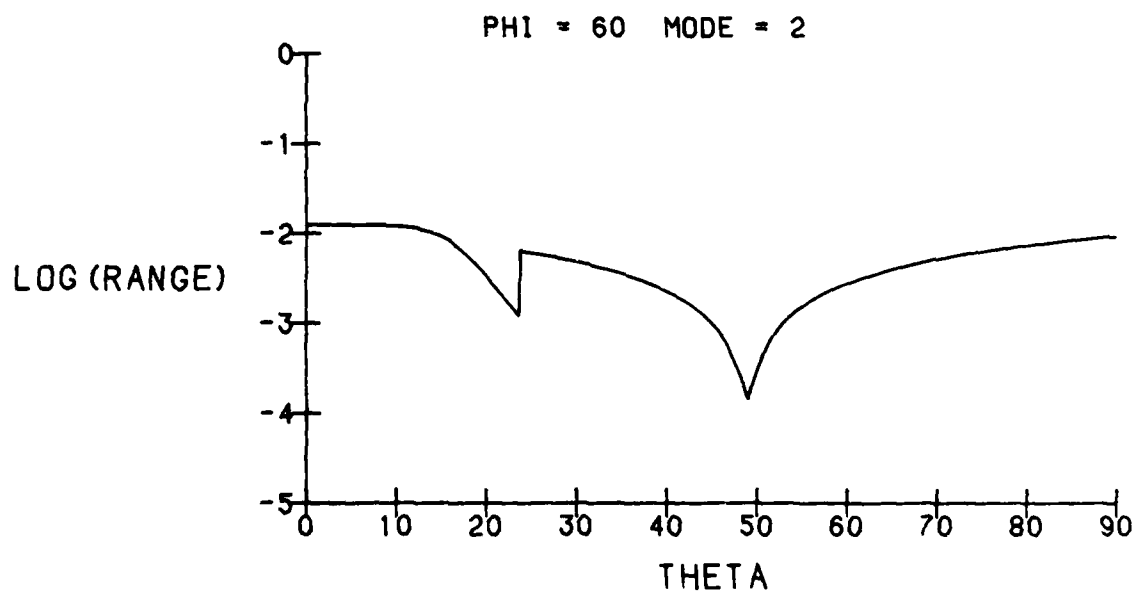
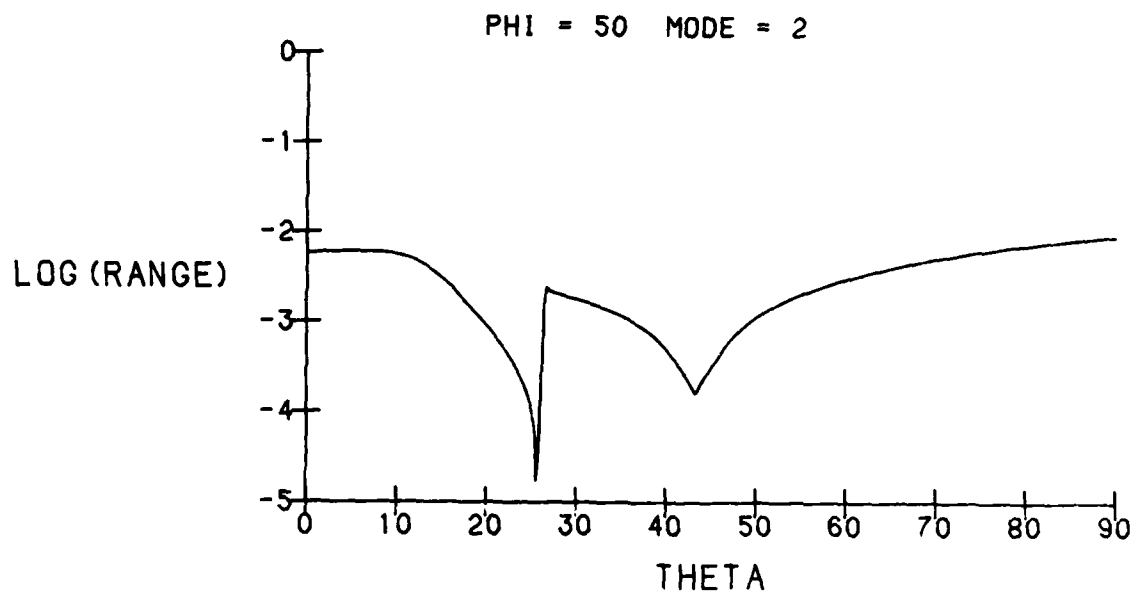


Figure 16: RANGE MEASURE OF TEMPERATURE SENSITIVITY (continued)

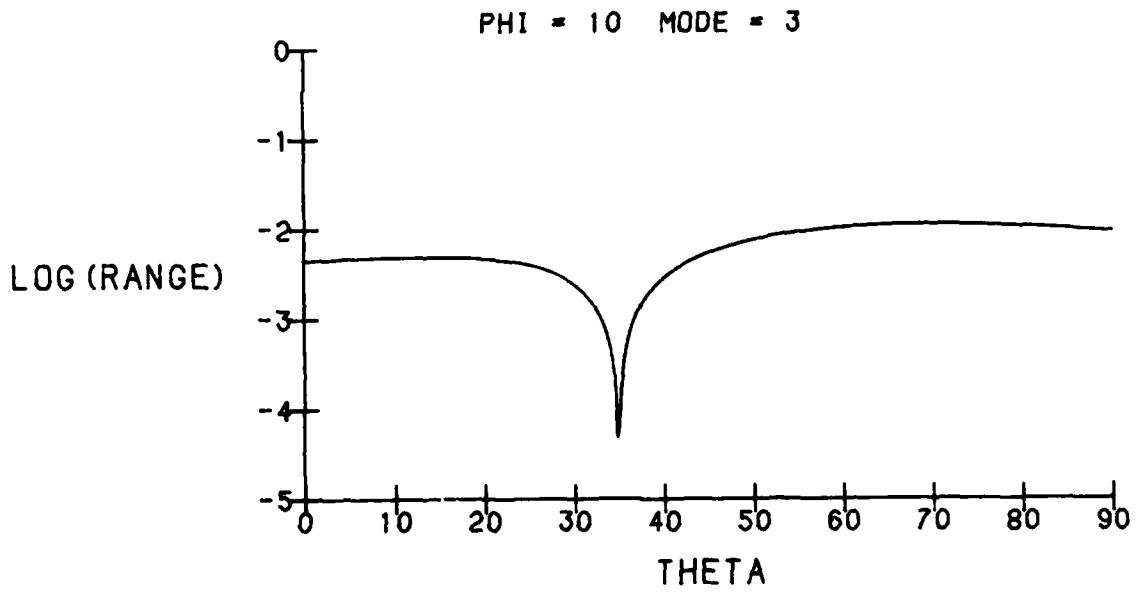
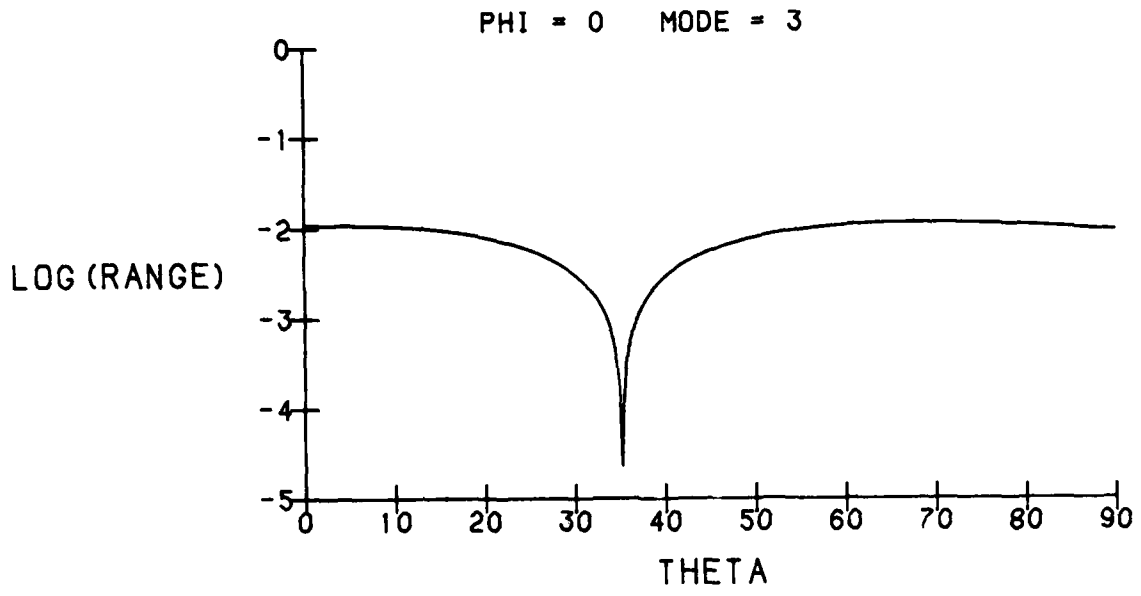


Figure 16: RANGE MEASURE OF TEMPERATURE SENSITIVITY (continued)

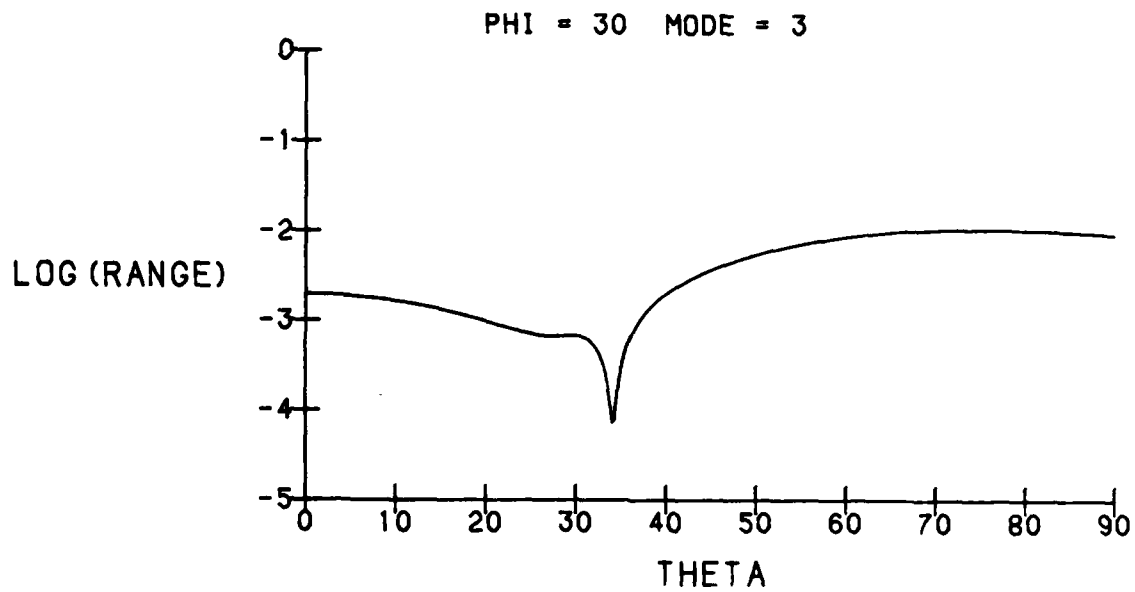
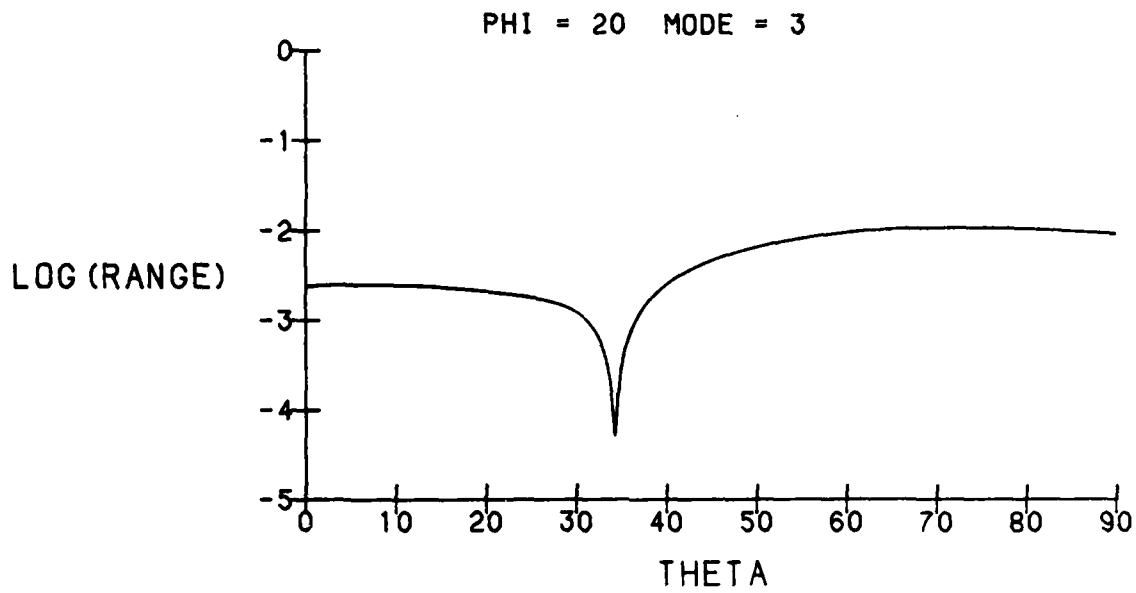


Figure 16: RANGE MEASURE OF TEMPERATURE SENSITIVITY (continued)

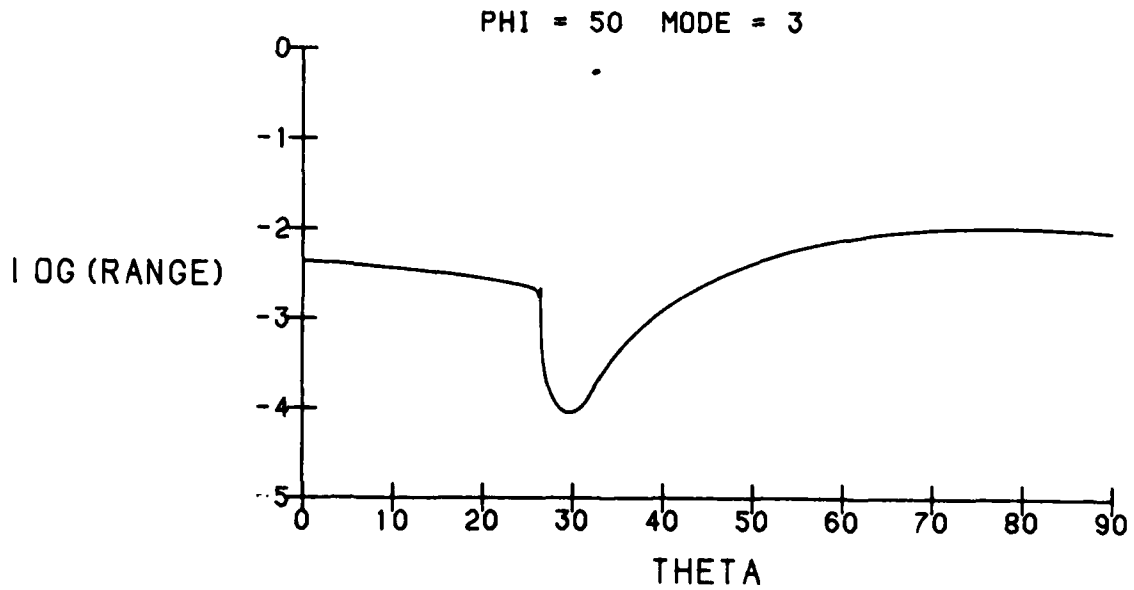
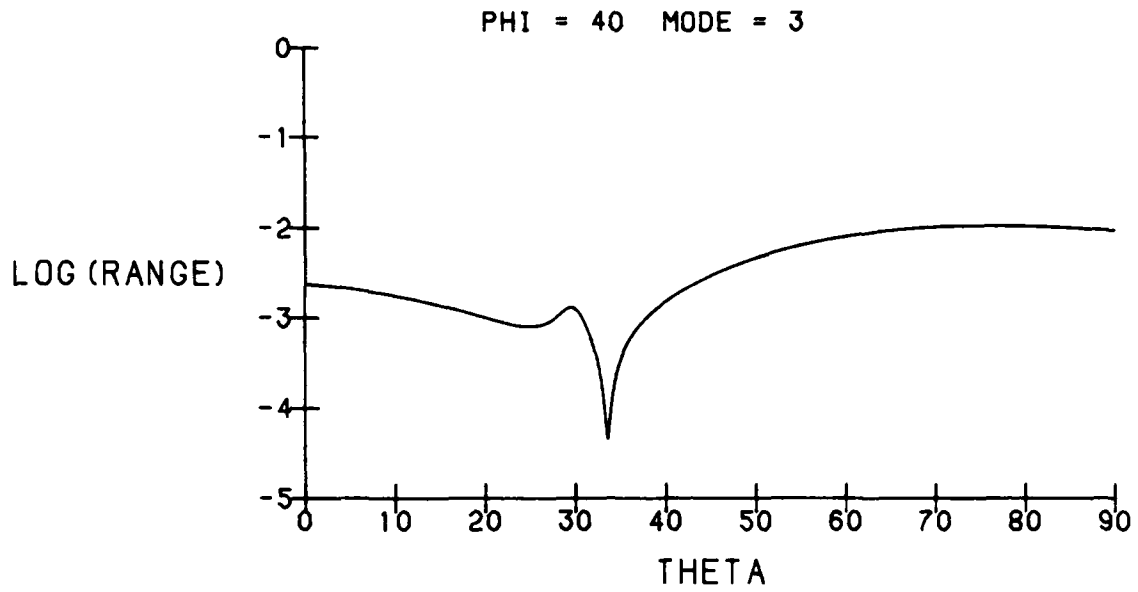


Figure 16: RANGE MEASURE OF TEMPERATURE SENSITIVITY (continued)

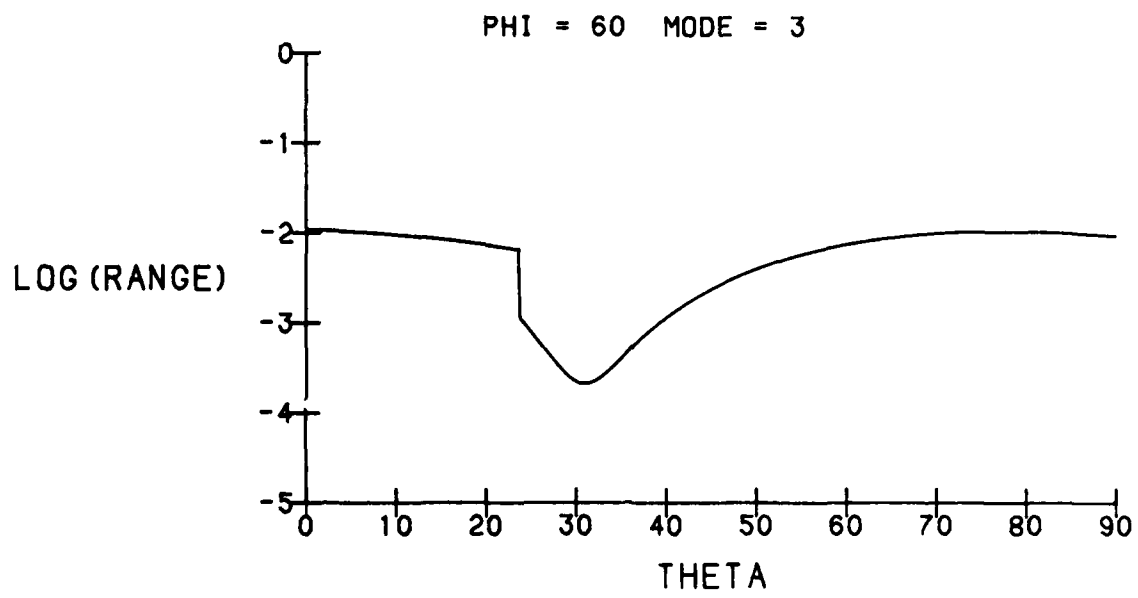


Figure 16: RANGE MEASURE OF TEMPERATURE SENSITIVITY (continued)

TABLE 1: Minima Using Measures M_1 , M_2 and M_3

MODE	θ	M_1 min		M_2 min		M_3 min	
		θ	M_1	θ	M_2	θ	M_3
C	0	35.1304	$.4035 \times 10^{-3}$	35.1720	$.1181 \times 10^{-4}$	35.3242	$.3782 \times 10^{-6}$
C	27	34.0644	$.2246 \times 10^{-2}$	34.0216	$.5897 \times 10^{-4}$	34.1258	$.1964 \times 10^{-5}$
C	42	33.2906	$.1564 \times 10^{-2}$	33.1912	$.4102 \times 10^{-4}$	33.1697	$.1369 \times 10^{-5}$
b	60	49.3832	$.5385 \times 10^{-2}$	48.9622	$.1393 \times 10^{-3}$	48.5290	$.4495 \times 10^{-5}$

The three measures that we have investigated all measure the sensitivity of a single mode. A slight generalization of these methods uses two modes, that is, measures the temperature sensitivity of the difference in frequency between two modes. Let mode i have temperature coefficient a_j ($j = 1, 2, 3$) and mode j have coefficient b_j ($j = 1, 2, 3$). By definition, we have:

$$f_i(T) = f_i(T_0) \left[1 + \sum_1^3 a_k (T - T_0)^k \right] \quad (58)$$

$$f_j(T) = f_j(T_0) \left[1 + \sum_1^3 b_k (T - T_0)^k \right] \quad (59)$$

Define the frequency difference between modes i and j by:

$$S_{ij}(T) = f_i(T) - f_j(T) \quad (60)$$

Substitution of (58) and (59) gives:

$$S_{ij}(T) = S_{ij}(T_0) + \sum_{k=1}^3 \left\{ a_k f_i(T_0) - b_k f_j(T_0) \right\} (T - T_0)^k \quad (61)$$

The fractional change in the frequency difference is thus:

$$\frac{\Delta S_{ij}}{S_{ij}} = \frac{S_{ij}(T) - S_{ij}(T_0)}{S_{ij}(T_0)} \quad (62)$$

$$= \sum_{k=1}^3 \left[W_i a_k - W_j b_k \right] (T - T_0)^k \quad (63)$$

where we have defined the weights:

$$W_i = \frac{f_i(T_0)}{f_i(T_0) - f_j(T_0)} \quad (64)$$

$$W_j = \frac{f_j(T_0)}{f_i(T_0) - f_j(T_0)} \quad (65)$$

These weights are dimensionless quantities which can be written in terms of the eigenvalues. For the fundamental frequencies of modes i and j , substitution of (55) into (64) and (65) gives:

$$W_i = \frac{\sqrt{\lambda_i}}{\sqrt{\lambda_i} - \sqrt{\lambda_j}} \quad (66)$$

$$W_j = \frac{\sqrt{\lambda_j}}{\sqrt{\lambda_i} - \sqrt{\lambda_j}} \quad (67)$$

These can also be written in terms of the modal velocities as:

$$W_i = \frac{v_i}{v_i - v_j} \quad (68)$$

$$W_j = \frac{v_j}{v_i - v_j} \quad (69)$$

Equation (63), with the weights defined by (66) and (67), was used to investigate the temperature sensitivity. Note that the quantity $S_{ij}(T)$ is a directly measurable quantity. The sensitivity was measured using the integral of the absolute value of (63) from -40° to 80° . The calculations and procedure were identical to those for the single mode measures. The results are summarized graphically in Figure 17. These graphs should be compared to the single mode data of Figure 7. This comparison shows that all the minima of the double mode measure are very weak. None of the minima of Figure 17 is less than 0.01. In contrast, our single mode integral measure has minima much less than this value (see also Table 1). The double mode measure will not be investigated further since it is inferior to the single mode measures.

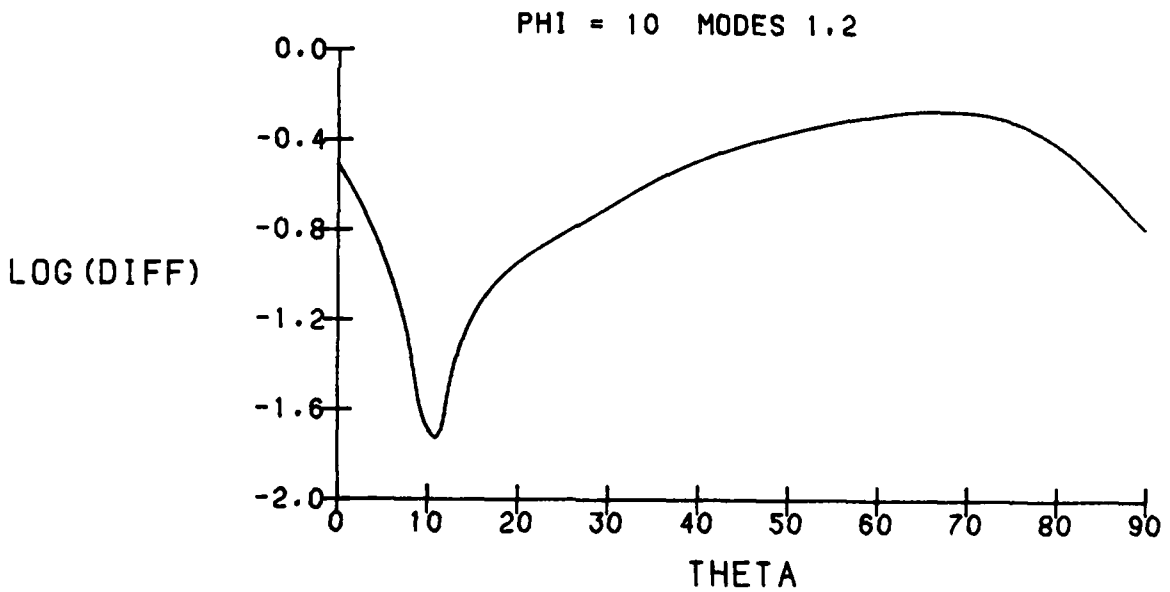
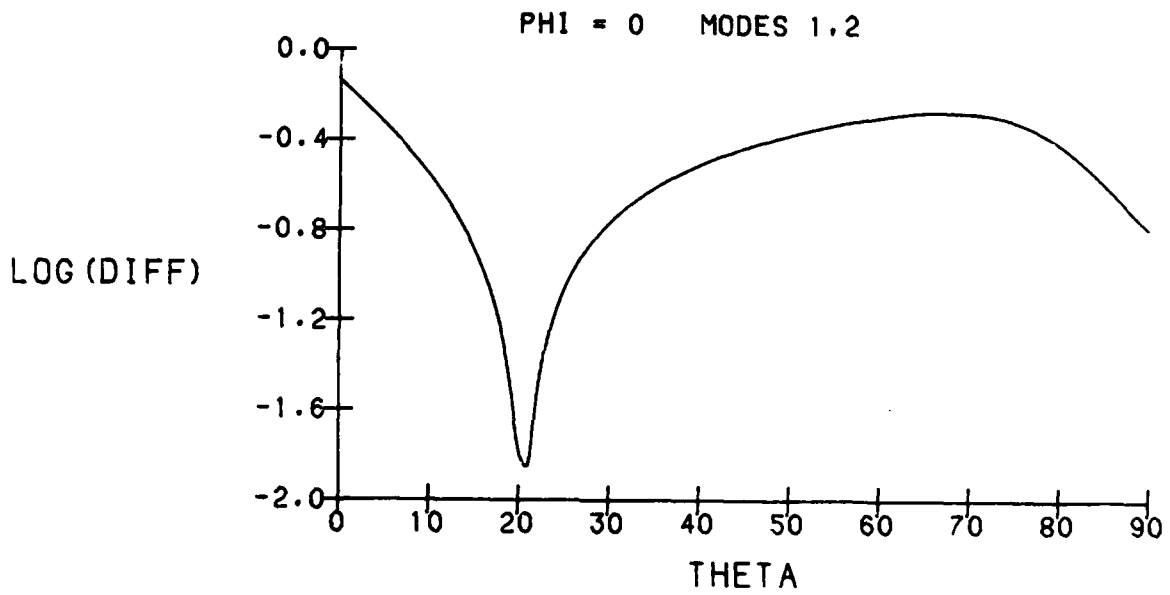


Figure 17: DIFFERENCE MEASURE OF TEMPERATURE SENSITIVITY

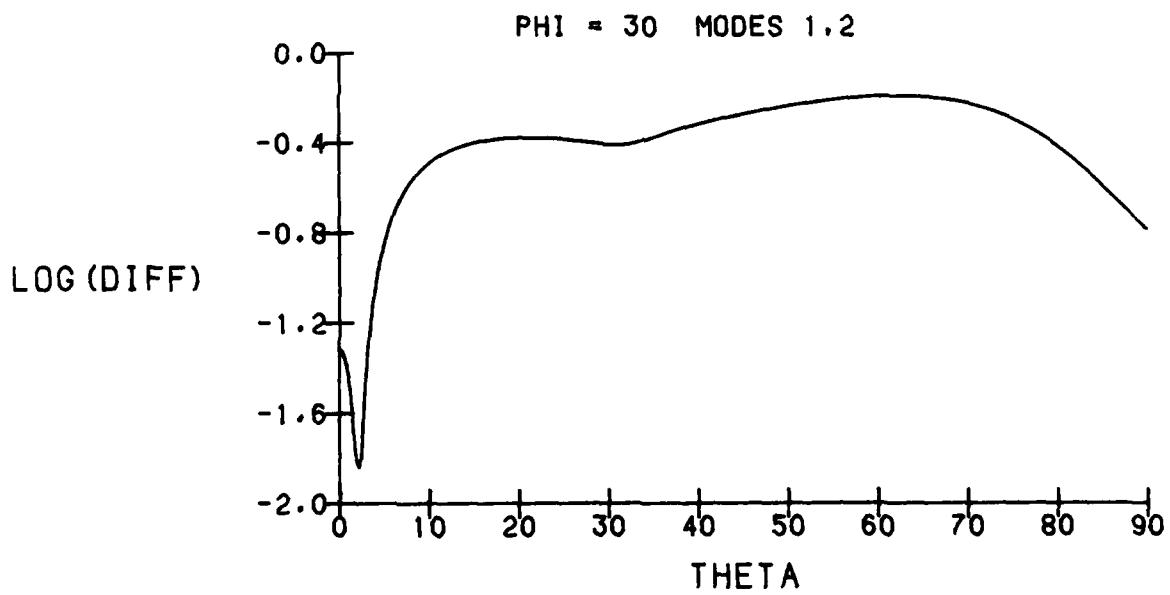
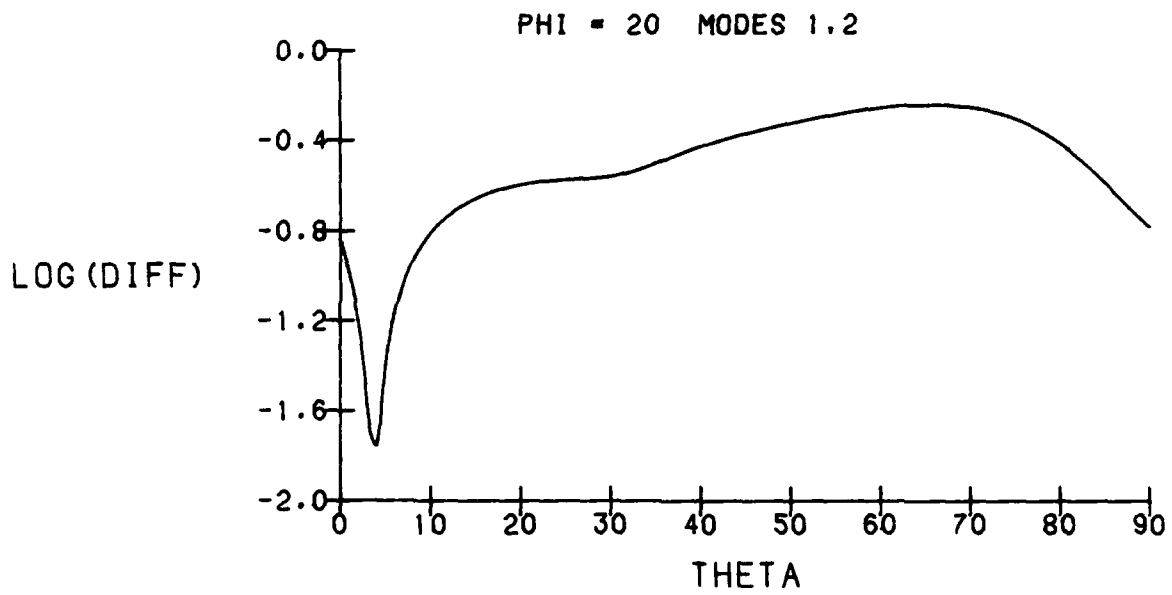


Figure 17: DIFFERENCE MEASURE OF TEMPERATURE SENSITIVITY (continued)

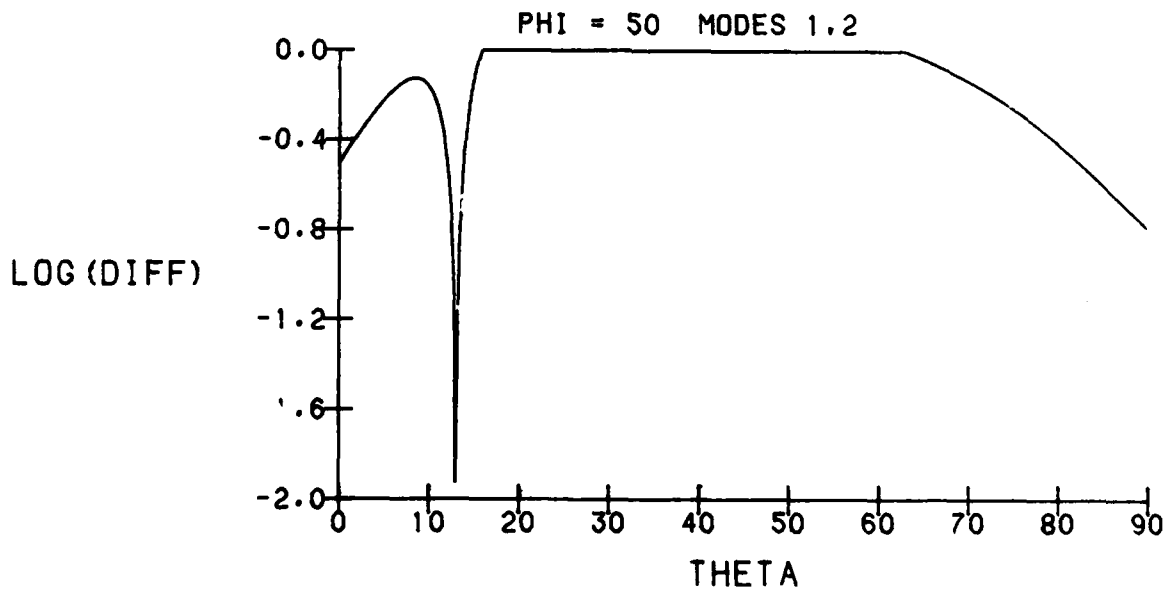
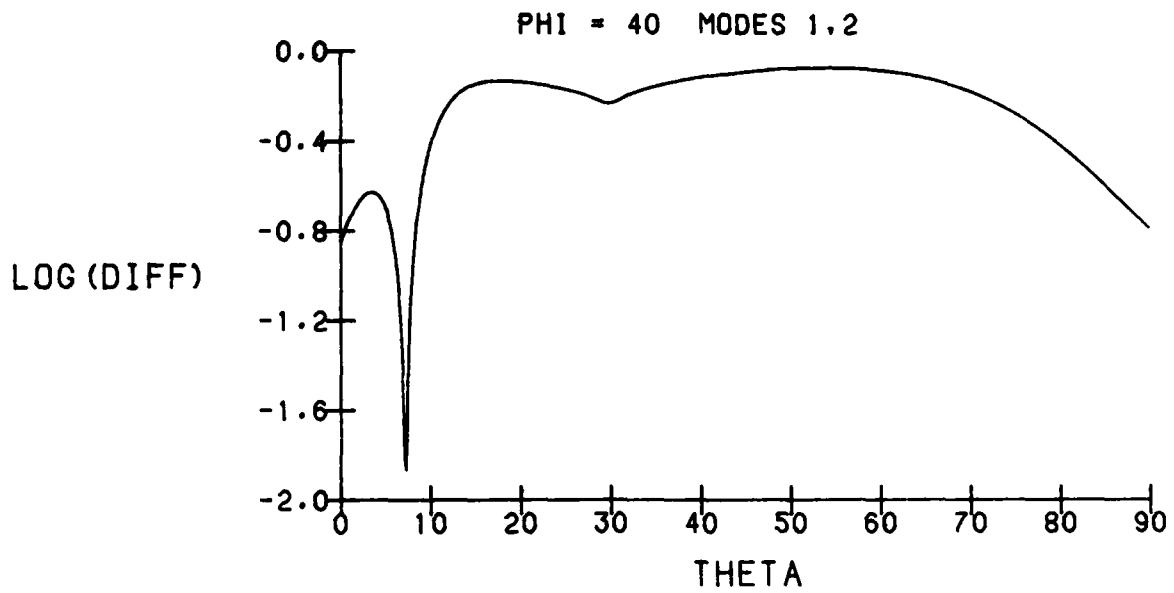


Figure 17: DIFFERENCE MEASURE OF TEMPERATURE SENSITIVITY (continued)

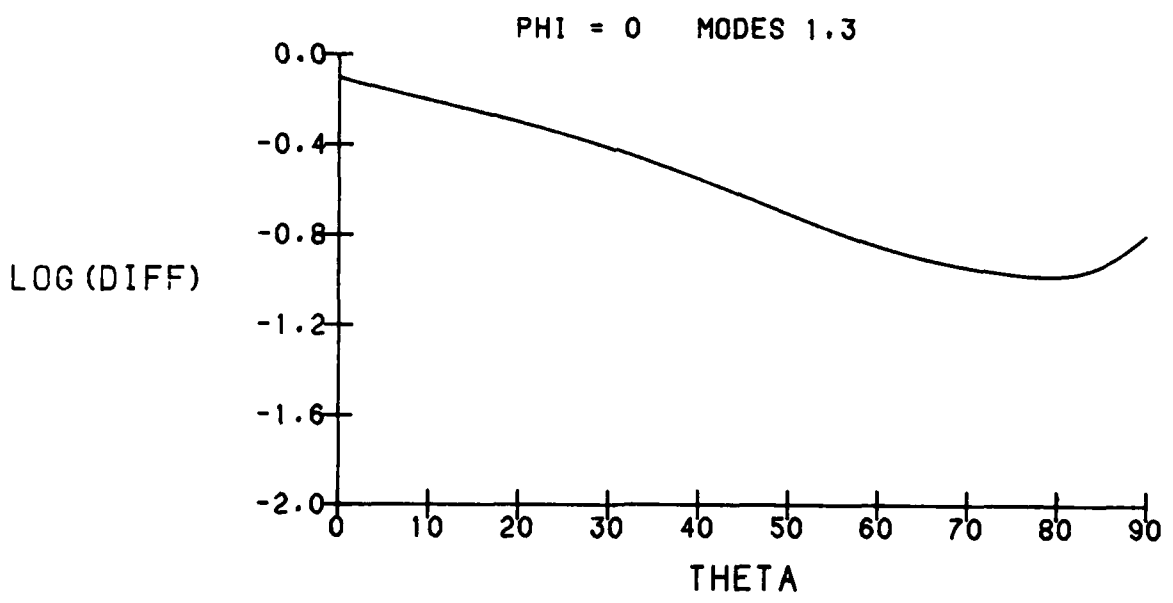
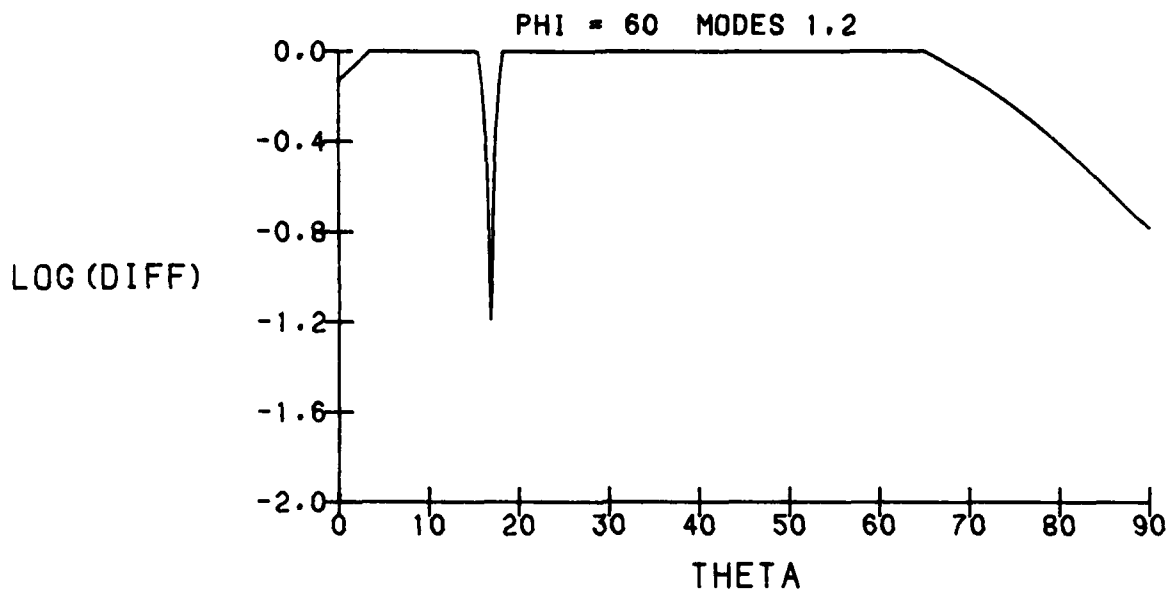


Figure 17: DIFFERENCE MEASURE OF TEMPERATURE SENSITIVITY (continued)

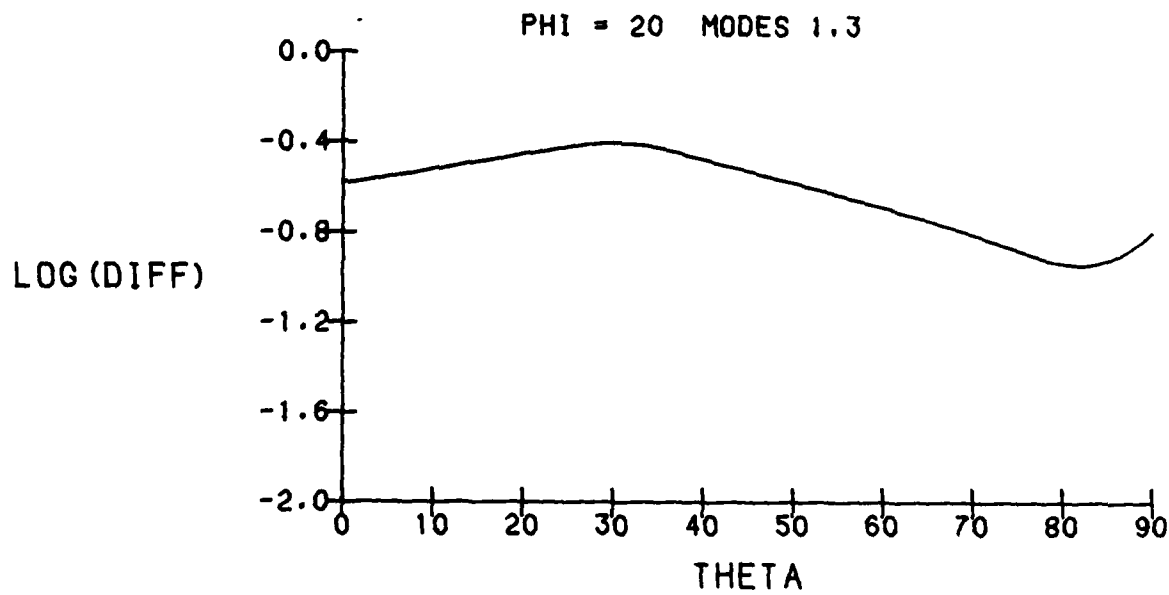
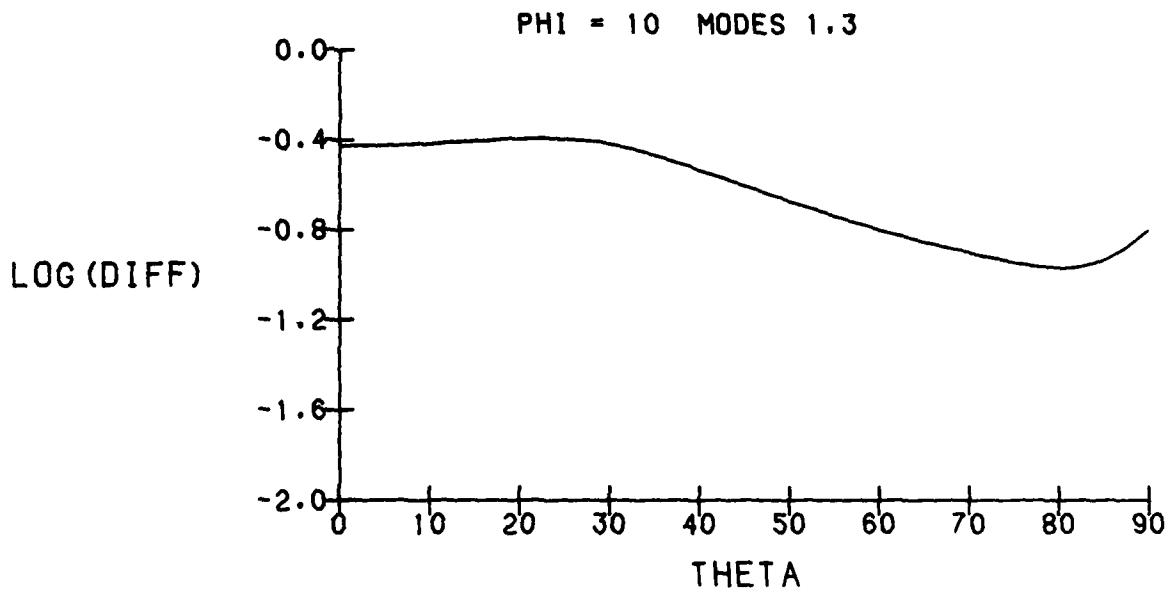


Figure 17: DIFFERENCE MEASURE OF TEMPERATURE SENSITIVITY (continued)

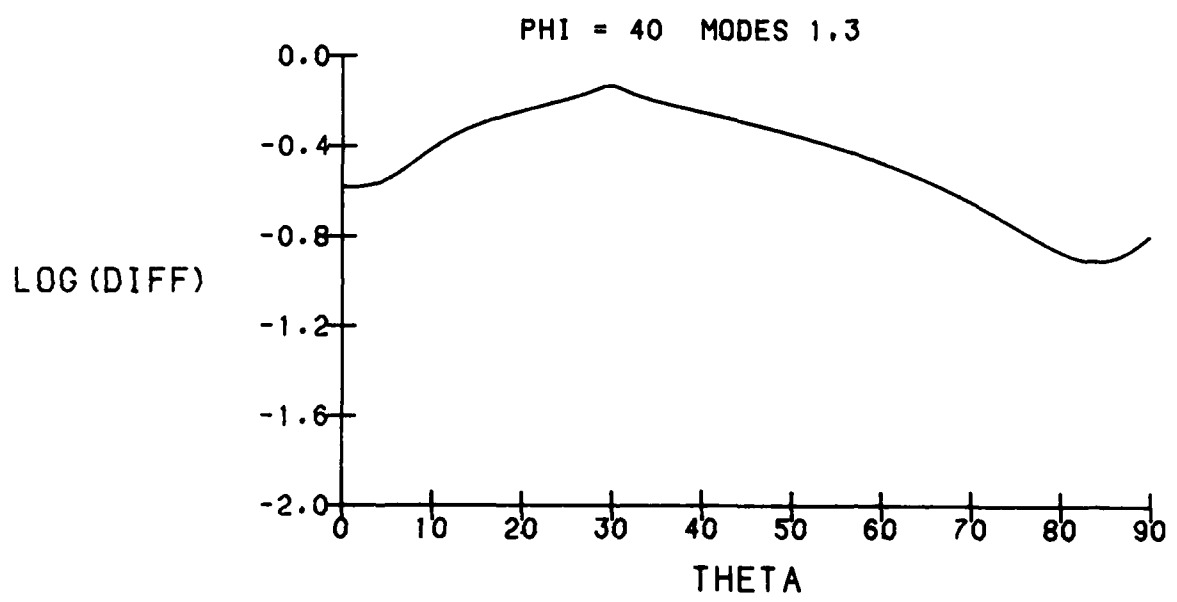
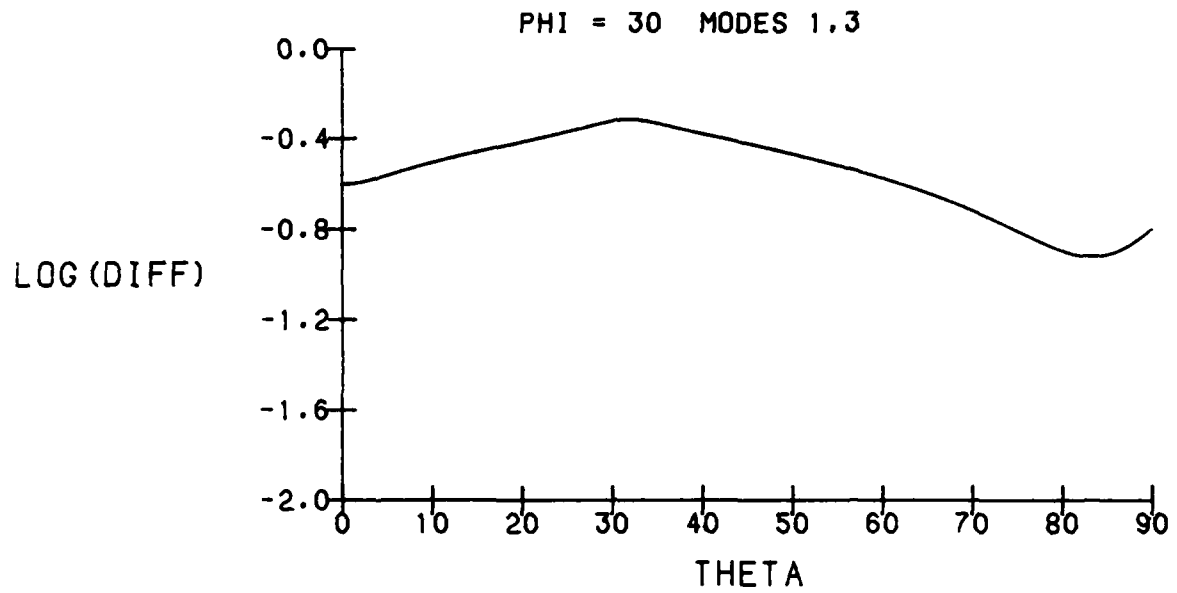


Figure 17: DIFFERENCE MEASURE OF TEMPERATURE SENSITIVITY (continued)

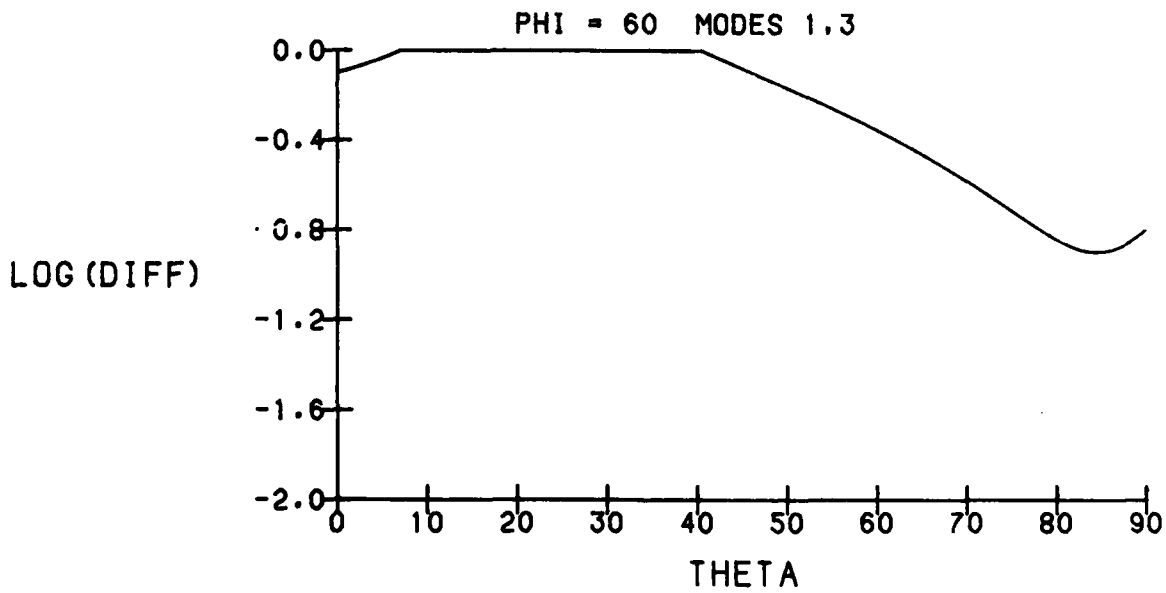
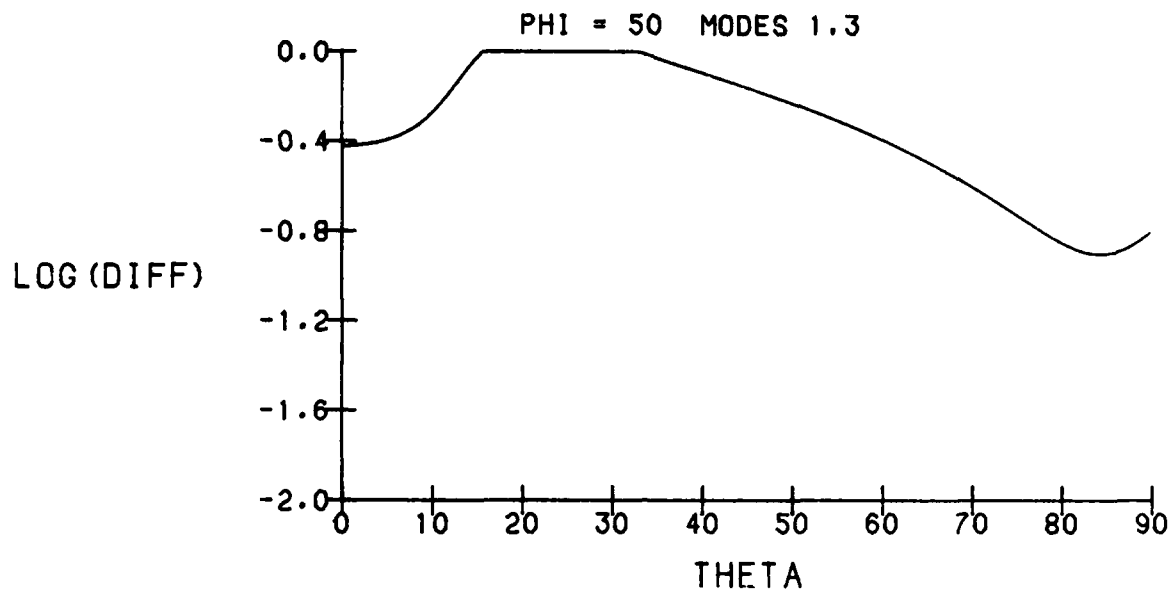


Figure 17: DIFFERENCE MEASURE OF TEMPERATURE SENSITIVITY (continued)

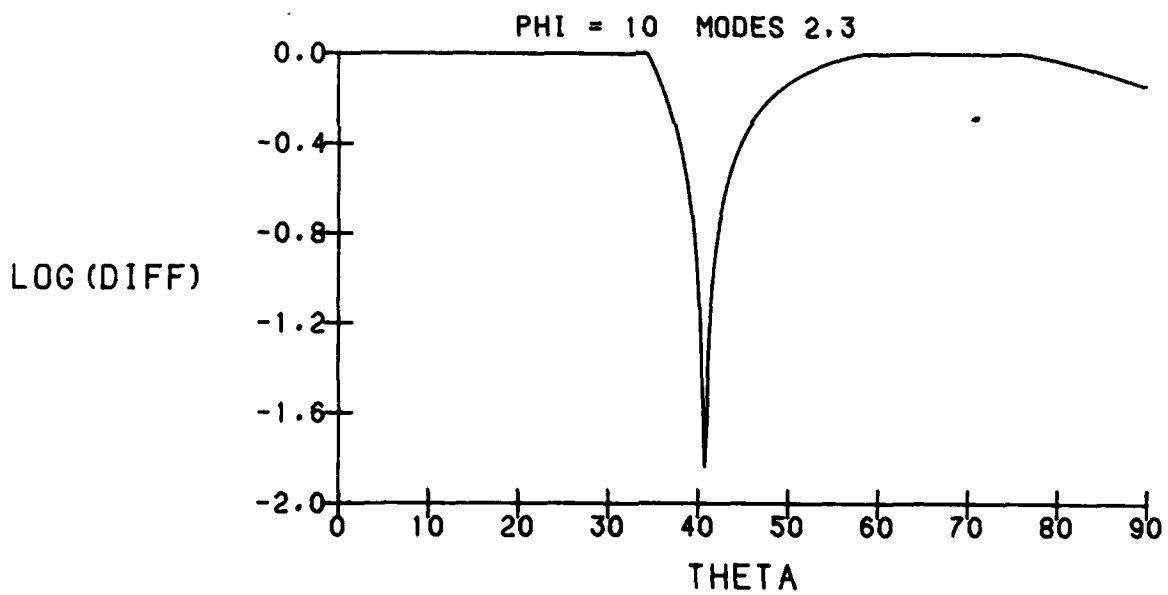
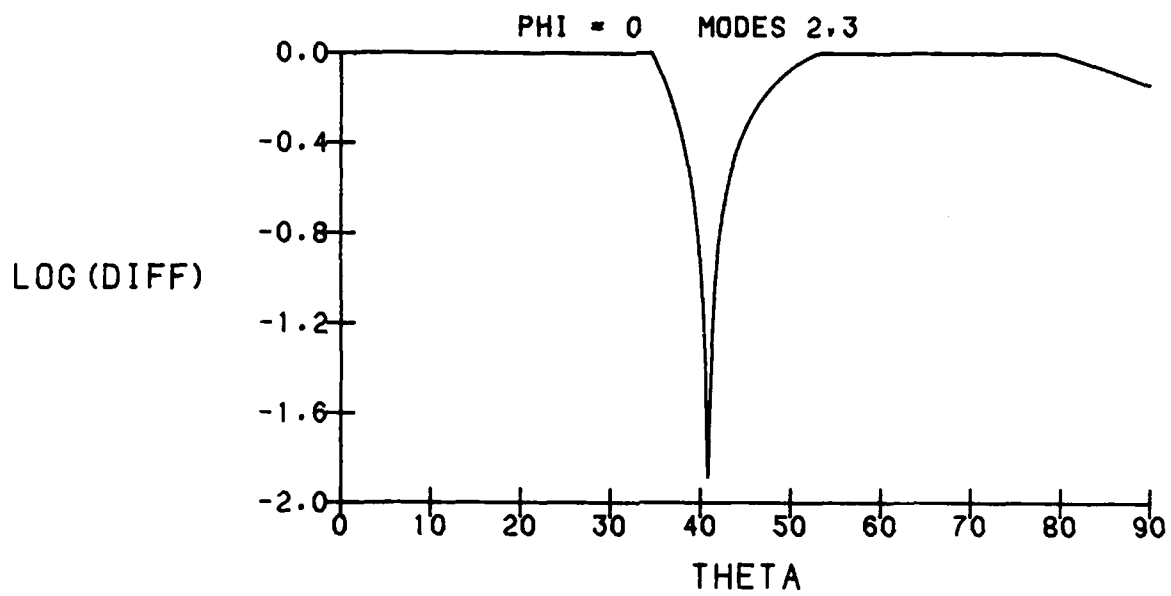


Figure 17: DIFFERENCE MEASURE OF TEMPERATURE SENSITIVITY (continued)

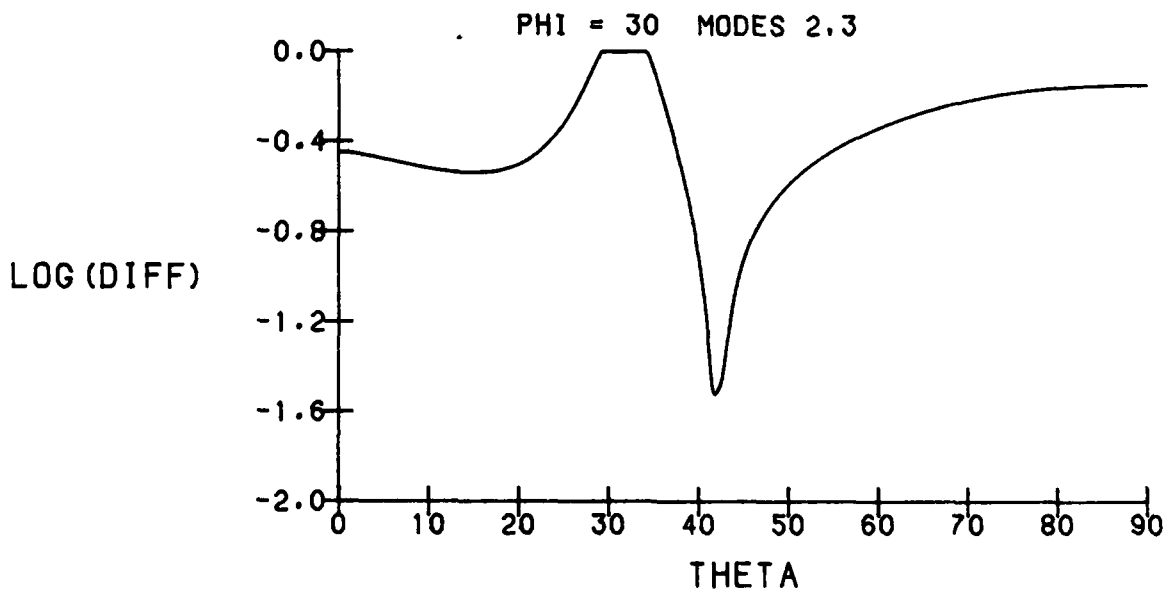
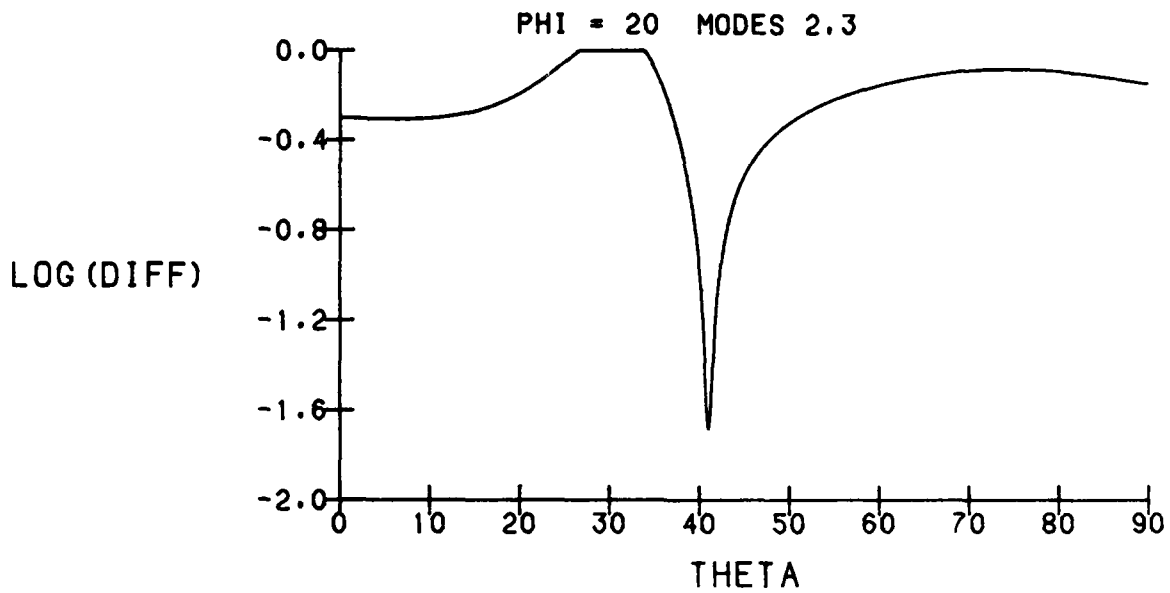


Figure 17: DIFFERENCE MEASURE OF TEMPERATURE SENSITIVITY (continued)

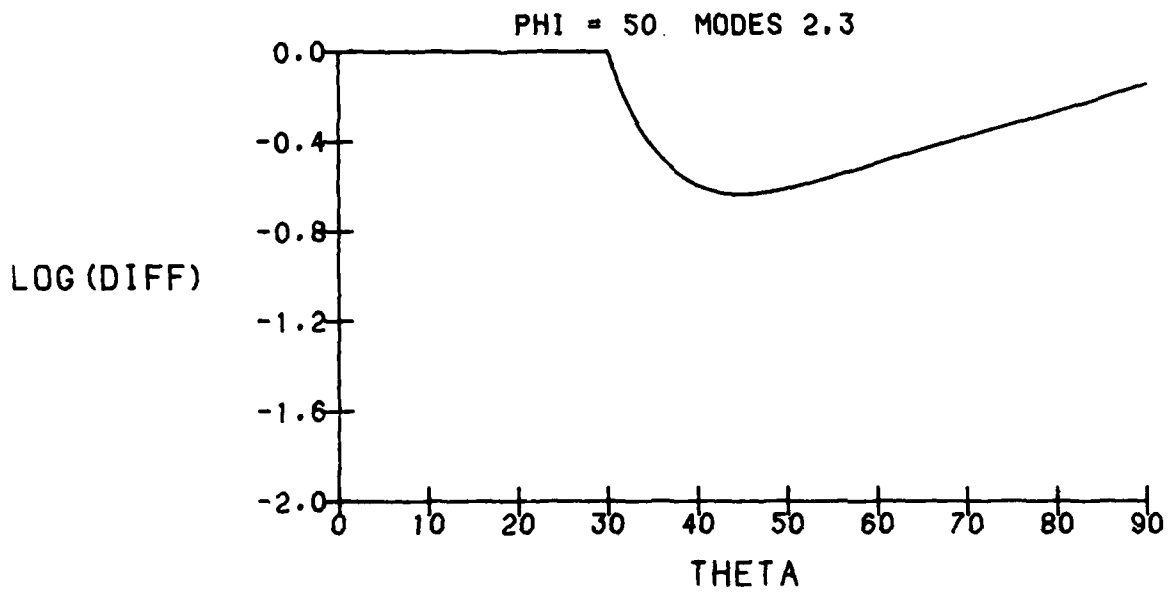
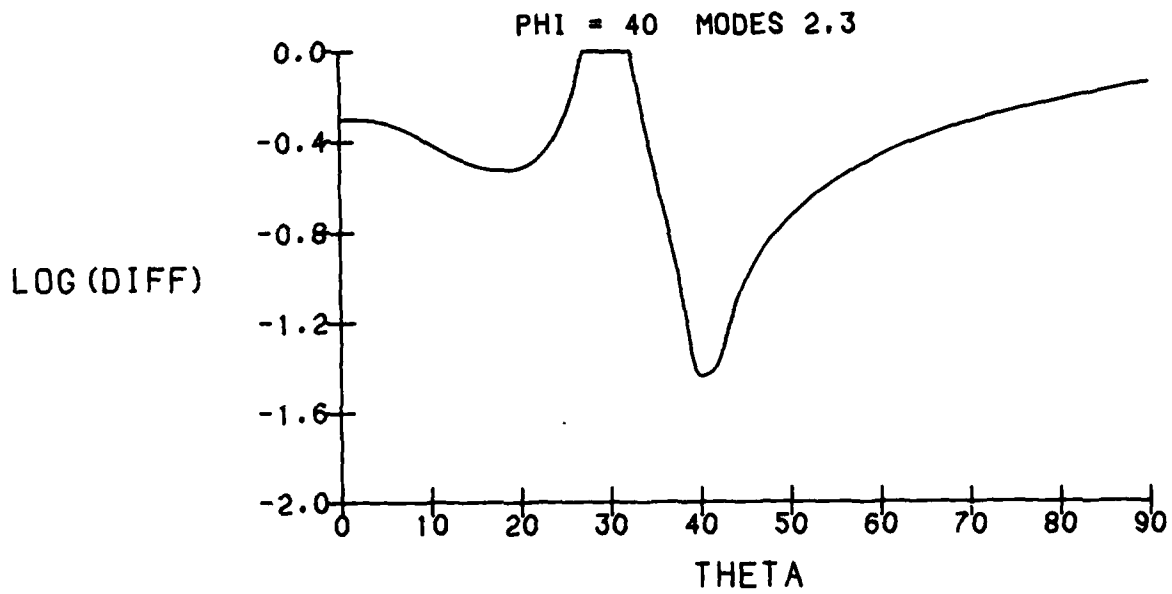


Figure 17: DIFFERENCE MEASURE OF TEMPERATURE SENSITIVITY (continued)

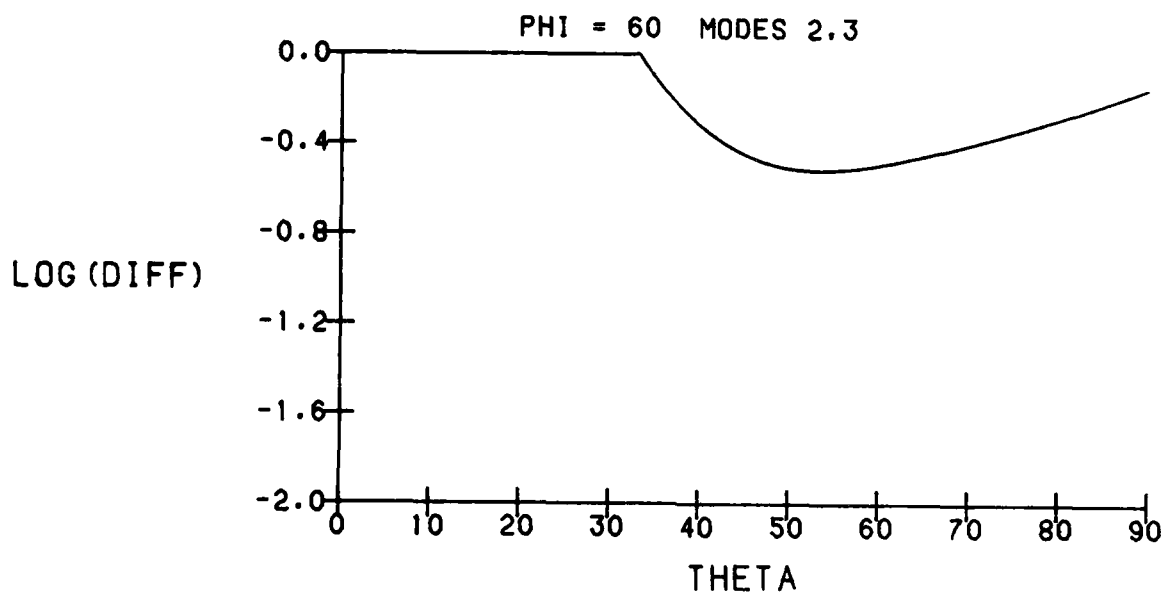


Figure 17: DIFFERENCE MEASURE OF TEMPERATURE SENSITIVITY (continued)

CONCLUSION

Previous work on the temperature sensitivity of quartz resonances used a local measure of temperature sensitivity, namely, the zeroes of the first order temperature coefficients. We have presented results of calculations using other measures of sensitivity in the temperature range $(-40^{\circ}, 80^{\circ})$ and have found that the minima for fixed ϕ occur in close proximity to the locus of zeroes of the first order temperature coefficients. Indeed, we have found that the locations of the minima vary only slightly between the different measures; the locations of the minima for the integral measure, the range measure and the slope measure are all in close proximity to each other and to the zeroes of the first order temperature coefficient. It seems likely that this characteristic is attributable to the cubic nature of the relative frequency difference expansion. Nonetheless, our results do go beyond an analysis of the zeroes of the first order temperature coefficient. Specifically, the measures we have used allow us to compare the temperature sensitivity of the various minima according to their magnitude. In addition, we have used three other practical criteria in comparing these doubly rotated cuts: angular stability, separation of modal frequencies and coupling strengths. In this fashion, we have presented four cuts with relatively stable temperature behavior. None of these four cuts is clearly superior to the others, but each has its advantages and disadvantages.

6.

REFERENCES

- Ballato, A., "Doubly Rotated Thickness Mode Plate Vibrators", Physical Acoustics, Vol. XIII, Academic Press, N.Y., 1977.
- Ballato, A. and Iafrate, G.J., "The Angular Dependence of Piezoelectric Plate Frequencies and Their Temperature Coefficients", 30th Annual Frequency Control Symposium, 141, 1976.
- Bechmann, R., "Frequency-Temperature-Angle Characteristics of AT-type Resonators Made of Natural and Synthetic Quartz", Proc. IRE, 44, 1600-1607 (1956).
- Bechman, R., Ballato, A. and Lukaszek, T.J., "Higher-Order Temperature Coefficients of the Elastic Stiffnesses and Compliances of Alpha-Quartz", Proc. IRE, 50, 1812-1822 (1962).
- Goldstein, H., Classical Mechanics, Addison-Wesley, Reading, MA, 1950.
- Kahan, A., Private communication (1982).
- Mason, W.P., Piezoelectric Crystals and Their Application to Ultrasonics, Van Nostrand, N.Y., 1950.
- Tiersten, H.F., Linear Piezoelectric Plate Vibrations, Plenum Press, N.Y., 1969.